KU Leuven
Biomedical Sciences Group
Faculty of Medicine
Department of Neurosciences
Vlaams Instituut voor Biotechnologie (VIB)
Center for Brain & Disease Research
Laboratory of Neurobiology

KU LEUVEN
DOCTORAL SCHOOL BIOMEDICAL SCIENCES

# THE INVOLVEMENT OF NOTCH SIGNALING IN AMYOTROPHIC LATERAL SCLEROSIS

*"a complex balance between the good and the bad"*

Annelies NONNEMAN

| | |
|---|---|
| Promotor: | Prof. Dr. Wim Robberecht |
| Co-promotor: | Prof. Dr. Ludo Van Den Bosch |
| Chair: | Prof. Dr. Peter Janssen |
| Jury members: | Prof. Dr. Mieke Dewerchin, KU Leuven<br>Prof. Dr. Patrick Callaerts, KU Leuven<br>Prof. Dr. Angeliki Louvi, Yale University<br>Prof. Dr. Nicholas Maragakis, Johns Hopkins University |

**Dissertation presented in partial fulfillment of the requirements for the degree of Doctor in Biomedical Sciences**

October 2018

# TABLE OF CONTENTS

# LIST OF ABBREVIATIONS

| | |
|---|---|
| Aβ | Amyloid beta |
| AD | Alzheimer's disease |
| ALDH1L1 | Aldehyde dehydrogenase 1 family member L1 |
| ALS | Amyotrophic lateral sclerosis |
| AMPA | α-amino-3-hydroxy-5-methylisoxazole-4-propionic acid |
| APP | Amyloid precursor protein |
| BDNF | Brain-derived neurotrophic factor |
| C9ORF72 | Chromosome 9 open reading frame 72 |
| $Ca^{2+}$ | Calcium |
| CADASIL | Cerebral autosomal dominant arteriopathy with subcortical infarcts and leukoencephalopathy |
| CD11b | Cluster of differentiation molecule 11b |
| CNS | Central nervous system |
| CNTF | Ciliary neurotrophic factor |
| DLL/Dll | Delta-like protein |
| DNA | Deoxyribonucleic acid |
| EAAT1 | Excitatory amino acid transporter 1 |
| EAAT2 | Excitatory amino acid transporter 2 |
| ER | Endoplasmic reticulum |
| fALS | Familial ALS |
| FTD | Frontotemporal dementia |
| FUS | Fused in sarcoma |
| G37R | Glycine to arginine mutation at position 37 |

| | |
|---|---|
| G85R | Glycine to arginine mutation at position 85 |
| G93A | Glycine to alanine mutation at position 93 |
| GAPDH/Gapdh | Glyceraldehyde 3-phosphate dehydrogenase |
| GDNF | Glial-derived neurotrophic factor |
| GFAP | Glial fibrillary acidic protein |
| GLAST | Glutamate aspartate transporter |
| GLT1 | Glutamate transporter 1 |
| GluR2 | Glutamate receptor 2 subunit |
| HES/Hes | Hairy and enhancer of split |
| HEY/Hey | Hairy enhancer of split related with YRPW motif |
| Hprt | Hypoxanthine phosphoribosyltransferase 1 |
| IBA-1 | Ionized calcium-binding adapter molecule 1 |
| IFN-γ | Interferon gamma |
| IGF-1 | Insulin growth factor 1 |
| IL-1β | Interferon 1 beta |
| IL-4 | Interleukin 4 |
| IL-10 | Interleukin 10 |
| Itgam | Integrin subunit alpha M |
| iNOS | Inducible nitric oxide synthase |
| LCM | Laser capture microdissection |
| MAML | Mastermind-like |
| MBP | Myelin basic protein |
| MCT-1 | Monocarboxylate transporter 1 |
| MMP-9 | Matrix metalloproteinase-9 |
| MS | Multiple sclerosis |
| $Na^+$ | Sodium |

| | |
|---|---|
| NG2 | Neural/glial antigen 2 |
| NICD | Notch intracellular domain |
| NMDA | N-methyl-D-aspartate |
| NO | Nitric oxide |
| NSC | Neural/neuronal stem cell |
| OPC | Oligodendrocyte precursor cell |
| PEST | Proline (P), glutamic acid (E), serine (S) and threonine (T) rich domain |
| PMI | *Post mortem* time interval |
| Polr2a | RNA polymerase II subunit A |
| PS1 | Presenilin-1 |
| PS2 | Presenilin-2 |
| RAN | Repeat-associated non-ATG |
| RBPjk | Recombination signal binding protein for immunoglobulin kappa J region |
| RNA | Ribonucleic acid |
| ROS | Reactive oxygen species |
| sALS | Sporadic ALS |
| SMA | Spinal muscular atrophy |
| SOD1 | Superoxide dismutase 1 |
| TDP-43 | TAR DNA binding protein 43 |
| TNFα | Tumor necrosis factor alpha |
| UBQLN2 | Ubiquilin-2 |
| UPR | Unfolded protein response |
| VCP | Valosin-containing protein |
| WT | Wild type |

# INTRODUCTION

**Part of the introduction is published in:**

**Nonneman A**, Robberecht W, Van Den Bosch L. The role of oligodendroglial dysfunction in amyotrophic lateral sclerosis. Neurodegener Dis Manag. 2014;4(3):223-39.

The progress in health care, medical knowledge, and availability of effective therapies is responsible for an enormous increase in life expectancy and a progressive increase in the number of older people. Neurodegenerative diseases are generally known to be strongly related to aging. Up to now, for most of them, no effective therapy or cure is available. Consequently, the growing number of patients with neurodegenerative diseases is becoming more and more problematic with a serious socio-economic impact (1). Besides Alzheimer's disease and Parkinson's disease, amyotrophic lateral sclerosis is one of the more common neurodegenerative diseases (2).

## 1. Amyotrophic lateral sclerosis: the basics

Amyotrophic lateral sclerosis (ALS) is a devastating neurodegenerative disease characterized by the selective loss of both upper and lower motor neurons (Figure 1A). This progressive disease starts at adult age by showing symptoms such as muscle weakness, atrophy, and spasticity due to muscle denervation (Figure 1B-C), and subsequently evolves into paralysis. Denervation of the respiratory muscles and the diaphragm leads to respiratory failure and death, which typically occurs 3 to 5 years after disease onset (3, 4). In spite of this simple classic textbook definition, ALS is a very heterogeneous

disease, with considerable variability in many aspects of the disease, including site of onset, age at onset, rate of disease progression, disease duration, familial occurrence, genetic causes, type of motor neurons involved, extent of extramotor involvement, and cognitive impairment (3).

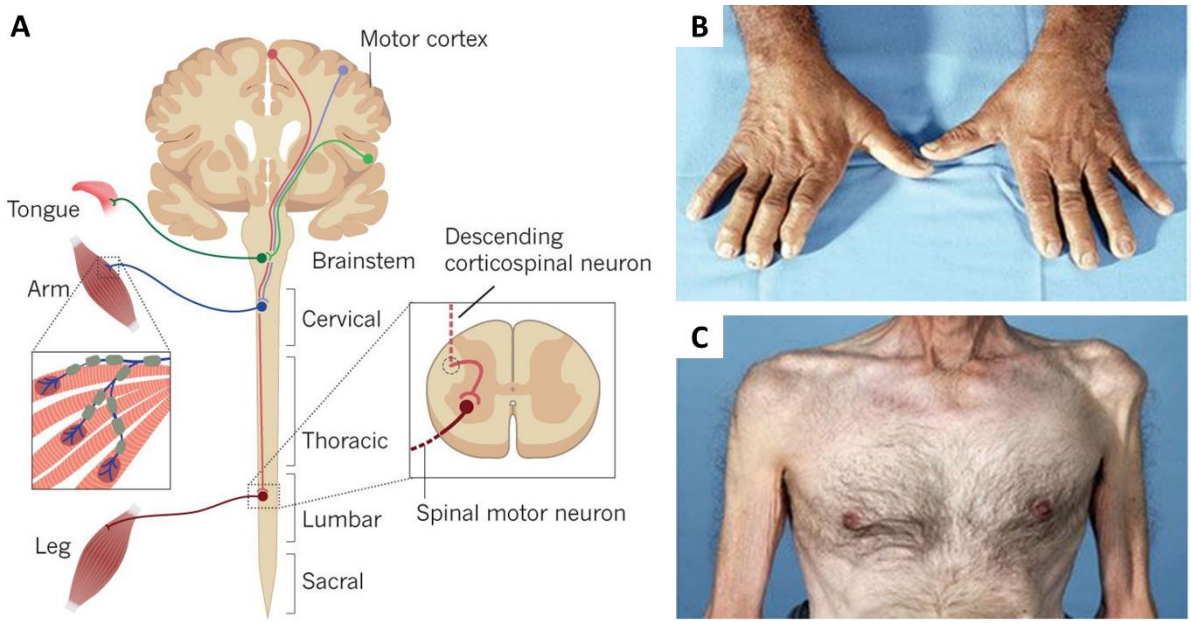


***Figure 1: Motor neuron degeneration in ALS results in a prominent muscle atrophy phenotype.*** *(A) ALS mainly affects the descending corticospinal motor neurons (upper motor neurons) that project from the motor cortex into synapses in the brainstem and spinal cord, and the bulbar or spinal motor neurons (lower motor neurons) that project into skeletal muscles. (B) The 'split hand' phenotype is shown, in which disproportionate wasting of the first dorsal interossei (i.e. muscle in the hand that lies between the thumb and the index finger) can be observed. (C) Patients with limb-onset ALS show prominent bilateral wasting of the shoulder girdles, pectoral muscles and proximal upper arms. Adapted from (5, 6) and reprinted with permission of Springer Nature and Copyright Clearance Center with copyright license numbers 4385601378801 (doi: 10.1038/nrneurol.2011.153) and 4385910787861 (doi: 10.1038/nature20413).*

In European populations, the incidence of ALS is 2–3 per 100,000 individuals per year, and the overall lifetime risk of developing ALS is 1:350 for men and 1:400 for women (7). As shown in figure 2, approximately 10% of patients have at least one affected relative and suffer from the hereditary form of ALS, defined as “familial ALS” (fALS). Genome analysis of these families allowed the identification of a variety of ALS-causing gene mutations, of which hexanucleotide repeat expansions in ‘Chromosome 9 open reading frame 72’ (*C9ORF72*) and mutations in ‘superoxide dismutase 1’ (*SOD1*) are the most prevalent (8, 9). Other less frequent ALS-causing mutations occur in ‘TAR DNA binding protein 43’ (*TDP-*

*43*) (10), 'fused in sarcoma' (*FUS*) (11), 'valosin-containing protein' (*VCP*) (12) and many others (13-15). The remaining 90% of patients are classified as having "sporadic ALS" (sALS) (3, 4, 13) (Figure 2). Of these, 10 % are misclassified as being clinically defined sporadic ALS cases, yet have a hereditary form, in spite of not reporting any known relative with the disease. For years, the main hypothesis explaining the sALS cases was the influence of environmental factors (16). The discovery of *C9ORF72* hexanucleotide repeat expansions being responsible for nearly 7% of sALS cases resulted in a shift in the understanding of the disease and in less strict borders between familial and sporadic cases (13, 17). Apart from genetic causes, as is the case for fALS patients, a genetic risk factor can be responsible for increased susceptibility. Possibly the genetic load in combination with environmental triggering factors over time can lead to ALS (13, 16, 17).

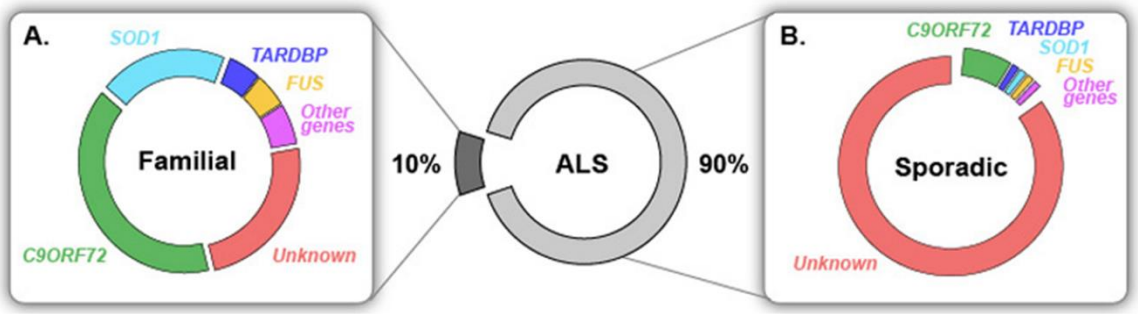


***Figure 2: Known genetic causes in familial and sporadic ALS.*** *Most ALS cases are sporadic (sALS) and only 10% are inherited, called familial (fALS). (A) 20% of fALS are caused by mutations in SOD1, which is the first known ALS-linked gene, identified in 1993. Mutations in the RNA/DNA-binding proteins TDP-43 and FUS cause a small fraction (~5%) of fALS each. Hexanucleotide repeat expansions in* C9ORF72 *are the most common genetic cause of ALS accounting for almost 40% of fALS in people of European ancestry. Several other genes have been identified as genetic causes of ALS and collectively today over 60% of fALS can be explained by known mutations. (B) While the aetiology of the vast majority of sALS remains unknown, mutations in genes known to cause fALS were identified in a small fraction of apparently sporadic patients. Most strikingly, hexanucleotide repeat expansions in C9ORF72 are causing approximately 7% of sALS without familial history in people of European ancestry. Reprinted from (18) with permission of Swiss Medical Weekly under the terms of the Creative Commons Attribution-Non Commercial-No derivatives 4.0 International type BY license (doi: 10.4414/smw.2015.14054).*

The growing number of ALS-causing genes and the study of the mutant proteins they encode revealed a variety of intracellular processes that are affected in ALS. Among them, protein misfolding and aggregation, mitochondrial dysfunction, axonal transport abnormalities, endoplasmic reticulum stress,

oxidative stress, glutamate-induced excitotoxicity, aberrant RNA processing, and neuroinflammation can contribute to the pathogenesis of ALS (15, 19) and will be described in chapter three, entitled '*Pathogenic mechanisms in ALS'*.

In spite of the enormous progress in the identification of the ALS-causing genes and underlying pathogenic mechanisms, no effective treatment beyond supportive care and two FDA-approved drugs with limited beneficial effects, namely riluzole and edaravone, is available to date (20-23). Riluzole, a glutamate release blocker, can prolong survival of patients by 2 to 3 months, compared to placebo. Edaravone, a free radical scavenger, is believed to protect neurons and glia against oxidative stress and results in a deceleration of motor performance decline (23). The lack of a major disease modifying therapy makes it compulsory for caretakers to focus on pharmacological and non-pharmacological treatments, including painkillers, physiotherapy, tracheostomy with mechanical ventilation for patients with respiratory insufficiency, gastrostomy and enteral feeding for those with dysphagia, in order to maintain the patient's quality of life and to extend life span as long as possible (20, 21). More profound investigation of the underlying disease mechanisms is necessary to identify new therapeutic targets.

## 2. Mouse models available for the study of ALS

Mouse models are the gold standard for the preclinical study of ALS, because these mammalian model systems have a high degree of genetic homology to humans and because mouse models exist for the genetic mutations that are most prevalent in fALS patients (24). Thanks to these models, important insights were obtained into the pathogenic mechanisms contributing to motor neuron degeneration in ALS.

## 2.1 Mutant SOD1 mouse models

Transgenic mice overexpressing human mutant *SOD1* under control of the human *SOD1* promotor and regulatory elements have been extensively used since 1994 to study ALS. The most commonly used human mutant *SOD1* mouse models carry one of the following mutations: G93A, G37R or G85R (25). They all develop adult-onset progressive motor neuron disease, but the age of onset and the disease progression rate may vary, as indicated in table 1, depending on the SOD1 mutation, the copy number of human mutant SOD1 inserted, and the genetic background (25).

***Table 1: The most commonly used human mutant SOD1 mouse models****. Adapted from (25).*

| ***SOD1 mutation*** | ***Disease onset **** | ***Survival **** | ***Copy number*** | ***Reference*** |
|---|---|---|---|---|
| G93A | 3 months | 4-5 months | 20-24 copies | (26) |
| G37R | 3.5-6 months | 7 months | 14 copies | (27) |
| G85R | 8 months | 8.5 months | 2-15 copies | (28) |

*(* Onset and survival ages when mice have the C57BL/6J genetic background)*

Mice overexpressing human wild type *SOD1* are used as controls (25). The latter do not develop motor neuron degeneration, however, at later ages they develop an axonopathy (25).

Of note, *Sod1* knockout mouse models cannot be used to study ALS, as they did not show motor neuron loss (29). However, the generation and characterization of these mice was important, as it suggests a toxic gain of function of mutant SOD1 in ALS, instead of a loss of function.

Much of the current understanding of the disease mechanisms involved in ALS is based on the human mutant *SOD1* overexpression mouse models (24), because they were the first available models that faithfully recapitulate human ALS pathology with adult-onset and progressive motor neuron degeneration and muscle atrophy, ultimately evolving into paralysis and death (26). However, the

disease in human mutant *SOD1* mouse models differs in some aspects from the disease developed in ALS patients (25). For instance, a fundamental feature of human ALS is cortical motor neuron degeneration, for which the evidence is rather limited in mutant *SOD1* mice. The origin of motor neuron loss and paralysis is also different: in mutant *SOD1* mice, the motor neurons of the ventral horn of the lumbar spinal cord degenerate first, followed by motor neurons in more rostral spinal cord regions. This explains the initiation of hind limb paralysis well before forelimb paralysis in mutant *SOD1* mice. In ALS patients however, disease can initiate at different regions, explaining why some patients develop speech and swallowing deficiencies before limb weakness (bulbar-onset ALS), while in others the disease follows the opposite course (spinal-onset ALS). These limitations have to be considered when utilizing these SOD1 mouse models, which nevertheless represent the best models currently available to study human ALS.

## 2.2 Other mouse models to study ALS

Besides the mutant SOD1 mouse model, many other mouse models have been generated for the study of ALS. The most important models are described below and listed in table 2.

Since the discovery of the involvement of TDP-43 in ALS, several mouse models have been generated to explore the role of TDP-43 in disease (25). The *Tdp-43* knockout mice are embryonic lethal and conditional floxed *Tdp-43* transgenic mice show that depletion of *Tdp-43* at adult ages leads to early death around 9 days after tamoxifen administration (25). Several mouse models overexpressing human mutant TDP-43 have also been generated. Different levels of overexpression (modest or high), different promotors for ubiquitous and neuronal specific expression and different mutations were evaluated (25). However, none of the TDP-43 mouse models seems to recapitulate the pathological hallmarks of ALS as seen in patients: the loss of cortical or spinal motor neurons is either very modest or absent, neuromuscular junction innervation is usually only mildly affected, these mice do not exhibit

early mortality, or the cause of death is unrelated to ALS pathogenesis. In addition, mice overexpressing human wild type TDP-43 also develop motor symptoms. (25)

***Table 2: Mouse models, other than the mutant SOD1 model, to study ALS***.

| ***Mouse models*** | ***Phenotype*** |
|---|---|
| *Tdp-43* knock-out | Embryonically lethal |
| Conditional floxed *Tdp-43* | Early lethality (unrelated to ALS) |
| Mutant human TDP-43 overexpression | Only limited pathology was observed:<br>- motor neurons loss is very modest/absent<br>- neuromuscular junction innervation is mildly affected<br>- no early mortality/cause of death is unrelated to ALS |
| Wild type human TDP-43 overexpression | Develop motor symptoms |
| *Fus* knockout | Early lethality (unrelated to ALS) |
| Mutant human FUS overexpression | Motor symptoms |
| Wild type human FUS overexpression | Motor Symptoms |
| Mutant human FUS (expressed at physiological levels) | Recapitulate adult-onset progressive motor neuron degeneration preceded by muscle denervation |
| Wild type human FUS (expressed at physiological levels) | No motor neuron loss or muscle denervation |
| C9ORF72 hexanucleotide repeat expansion models | Motor neuron loss is limited |

To understand the role of FUS in ALS, different types of FUS mouse models have been generated. *Fus* knockout resulted in early lethality that was not associated with ALS (30). Several human mutant FUS overexpressing mice and human wild type overexpressing mice were generated, but both the mutant models and the wild type models do developed motor symptoms (30). Only very recently, human FUS mouse models expressing mutant and wild type FUS at physiological levels were successfully generated (31, 32). These mutant FUS models recapitulate adult-onset progressive motor neuron degeneration preceded by structural and functional abnormalities at the level of the neuromuscular junction. In contrast, control mice expressing human wild type FUS at endogenous levels did not develop motor

neuron loss or muscle denervation. Further study of these models will elucidate their potential for the study of ALS.

Recently, several C9ORF72 hexanucleotide repeat expansion mouse models were generated and characterized (33). In general, the motor neuron loss in these models is rather limited and there is large variability in the clinical phenotype between the different C9ORF72 mouse models.

In conclusion, many mouse models have been generated for the study of ALS. These models have provided insights into certain aspects of the pathogenesis of ALS that will be described in the next chapter. Working with mouse models also has some disadvantages, including the high cost for maintenance and the long duration of the studies (24). In addition, drawing conclusions based on results obtained with mouse models has to be done very carefully, as these mice are often overexpression models, and inbred in nature, which does not reflect the human situation (24). However, overall mouse models remain the gold standard in preclinical testing.

# 3. Pathogenic mechanisms in ALS

The pathogenesis of ALS remains largely unknown. A plethora of toxic mechanisms that could mediate motor neuron degeneration have been proposed (Figure 3), based on the knowledge about the biology and functions of the ALS-causing genes and the mutant proteins which they encode.

ALS-genes and proteins can be grouped according to their physiological functions and properties into the following pathologically affected processes: aberrant RNA homeostasis, impaired protein homeostasis and protein quality control, disturbed cytoskeletal dynamics and defective DNA damage response (6). Other processes that are known to be involved in the pathogenesis of ALS include oxidative stress, glutamate-induced excitotoxicity, mitochondrial dysfunction, axonal transport abnormalities, and endoplasmic reticulum (ER) stress.

In addition to these dysregulated molecular pathways in motor neurons, non-neuronal neighboring cells including astrocytes, microglia, and oligodendrocytes play an important role in the disease process. Moreover, these cells could also adversely influence the progression of ALS (6, 15, 19, 34-36).

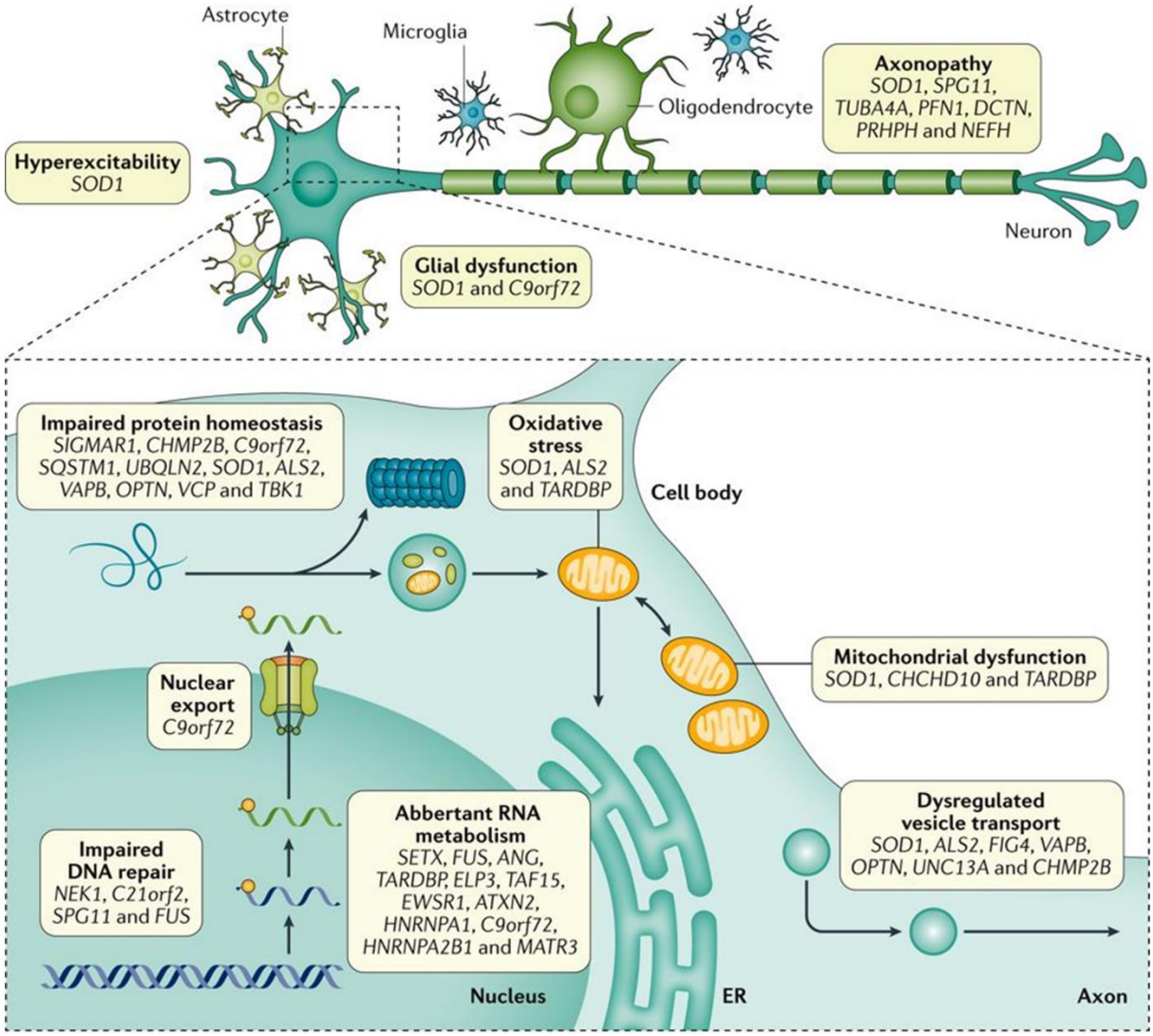


***Figure 3: Proposed pathogenic mechanisms in ALS.*** *Based on mutations in several genes it was suggested that motor neuron injury is exerted through many pathophysiological mechanisms that are often interlinked. SOD1 is the longest-studied gene implicated in ALS and has been linked to the greatest number of pathophysiological mechanisms, whereas the effects of some other gene mutations are still unknown. The most commonly suggested pathogenic mechanisms are depicted in this figure. Among them, aberrant RNA metabolism and impaired protein homeostasis are predominant factors linking multiple ALS causative genes to neuronal injury. Mitochondrial dysfunction leads to an increase in oxidative stress, which puts further stress on an already impaired protein homeostasis system. Other mechanisms of ALS can directly alter neuronal function (such as impaired nuclear export, impaired DNA repair and dysregulated vesicle transport) and dysfunction of glial cells. In addition, neuronal hyperexcitability and axon dysfunction have been implicated in ALS. The interplay of mechanisms is indicated by arrows. ER, endoplasmic reticulum. Adapted from (37) and reprinted with permission of Springer Nature and Copyright Clearance Center with copyright license number 4385600221384 (doi: 10.1038/nrdp.2017.71).*

The separation between these different pathogenic mechanisms is artificial and a combination of different interacting mechanisms is more likely to happen (Figure 3). Moreover, to which extent each of these mechanisms contributes to the overall pathogenesis of ALS is currently unknown (37). However, these mechanisms contribute to a general final pathway of denervation, axonal retraction, and motor neuron loss.

## 3.1 Aberrant RNA homeostasis

The identification of ALS-causing mutations in the RNA binding proteins TDP-43 (10, 38) and FUS (11, 39), has led to the hypothesis that disturbances in RNA homeostasis might be involved in ALS pathogenesis (6). TDP-43 and FUS are proteins that regulate RNA metabolism at every stage of the RNA life cycle and can bind to thousands of different RNAs. This means that mislocalization of these proteins from the nuclear to the cytoplasmic compartment will result into disruption of their function and will also have serious adverse effects on RNA metabolism in general (37). Also the hexanucleotide GGGGCCC repeat expansion in the non-coding region of the C9ORF72 gene has been described to disturb RNA homeostasis and result into RNA toxicity (37), because it can a) form G-quadruplex structures that interact with RNA processing factors; b) induce the production of abnormal RNA species that are retained in the nucleus, defined as nuclear RNA foci, which induce the sequestration of RNA-binding proteins; c) lead to the formation of RNA-DNA hybrid structures, so-called R-loops, which increase the susceptibility to DNA damage and lead to genome instability.

## 3.2 Impaired protein homeostasis, degradation and quality control

The presence of protein aggregates containing products of ALS genes, such as SOD1, TDP-43, FUS, UBQLN2 or C9ORF72 dipeptides, in affected motor neurons is generally known as a pathological

hallmark of ALS (15, 40). These aggregates highly likely disturb protein homeostasis and induce cellular stress by interfering with various cellular functions, such as protein clearance pathways, axonal transport, cytoskeletal architecture and mitochondrial functioning (35). Protein aggregates may also sequester RNA and other proteins essential for normal cellular function (36). Ultimately, this leads to axonal retraction, denervation, and cell death (41). In addition, mutations in some proteins, including SOD1, UBQLN2 and VCP, can lead to protein misfolding and abnormal cellular localization, that directly or indirectly impairs the proteasome or the autophagy machinery and consequently impairs protein degradation (37). Dipeptide repeat-proteins generated from C9ORF72 repeat expansions through repeat-associated non-ATG (RAN) translation, an unconventional form of translation initiated through an expanded repeat and independent of a start codon, can also disrupt protein homeostasis and lead to neurotoxicity (37).

## 3.3 Disturbed cytoskeletal dynamics and axonal transport

Motor neurons are the most asymmetric cells in nature since they have very long axons that reach more than 1 meter (6). Consequently, these cells highly rely on axonal transport to deliver all necessary components synthesized in the cell body to the axons and the synapses, including mRNA, proteins, lipids, organelles, and vesicles (42). In ALS, disorganization of the axonal cytoskeleton and slower axonal transport, both anterograde and retrograde, are a common feature and have been reported before symptom onset, with devastating consequences on the health of the motor neurons (6). Up to now the underlying cause of axonal transport defects in ALS is not fully understood, since mutations in the axonal transport machinery, such as mutations in the motor protein dynactin, have only been reported in a small number of cases (42).

## 3.4 DNA damage and defective DNA repair

Damage of the DNA and impairment of the DNA repair machinery are also suggested to be involved in the pathogenesis of ALS (37). FUS mutations are linked to the failure of DNA repair and accumulation of DNA damage. This might result in additional cytoplasmic FUS mislocalization and consequently FUS aggregation and neurodegeneration (43). It is also reported that R-loops, which are generated by the repeat expansion in C9ORF72, are able to trigger DNA damage and genome instability (37). In an attempt to repair the damage, cells then activate the DNA damage response, but when this damage cannot be repaired, apoptosis is induced (44).

## 3.5 Glutamate-induced excitotoxicity

Excitotoxicity is toxicity induced by excessive glutamate stimulation that leads to abundant calcium ($Ca^{2+}$) entry into the neurons (37). Motor neurons are very sensitive to this massive $Ca^{2+}$ influx, since they have a low $Ca^{2+}$ buffering capacity and express more $Ca^{2+}$ permeable α-amino-3-hydroxy-5-methylisoxazole-4-propionic acid (AMPA) receptors, as they have fewer GluR2 subunits than other types of neurons (37). In addition, the expression of the excitatory amino acid transporter 2 (EAAT2), which is responsible for the synaptic glutamate reuptake, is downregulated in the astrocytes in ALS (45). Consequently, this results in excessive amounts of glutamate in the synaptic cleft that induce the neurotoxic $Ca^{2+}$-influx. Of note, Riluzole, one of the two FDA-approved drugs for ALS that modestly extend survival, acts via inhibiting the glutamate release (46).

## 3.6 Mitochondrial dysfunction

Mitochondria play a key role in energy production and $Ca^{2+}$ buffering. In ALS, dysfunction and morphological changes of the mitochondria have been reported (37). Protein aggregates in the

mitochondrial inter-membrane space disrupt protein import and oxidative damage to the mitochondrial proteins disrupts the functioning of the respiratory chain. Consequently, reactive oxygen species (ROS) are generated that may trigger apoptotic cell death mechanisms and impairment of neuronal health and functioning (47). In addition, defective axonal transport of mitochondria may induce axonal degeneration as well due to local energy deficits (48).

## 3.7 Endoplasmic reticulum stress

The endoplasmic reticulum (ER) is a cellular compartment that is responsible for protein synthesis, posttranslational processing, protein folding, and delivery of the biologically active proteins to their proper target site (6, 49). These processes are $Ca^{2+}$ dependent. In addition, the ER is also involved in intracellular $Ca^{2+}$ homeostasis and redox balance. An imbalance in ER $Ca^{2+}$ homeostasis, accumulation of mutant SOD1 or damage induced by ROS can disrupt the physiological state of the ER and results in ER stress (49). In order to return to a normal physiological state, the unfolded protein response (UPR) is activated. However, in ALS this UPR fails to restore the normal state and consequently cell death signaling cascades are activated and apoptosis is induced (6, 49).

## 3.8 Oxidative stress

Substantial evidence supports an involvement of oxidative stress in ALS pathogenesis (47). For instance, elevated markers of oxidative damage in the spinal cord and cerebrospinal fluid of ALS patients were reported, and the discovery of mutations in the SOD1 gene that were responsible for approximately 20% of fALS cases supported the implication of oxidative stress in ALS pathogenesis. Oxidative stress is the result of the imbalance between the production of ROS and the capacity of the system to remove the ROS and repair the induced damage. Most of the ROS are generated by the

mitochondria due to leakage of electrons from the mitochondrial respiratory chain during oxidative phosphorylation. ROS are capable to induce serious damage in DNA, proteins and lipids, including DNA mutations, changes in protein conformation and altered cellular membrane dynamics that are harmful for motor neurons. (47)

## 3.9 Non-cell autonomous toxicity in the pathogenesis of ALS

### *Evidence for non-cell autonomous toxicity*

In ALS, motor neuron degeneration is not only arising through cell intrinsic mechanisms, but non-cell autonomous-mediated mechanisms actively contribute to the degeneration of the motor neurons as well (41). Evidence came from the study of human mutant *SOD1* mouse models. Expression of human mutant SOD1 only in motor neurons was not sufficient to induce motor neuron degeneration in mice (50, 51). Only when expressed at very high levels, it can induce disease at late ages with a progression rate that is much slower than in mice expressing human mutant SOD1 ubiquitously (52). In addition, deletion or reduction of human mutant SOD1 specifically in motor neurons delayed disease onset, but cannot alter disease progression after symptom onset (53, 54). These findings suggest the involvement of non-neuronal cells in the pathogenesis of ALS.

Removal of human mutant SOD1 selectively from oligodendroglial cells delayed disease onset (55). Transgenic mice expressing mutant SOD1 restricted to astrocytes developed astrocytosis in the absence of motor degeneration (56), while astrocyte-specific deletion of mutant SOD1 significantly slowed down disease progression, without altering disease onset (57). This effect on disease progression was accompanied by a delay in microglial activation, suggesting the interaction between diseased astrocytes and microglia. Selective mutant *SOD1* gene excision from microglia could also substantially decelerate disease progression without affecting onset (54). Thus, at least in mouse

models, motor neurons and oligodendrocytes affect disease onset without influencing disease progression, while astrocytes and microglia are responsible for accelerating disease progression (41).

### *How do different types of glial cells contribute to motor neuron degeneration in ALS?*

The ***oligodendrocytes*** are a glial cell type of major importance to CNS neurons as they insulate axons with a myelin sheath (58-60) and provide neurons with metabolic support (61, 62). Abnormalities in one of these two functions can seriously affect the health of the associated (motor) neurons (58, 59, 61, 62) (Figure 4).

In the gray matter of the ventral spinal cord of sALS and fALS patients (55) and ALS mice (55, 63, 64), oligodendroglial inclusions, myelin abnormalities, demyelination and even oligodendrocyte degeneration were observed. Besides the oligodendrocytes, oligodendroglial precursor cells (OPCs) are also affected (55, 63, 65). The OPCs show a clear augmentation of the Neural/Glial antigen-2 (NG2) immunoreactivity and thick hypertrophic NG2+ processes. The exact importance of oligodendrocytes and their NG2+ precursors and how they are involved in the pathogenesis of ALS has been elucidated through extensive studies in mouse and rat ALS models (55, 61, 63, 65, 66). Oligodendrocytes were discovered to degenerate already before the first symptoms of motor neuron degeneration become apparent and progressively more oligodendrocytes degenerate during the course of disease (55, 63). However, the overall number of oligodendrocytes does not change throughout the course of disease and is similar to the number of oligodendrocytes in healthy control mice (55, 63). This is because OPCs proliferate and differentiate in order to generate new oligodendrocytes to replace ones that are lost (63, 65). However, these new oligodendrocytes show several functional defects. For example, the structure and protein composition of the myelin sheath is altered (66) and the levels of myelin-forming proteins are progressively decreasing during disease (55, 63). Most prominent is the decrease in the level of myelin basic protein (MBP), the second most abundant protein component of myelin

responsible for the formation, compaction, and stabilization of myelin (67). These myelin defects are also detected in the spinal cord and motor cortex of ALS patients, but are absent in control subjects (55). A thick, well-developed, well-organized and compact myelin sheath has neuroprotective properties (68), and is very important for fast and efficient propagation of action potentials along the axons. Obviously, the myelin abnormalities in ALS are detrimental for the health of motor neurons and can be considered a contributing factor to neurodegeneration. However, the absence of myelin alone is not sufficient for axonal degeneration, unless it occurs in combination with oligodendroglial injury or inflammation (58). Besides the above described myelin defects, oligodendrocytes also fail to supply axons with metabolic energy substrates (61, 63). Monocarboxylate transporter 1 (MCT-1) is a marker for metabolic support provided by the oligodendrocytes, as it is the major transporter of energy substrates (including lactate, pyruvate and ketone bodies) to the CNS neurons and it is abundantly expressed in oligodendrocytes (61, 62, 69). In ALS affected spinal cord, both from patients and from mouse models, less MCT-1 is expressed (61, 63). Due to this reduction of MCT-1 expression levels, the lactate transport from oligodendrocytes to neurons is thought to be diminished, causing disturbances of the local energy supply and leading to axonal dysfunction, axonal damage and even neuronal loss in cell culture models, as well as mouse models (58, 61, 62, 69). Of note, the reduction in MBP and MCT-1 levels in the spinal cord of *SOD1*$^{G93A}$ mice cannot be explained by loss of oligodendrocytes, as their density does not change during disease progression due to continuous generation of newly differentiated oligodendrocytes (55, 63). However, this indicates that the new oligodendrocytes are unable to function properly, probably due to an immature developmental state. In this way, oligodendrocytes could actively contribute to the motor neuron degeneration in ALS.

Besides oligodendroglial cells, ***microglia and astrocytes*** also contribute to the degeneration of motor neurons by causing neuroinflammation, a local inflammatory response characterized by morphological changes, proliferation, and migration of these cells to the site of injury and secretion of pro-inflammatory mediators (70, 71) (Figure 4).

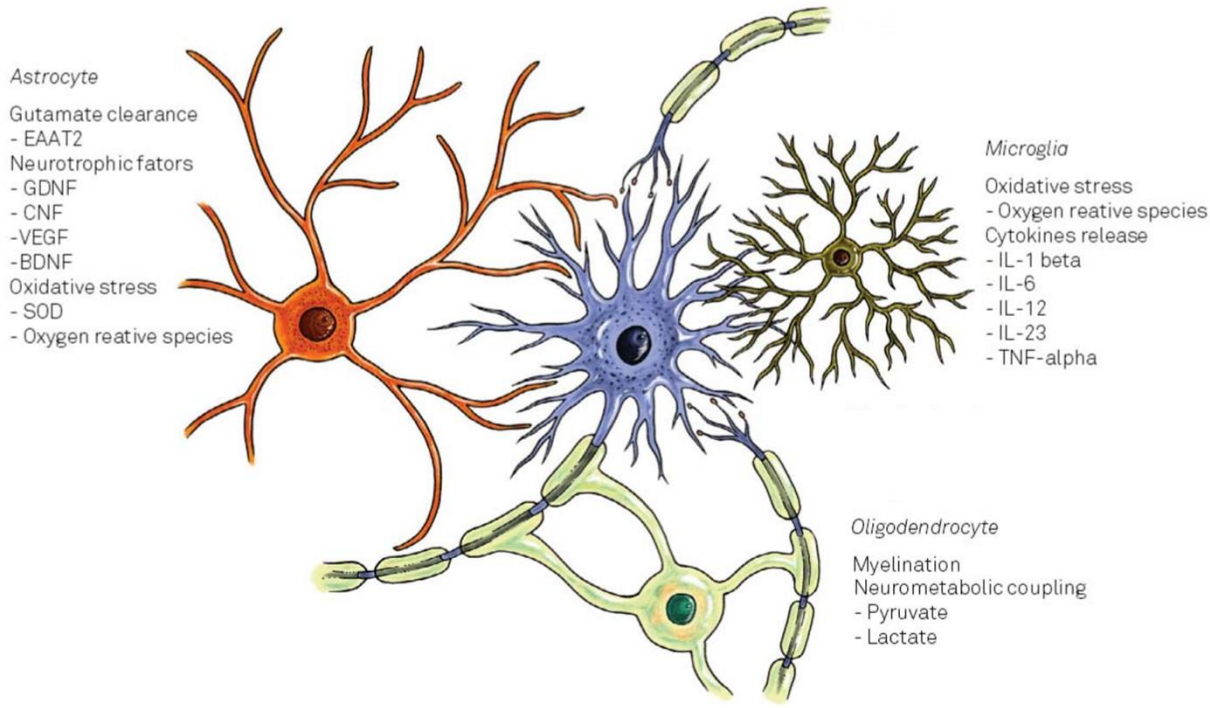


***Figure 4: Different types of glial cells contribute to motor neuron degeneration in ALS.*** *Astrocytes, microglia and oligodendrocytes interact in many different ways with neurons to maintain the neurons healthy. The most important molecular mechanisms implicated in the pathogenesis of ALS are listed for each glial cell type. Adapted from (72) and reprinted with the permission of Arquivos de Neuro-Psiquiatria under the terms of the Creative Commons Attribution 4.0 International type BY license (doi: 10.1590/0004-282X20160117).*

***Microglia*** are the resident immune cells of the central nervous system (CNS) and continuously screen their microenvironment with motile processes (70, 71). When they encounter a damaging hazard, microglia start to release a range of inflammatory cytokines and chemokines in order to maintain homeostasis (70, 71). In an initial phase of activation, the so-called 'M1 activated state', microglia will release pro-inflammatory factors (for example tumor necrosis factor alpha (TNFα), interleukin 1beta (IL-1β), chemokines, nitric oxide (NO), ROS, and interferon gamma (IFN-γ)) as an attempt to clear, or at least limit, the effects of the damaging hazard (70, 71). The 'M1 activated state' is followed by the 'M2 alternatively activated state', characterized by phagocytosis of cellular debris and by the release of anti-inflammatory factors (for example interleukin 4 (IL-4), interleukin 10 (IL-10), insulin growth factor 1 (IGF-1) to suppress inflammation and mediate repair and restoration (70, 71). Of note, this M1/M2 paradigm with distinct M1 and M2 phenotypes may be an oversimplification of the actual

situation (73), suggesting a continuum between these two phenotypes to be a more realistic representation of the actual situation (70, 74). The damaging hazard activating the microglia can be very diverse in nature, including neuronal injury, ischemic insults, infections, toxic metabolites, disease proteins and peptides, cytokines and autoimmunity (75).

In sALS and fALS patients, as well as in ALS mouse models, the presence of reactive microgliosis has been reported (71). This reactive microgliosis is characterized by a strong upregulation of several markers that are generally used to identify them, such as 'cluster of differentiation molecule 11b' (CD11b) and 'ionized calcium-binding adapter molecule 1' (IBA-1), by an increase in the number of reactive microglia present in the spinal cord ventral horn due to active proliferation of the resident local microglia, and by morphological changes, including a larger cell body and very short, thick and less branched processes (70, 71, 74, 76). In autopsy tissue of ALS patients, reactive microgliosis was observed in areas of significant motor neuron loss, including the motor cortex, the motor nuclei of the brainstem, the corticospinal tract, the ventral horn of the spinal cord, and even in areas of only mild degeneration (74). In addition, a positron emission tomography study in ALS patients revealed that microglial activation takes place throughout disease (77). The study of ALS mice confirmed that the activation of microglia starts well before motor symptom onset and gradually increased with disease progression (76). Based on their morphology, ALS microglia can be divided into four groups (76). Type S microglia, named after surveilling microglia, have a typical ramified morphology with a small cell body and are mainly observed in healthy situations and possibly very early in the asymptomatic phase of disease. Type R1 microglia, named after reactive microglia, have a small cell body with shorter and less branched processes and are observed only at the early stage of disease. Type R2 microglia resemble type R1 microglia, but their processes are further shortened and are only transiently present during the period of symptom onset and easily change into type 3 microglia. These type 3 microglia have the clear morphology of very reactive microglia with a large cell body and very short, thick and less branched processes. The number of type 3 microglia gradually increases throughout the symptomatic stage of disease and ultimately become the vast majority of the microglial

population in ALS mice. Besides the alterations in number and morphology, the function of reactive ALS microglia appears to change as well. In the initial pre-onset and onset phase of disease, microglia attempt to slow down disease progression and have the characteristics of neuroprotective M2 alternatively activated microglia that phagocytose cellular debris and release anti-inflammatory factors to suppress inflammation and mediate repair and restoration (74, 78). In contrast, at later disease stages, microglia gradually transform into neurotoxic over-activated M1 microglia, that produce and release more and more ROS and pro-inflammatory cytokines, thereby inducing motor neuron injury, aggravating and amplifying the initial damage to motor neurons and consequently accelerating disease (74, 78). When mediating this neuroinflammatory response, microglial cells function in close interaction with astrocytes and are able to mutually activate each other (71, 78, 79).

***Astrocytes***, another very important multi-functional cell type in the CNS, are involved in regulating neurotransmitter concentration at the synapses, as well as ion homeostasis, and provide metabolic support and neurotrophic factors to surrounding neurons in order to allow proper neuronal functioning and neurotransmission (71, 80). To achieve these important tasks, astrocytes closely interact with neurons at the level of the synapse by engulfing the neuronal synapses, which enables them to influence and respond to synaptic activity. One of the most important functions of astrocytes at the synapse is their role in the uptake of glutamate from the synaptic cleft between presynaptic and postsynaptic neurons (71, 80). Glutamate is the most abundant neurotransmitter in the CNS mediating the excitatory synaptic communication between neurons (81). The glutamate released from the presynaptic neuron activates the ionotropic glutamate receptors present on the postsynaptic neuron, namely the $Ca^{2+}$-permeable AMPA and N-methyl-D-aspartate (NMDA) receptors, thereby inducing the influx of $Na^{+}$ and $Ca^{2+}$ ions into the cell, which leads to depolarization and ultimately to the generation of an action potential (82). Astrocytes express the glutamate transporters GLAST and GLT1 (in humans, EAAT1 and EAAT2, respectively) that are powerful uptake systems for glutamate (71). The astrocytic uptake of glutamate is very important to avoid glutamate-mediated excitotoxicity (82). Following the

astrocytic glutamate uptake, astrocytes convert glutamate into glutamine, which is then shuttled back to the presynaptic neuron to generate new glutamate used for neurotransmission (83). Besides glutamate shuttling, astrocytes are also necessary for the release of neurotrophic factors, including glial-derived neurotrophic factor (GDNF), brain-derived neurotrophic factor (BDNF), and ciliary neurotrophic factor (CNTF), and for the supply of metabolic nutrients to the neurons upon increased metabolic demand (80). In order to do so, astrocytes receive their input to respond to the synaptic transmission through the neurotransmitter receptors expressed on their surface (84). Upon activation of these receptors, the intracellular astrocytic $Ca^{2+}$ levels increase, thereby instructing them to respond and communicate with other astrocytes over long distances through $Ca^{2+}$ shuttling via connexin gap junctions. This $Ca^{2+}$ flux triggers the release of vasoactive compounds at the end feet of astrocytes enveloping neighboring arterioles and capillaries thereby inducing vasodilatation or vasoconstriction (84). In this way, astrocytes can control the blood flow in the CNS and consequently also the supply of glucose and oxygen. At the astrocytic end feet, glucose transporters enable the uptake of energy substrates from the blood. Subsequently, the astrocytes convert glucose into lactate (glycolysis is driven by the astrocytic glutamate uptake) and they shuttle this metabolic energy substrate towards the neurons, where it is used as fuel for neuronal metabolism to meet their energy demands (71, 84). Additionally, astrocytes are also able to store energy for the neurons in the form of glycogen that can be converted into lactate and shuttled when necessary (84). Thus, astrocytes are able to respond to the increased metabolic substrate demand upon increased neuronal activity and are important for the health and survival of neurons.

In both sALS and fALS patients, as well as in ALS mouse models, reactive astrogliosis is widespread throughout the brain and the spinal cord (71, 85-88). The study of mutant *SOD1* mice revealed the presence of reactive astrocytes well before symptom onset and reactive astrogliosis becomes more prominent with disease progression (71, 83, 89). Characteristic for reactive ALS astrocytes is the strong upregulation of several markers, generally used to identify them, such as 'glial fibrillary acidic protein' (GFAP) and 'aldehyde dehydrogenase 1 family member L1' (ALDH1L1) (71, 90). Reactive astrocytes also

acquire a distinct reactive morphology with a hypertrophic cell body, and long and thick processes with increased content of GFAP (89). In contrast to reactive microgliosis, reactive astrocytes do not proliferate (71). Typical for reactive astrocytes in the disease context of ALS, is their decreased expression of the glutamate transporter GLT1 (or EAAT2 in humans) (28, 45). Consequently, glutamate accumulates at the synaptic cleft and induces the harmful condition of glutamate-mediated excitotoxicity that contributes to the degeneration of the motor neurons (80, 83). In addition, it was shown that mutant *SOD1* expressing astrocytes secrete factors that lower the expression of the GluR2 glutamate receptor subunit, which makes the AMPA receptors on motor neurons more $Ca^{2+}$ permeable and makes the motor neurons more prone to AMPA receptor-mediated excitotoxicity (91). As described above, astrocytes are important suppliers of energy for the motor neurons. Consequently, lower production of lactate by ALS astrocytes and defective lactate shuttling between astrocytes and motor neurons that were demonstrated (80), may affect the health of the motor neurons. Besides excitotoxicity and reduced lactate supply, reactive ALS astrocytes can actively contribute to motor neuron degeneration by several additional mechanisms. For example, reactive ALS astrocytes produce and release toxic pro-inflammatory cytokines, they have mitochondrial defects contributing to increased production of harmful ROS, they express more inducible nitric oxide synthase (iNOS) causing an increase of nitric oxide (NO) production, and their release of neurotrophic factors is insufficient to maintain neuronal health (80, 83, 89, 92, 93). Together, these mechanisms could be responsible for the deleterious effect of reactive ALS astrocytes on motor neurons.

## 3.10 Selective vulnerability of the motor neurons

The question why motor neurons are the neuronal subtype mainly affected in ALS, is still not answered. However, several possible explanations for this selective vulnerability were proposed, depending on motor neuron size and morphology, their unique functional properties, their energy metabolism and their gene/protein expression signatures (94).

Motor neurons are cells with very large somata, particularly long axons and complex dendritic trees (94). They have a large biosynthetic load and show high firing rates (95). This obviously requires a robust supply of high levels of energy metabolites, for which motor neurons completely rely on other neighboring cell types, such as oligodendrocytes and astrocytes that are in close contact with the motor neurons. As described above, pathological abnormalities in both oligodendrocytes and astrocytes in ALS pathogenesis are responsible for an impaired energy supply towards the motor neurons and can seriously affect the health of this specific neuronal subtype (61, 80).

In addition, motor neurons are more sensitive to glutamate-mediated excitotoxicity than other types of neurons, since they have lower intrinsic $Ca^{2+}$ buffering capacity and their AMPA receptors have less GluR2 subunits compared to other types of neurons, resulting in the presence of $Ca^{2+}$-permeable AMPA receptors on motor neurons. Consequently, motor neurons suffer from the detrimental effects of high intracellular $Ca^{2+}$ levels (94, 95).

Together these proposed motor neuron characteristics may explain their selective vulnerability. Of note, even within the pool of motor neurons there are different subpopulations experiencing differential vulnerability to degeneration. The motor neurons controlling the eye movements and the motor neurons in the Onuf's nucleus in the sacral spinal cord controlling the pelvic floor muscles tend to be less vulnerable and persist throughout disease (94, 96). Also among spinal motor neurons a spectrum of vulnerability is reported, with motor neurons innervating fast-twitch muscles being more severely affected at the early phase of disease, while motor neurons innervating slow-twitch muscles only degenerate later in disease (94). Distinct gene and protein expression signatures are a potential determinant of this selective motor neuron vulnerability (94). For example, the expression of matrix metalloproteinase-9 (MMP-9) was only observed in a subset of motor neurons and is considered a marker for vulnerable motor neurons (97). Also, for Calreticulin and SIL1 a subtype specific expression pattern was observed: resistant motor neurons express high levels, while the expression in vulnerable

motor neurons is progressive decreasing throughout disease. Reduced expression of these proteins is believed to induce ER-stress and consequently cell death (94).

Together, this shows that the pathogenic mechanism of ALS is very complex, with both cell-intrinsic and non-cell autonomous mechanisms that have to be taken into account. More research is needed to better understand the full picture of this disease.

# 4. Notch signaling

## 4.1 The Notch signaling pathway

The Notch signaling pathway is a critical mediator of cell-cell interactions that plays a key role in a wide range of tissues, including the CNS, both during development and in adulthood (98, 99). In general, Notch signaling controls cell fate, proliferation, differentiation, survival, and apoptosis.

The Notch pathway converts an extracellular signal received from a ligand-carrying neighboring cell into gene expression changes in the nucleus of the Notch receptor-carrying cell, a process called *trans*-activation (Figure 5). In mammals, four transmembrane Notch receptors (NOTCH-1, -2, -3, -4) and five transmembrane canonical ligands (JAGGED-1, -2, DELTA-LIKE-1, -3, -4) have been identified. Upon ligand binding, the Notch receptor is cleaved by α- and γ-secretases, resulting in the release of the Notch intracellular domain (NICD), which serves as the active signaling fragment. Subsequently, NICD translocates to the nucleus, where it forms a transcription-activation complex with the co-factors 'recombination signal binding protein for immunoglobulin kappa J region' (RBPjk) and 'mastermind-like proteins' (MAML-1, -2, - 3) and initiates the transcription of target genes, such as the *HES* (*HES-1, -5, -7*) and the *HEY* genes (*HEY-1, -2, -L*), that function as transcriptional repressors (100-102).

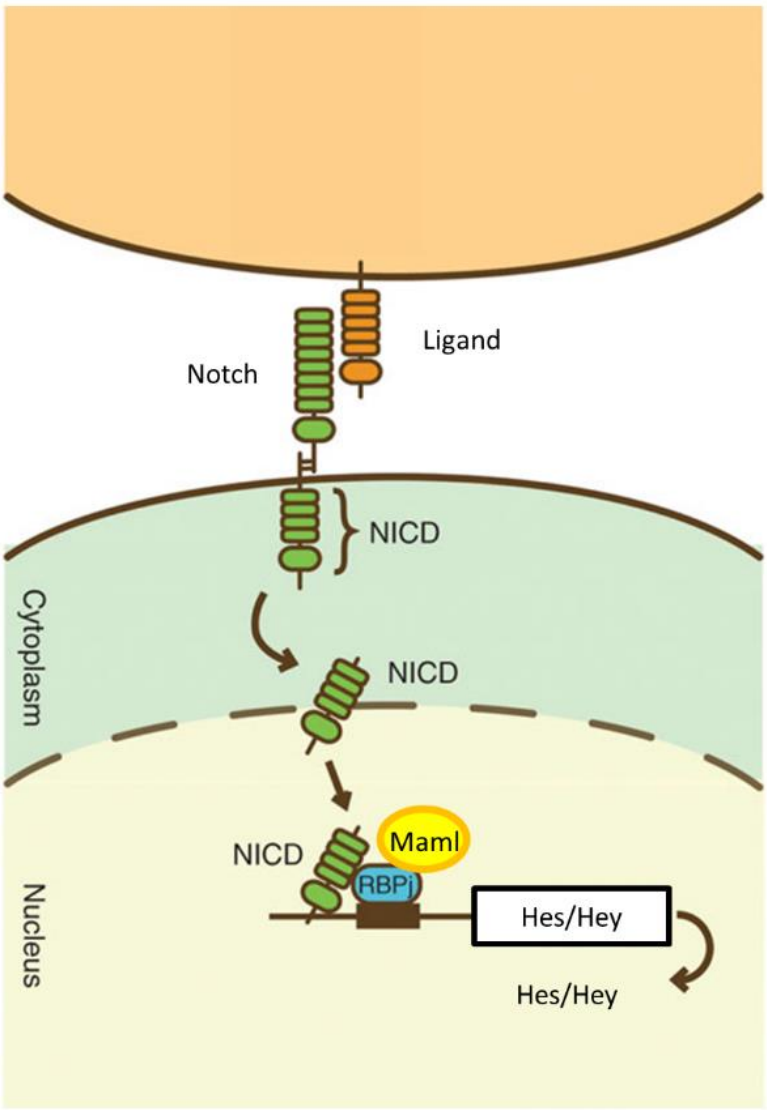


***Figure 5: The canonical Notch signaling pathway.*** *Notch signaling is activated upon binding of a canonical ligand expressed on the cell surface of one cell to the Notch receptor expressed on a neighboring cell. Upon activation, the Notch intracellular domain (NICD) is released from the transmembrane region and transferred to the nucleus, where it forms a transcription activation complex with RPBjk and Mastermind-like (Maml), and induces the expression of the Hes and Hey genes. Adapted from (103) and reprinted with permission of Springer Nature and Copyright Clearance Center with copyright license number 4386071234931 (doi: 10.1038/nn.2208).*

However, when a cell carries both the Notch receptor and the ligand, then this ligand impedes the activation of the receptor, a process called *cis*-inhibition (104).

Interestingly, besides the above described canonical Notch signaling pathway (shown in Figure 5), also a non-canonical Notch signaling pathway exists (105, 106). This type of signaling is RBPjk-independent

and can either be initiated by non-canonical ligands, such as F3/Contactin-1 and NB3/Contactin-6, or can be ligand-independent (105, 106).

Tight regulation of Notch signaling is necessary for its proper function (100, 106, 107). Glycosylation of both the Notch receptors and the ligands regulates the strength of the receptor-ligand interactions (106, 107). Ubiquitination regulates the level of receptors and ligands available on the cell surface, as the addition of ubiquitin serves as a signal for endocytosis and consequently degradation (106, 107). In addition, NICD has a short half-life to ensure optimal signaling strength and avoid deleterious sustained NICD accumulation, as most Notch-mediated processes require a transient signaling pulse (100). This is achieved by phosphorylation of NICD in a domain rich of proline (P), glutamic acid (E), serine (S) and threonine (T), the so-called PEST domain, followed by ubiquitination and proteasomal degradation (100).

## 4.2 Notch signaling and the central nervous system

The Notch signaling pathway has been extensively studied as a developmental pathway regulating cell-cell communication and controlling cell-fate specification by inhibiting cell differentiation and promoting proliferation (98, 101). The knowledge about the role of this Notch pathway in the post-natal and adult CNS is less abundant (108, 109).

***During development*** of the CNS, the Notch pathway is of major importance for different cell types. For instance, the Notch pathway functions as a key regulator of the pool of neuronal stem cell (NSC), as it strictly regulates proliferation, survival, self-renewal and differentiation of these cells to balance between maintenance of the NSC pool and the generation of enough neurons and glial cells for proper development of the CNS (110-112). Activation of the Notch pathway inhibits neurogenesis and neuronal maturation, and promotes astrogliogenesis (112). Besides its role in NSCs, neurogenesis and

astrogenesis, Notch signaling is also involved in oligodendrogenesis: activation of the Notch pathway promotes the generation and proliferation of oligodendrocyte precursor cells, but it inhibits their differentiation and maturation into oligodendrocytes (112).

The study of Notch signaling in ***post-natal and adult*** organisms was hampered for a long time because loss of Notch signaling causes severe embryonic phenotypes and early lethality (112-116). The availability of inducible Cre-loxP targeting technology makes it possible to choose the timing and tissue type in which Notch signaling is modulated and allows to investigate the role of Notch signaling in adulthood and in adult-onset disease models (108, 117). In the post-natal and adult CNS, Notch signaling remains important for both progenitor cells and mature cell types, but depending on the time point studied different (sometimes contradictory) results were obtained, which makes it difficult to understand the exact role of Notch signaling in adulthood (108). However, a concise overview of the current knowledge about the role of Notch signaling in the post-natal and adult CNS is given below and more information about the involvement of Notch signaling in CNS pathology conditions and neurodegeneration is provided in the next section entitled '*Notch signaling and its involvement in CNS pathology and neurodegeneration*'.

For instance, Notch signaling plays a key role in the neural stem cell pools that are maintained during adulthood, including the ependymal cells that line the central canal of the spinal cord, the neural stem cells (NSCs) in the subventricular zone of the lateral ventricle and the neural stem cells in the dentate gyrus of the hippocampus (109, 118-121). Notch signaling is considered a key mediator of NSCs maintenance by inhibiting the expression of pro-neuronal genes to avoid neuronal differentiation and by supporting progenitor cell survival (109). For the maintenance of the adult NSC pools, it is important to have a healthy balance between proliferation and quiescence. This balance is also regulated by the Notch signaling pathway: low Notch levels allow proliferation, while high Notch levels induce a quiescent state and lead to growth arrest (109). In addition to NSC maintenance in adulthood, Notch signaling is also involved in the process of generating new neurons in adulthood (109, 118), since it was

observed that reduced Notch signaling activation can result into depletion of the NSC pools due to the generation of new mature neurons (109, 118).

Besides NSC pool maintenance and neurogenesis, Notch signaling is also important for mature post-mitotic neurons where Notch is implicated in neurite remodeling and the regulation of synaptic plasticity (108, 110): Notch signaling activation promotes neurite retraction, inhibits neurite outgrowth, promotes dendritic branching and can reduce the density of the dendritic spines (Figure 6). However, contradictory results were obtained about Notch signaling and its role in long-term potentiation (LTP) and long-term depression (LTD) and consequently its involvement in learning and long-term memory (108). Of additional importance is the crucial role of Notch signaling for neuronal survival, as Notch activation predisposes neurons to apoptosis (108).

The Notch signaling pathway also plays an important role in the health of glial cells (Figure 6), including astrocytes, microglia, oligodendrocyte precursor cells, and oligodendrocytes (108). In brief, Notch signaling is involved in promoting the activation of astrocytes and microglia, and similar to development, Notch induces proliferation of oligodendrocyte precursor cells and inhibits their differentiation into mature functional oligodendrocytes. As these phenomena take place in a context of neurodegeneration and disease, the involvement of Notch signaling in astrocytic and microglial activation, OPC proliferation and oligodendrocyte differentiation will be discussed in more detail in the next section entitled '*Notch signaling and its involvement in CNS pathology and neurodegeneration*'.

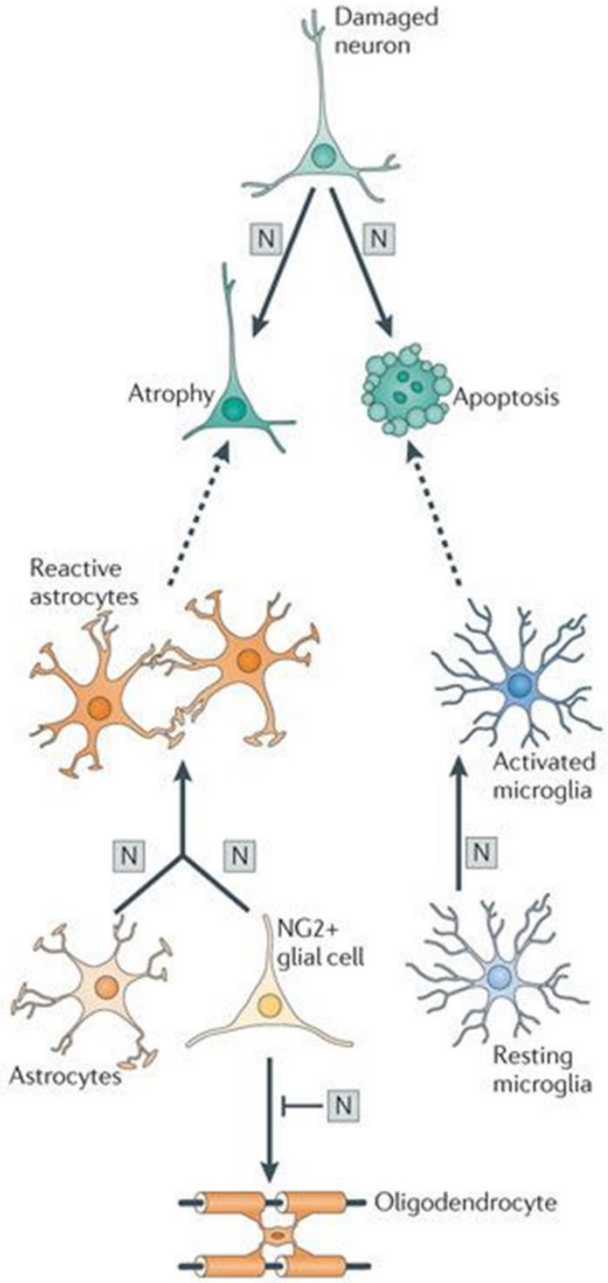


***Figure 6: Pleiotropic roles for Notch signaling in the adult CNS following injury or degeneration.*** *Upon injury or degeneration of the CNS, the developmental programs of Notch are reactivated to control a diverse set of responses to the insult, including promoting neuronal atrophy and death, increasing microglial activation, and potentially regulating reactive gliosis by initiating proliferation and astrogliogenesis from resident progenitors. However, the response is counter-productive and Notch activation limits the ability of oligodendrocytes to differentiate and remyelinate damaged neurons. Adapted from (108) and reprinted with permission of Springer Nature and Copyright Clearance Center with copyright license number 4424880370073 (doi: 10.1038/nrn.3024).*

## 4.3 Notch signaling and its involvement in CNS pathology and neurodegeneration

The importance of Notch signaling for normal human adult CNS function was demonstrated by the involvement of several mutations in genes of the Notch signaling pathway in diverse CNS pathologies (109, 121). For example, *JAGGED-1* and *NOTCH-2* mutations are implicated in the developmental complex multisystem disorder ***Alagille***, that (among many other symptoms) is associated with mental retardation, mutations in *NOTCH-3* are linked to a hereditary adult-onset disease causing ischemic stroke and dementia, called ***CADASIL*** (Cerebral Autosomal Dominant Arteriopathy with Subcortical Infarcts and Leukoencephalopathy), and a *NOTCH-4* polymorphism was found to be associated with susceptibility to ***schizophrenia*** (109, 122-124).

The Notch signaling pathway has also been linked to several neurodegenerative diseases (109, 121), including Alzheimer's disease (125, 126), multiple sclerosis (127-129), spinal muscular atrophy (130), prion disease (131) and ischemic stroke (132).

Several observations point to the possible involvement of Notch signaling in ***Alzheimer's disease (AD)*** (125, 126). For instance, a two-fold increase in the expression of Notch-1 was observed in *post-mortem* brains from AD patients when compared to brains from age-matched control individuals (126), however this does not necessarily mean that the pathway is more active. Second, the γ–secretase enzyme that is responsible for the cleavage of the amyloid precursor protein (APP) and consequently the generation of the toxic Aβ, is also needed to cleave the Notch receptors and consequently release the activated NICD (125). Mutations in the presenilins PS1 and PS2, which are catalytic components of γ–secretase, are linked to AD and alter the proteolytic activity of γ–secretase, and consequently may also affect Notch signaling activation (125). Although controversial, the possible involvement of Notch signaling in memory formation, which is impaired in AD patients, may suggest the potential involvement of the Notch signaling pathway in the pathogenesis of AD (108, 125). Of additional interest

is the knowledge that overexpression of NICD-1 can activate Caspase-3 in neurons and consequently results in neuronal death, a process that can potentially be involved in the neurodegeneration seen in AD as well (125). However, more studies are needed to further explore the exact role of Notch signaling in this disease.

Extensive evidence shows that the Notch signaling pathway is also implicated in the pathogenesis of ***multiple sclerosis (MS)***, a neuroinflammatory disease characterized by demyelination that results in axonal degeneration (127-129). In an attempt to repair the lesions, a process of remyelinisation takes place, however, with a limited success rate (127-129). In the demyelinated lesions, the ligand Jagged-1 was found to be expressed at high levels by hypertrophic astrocytes, and the Notch-1 receptor and the downstream target Hes-5 were observed in oligodendrocyte precursor cells and immature oligodendrocytes (127-129). In contrast, in the remyelinated MS lesions Jagged-1 was found to be absent (127). These observations, both in MS patients and rodent models, indicate that the Jagged-1 mediated Notch signaling pathway plays a role within the MS lesions and suggest that Jagged-1 mediated Notch signaling may be responsible for the failure of remyelination in MS, since it is known that the canonical Notch pathway can block oligodendrocyte differentiation and maturation (127-129, 133). In contrast, when the non-canonical Notch signaling pathway is activated by the F3/Contactin-1 ligand, it can promote oligodendrocyte differentiation and maturation (129, 134). The expression of F3/Contactin-1 was observed on demyelinated axons in brain samples from MS patients (135). These findings suggest that the balance between the Jagged-1-mediated canonical and the F3/Contactin-1-mediated non-canonical signaling determines the success or (partial) failure of remyelination of the MS lesions. Of additional interest is the observation that inhibition of Notch signaling by the use of gamma-secretase inhibitors can delay disease onset, reduce clinical symptoms, reduce axonal damage and promote remyelination in experimental mouse models of MS, when compared to vehicle treated MS mice (128, 136). Together, these findings support the involvement of the Notch signaling pathway in the pathogenesis of MS.

The Notch signaling pathway was also linked to ***spinal muscular atrophy (SMA)***, a neuromuscular disorder characterized by the loss of motor neurons and progressive muscle atrophy (130). In the SMNΔ7 mouse model of SMA, more reactive astrocytes were found positive for the ligands Jagged-1 and Delta-1 and increased NICD-1 levels were reported in the nuclei of motor neurons (130).

The involvement of Notch signaling in ***prion diseases*** was suggested by the observation of higher levels of NICD-1 in the brains of prion-infected mice, when compared to uninfected control mice and by a strong correlation between prion protein accumulation, NICD-1 levels and dendritic atrophy (131). In addition, scrapie-infected neuroblastoma cells show increased levels of NICD-1 compared to control cells and the NICD-1 levels correlate with prion protein accumulation and defective neurite growth as well (131). Inhibition of Notch-1 activation by Notch-1 siRNAs was able to reduce the neurite phenotype in the scrapie-infected neuroblastoma cells (131), but no *in vivo* data are currently available.

In ***ischemic stroke***, it was observed that higher NICD-1 levels were present after stroke in mice when compared to sham control mice, which reflects increased activation of the Notch signaling pathway after stroke (132). The aberrantly upregulated Notch signaling activation was demonstrated to be responsible for worsening the brain damage and the functional outcome after stroke, since inhibition of the Notch pathway results in a reduction of the infarct area and an improvement of the neurological deficits (132). Lowering the Notch signaling activation was found to exert neuroprotective effects (132, 137, 138) and it could lead to the presence of fewer neurotoxic reactive microglia and astrocytes, and to reduced infiltration of pro-inflammatory leukocytes (132, 139, 140). These data suggest that the Notch signaling pathway plays an important role in the increased vulnerability of neurons to apoptosis, in the activation and the neurotoxic activity of microglia and astrocytes, and in the infiltration of leukocytes after stroke.

In ***ALS***, the knowledge about the involvement of the Notch signaling pathway is rather limited and the results from animal models are contradictory. In *Drosophila*, one study showed that loss-of-function mutations of Notch or of downstream target genes extended the lifespan of TDP-43 transgenic flies

(141), whereas another study showed that increased Notch expression suppressed the toxicity induced by the GR dipeptide repeats associated with C9ORF72 expansions (142). In ALS mouse models, almost no functional Notch studies have been performed. Only increased expression of Notch-3 and the downstream target gene *Hes-1* has been reported in the gastrocnemius muscle of the mutant *SOD1* mouse (143). Despite the lack of functional studies about Notch signaling in ALS, we hypothesize that this pathway may be involved in the pathogenesis of ALS. This is because, as described above, the Notch pathway is implicated in several processes that are relevant to the pathogenesis of ALS. For example, the Notch signaling pathway plays an important role in axonal outgrowth and retraction (144-149), neuromuscular junction maturation (150), microgliosis (128, 132, 139, 151-156), astrocytosis (140, 157-160), proliferation and differentiation of oligodendrocyte precursor cells into mature oligodendrocytes (133, 161-169), and even cell death (137, 170, 171), which are all processes that are relevant to the pathogenesis of ALS.

# AIMS OF THE STUDY

Based on the knowledge that the Notch signaling pathway is involved in processes that are relevant to the pathogenesis of ALS, such as axonal outgrowth and retraction (144-149), neuromuscular junction maturation (150), microgliosis (128, 132, 139, 151-156), astrocytosis (140, 157-160), proliferation and differentiation of oligodendrocyte precursor cells into mature oligodendrocytes (133, 161-169), and cell death (137, 170, 171), ***we hypothesized that the Notch signaling pathway could be involved in the pathogenesis of ALS***. Moreover, the Notch signaling pathway is described to be involved in other neurodegenerative diseases as well, including Alzheimer's disease (125, 126), multiple sclerosis (127-129, 133-136), spinal muscular atrophy (130) and ischemic stroke (132, 137-140).

To evaluate this hypothesis, we focused on the following major aims:

## AIM 1: To characterize the Notch signaling pathway in ALS

In this first part, we characterized the different components of the Notch signaling pathway, including the different Notch receptors, ligands, co-factors and downstream targets, in the affected lumbar spinal cord of the *SOD1*$^{G93A}$ mice, and in the affected lumbar spinal cord of sALS patients. In this regard, we addressed the following questions: (i) Is the expression of the different components of the Notch signaling pathway altered in ALS and does the expression change with disease progression; (ii) What is the activation status of the Notch signaling pathway; (iii) Which cell types are involved in mediating Notch signaling in ALS.

## AIM 2: To explore whether interfering with the Notch pathway affects the course of disease in an ALS mouse model

After characterizing the Notch signaling pathway in ALS mice and sALS patients, we evaluated whether interfering with the Notch signaling pathway can influence the course of disease in the *SOD1*$^{G93A}$ mice. By using inducible Cre-LoxP targeting technology, we wanted to evaluate the effects of ligand- and receptor-based modulation approaches.

The overall goal of this study was to evaluate the involvement of the Notch signaling pathway in the pathogenesis of ALS and to explore the functional and therapeutic implications of Notch signaling activation in this disease context.

# MATERIALS & METHODS

*Mice*

Mice overexpressing human mutant SOD1 (*SOD1$^{G93A}$*, B6.Cg-Tg(SOD1*G93A)1Gur/J, JAX stock number 004435) and human wild-type SOD1 (*SOD1$^{WT}$*, B6.Cg-Tg(SOD1)2Gur/J, JAX stock number 002298), control non-transgenic mice (C57BL/6J, JAX stock number 000664), *Jagged-1$^{lox/lox}$* mice (B6;129S-*Jag1$^{tm2Grid}$*/J, JAX stock number 010618), *Notch-1$^{lox/lox}$* mice (B6.129X1-*Notch1$^{tm2Rko}$*/GridJ, JAX stock number 007181), *Rosa-$^{lox}$STOP$^{lox}$-YFP* mice (B6.129X1-*Gt(ROSA)26Sor$^{tm1(EYFP)Cos}$*/J, JAX stock number 006148) and *CAGG-CreER* mice (B6.Cg-Tg(CAG-cre/Esr1*)5Amc/J, JAX stock number 004682) were obtained from The Jackson Laboratory (Bar Harbor, Maine, USA). *Cx30-CreER* mice (172, 173) were kindly provided by Frank W. Pfrieger (INCI, Strasbourg, France). Cre-mediated recombination was induced at the age of 60 days by administering tamoxifen (200 mg/kg/day in sunflower seed oil with 10 % ethanol; Sigma-Aldrich, Saint-Louis, MO, USA) by oral gavage for four consecutive days, as described before (63). Maintenance of mice used in this study and all experiments were carried out in strict accordance with protocols approved by the Ethical Committee of the University of Leuven, Belgium (P149/2011 and P281/2015).

*Human samples*

The expression data set of the whole-genome exon splicing array provided by the group of John Ravits (University of California, La Jolla, San Diego, CA, USA) on motor neurons and the remaining anterior horn (174) is publicly available (www.ncbi.nlm.nih.gov/geo, accession number GSE18920). Motor neurons were isolated by Laser Capture Microdissection (LCM) from lumbar spinal cords of 12 sporadic ALS patients (sALS) and 10 control individuals. The GeneChip raw data CEL-files were reanalyzed using

the Affymetrix Expression Console to obtain summarized expression values for transcripts presented as normalized probe intensity units.

Human formalin-fixed paraffin-embedded lumbar spinal cord samples used for histology were kindly provided by John Ravits (University of California, La Jolla, San Diego, CA, USA). All human lumbar spinal cord samples from 6 patients diagnosed with ALS using revised El Escorial criteria (4 males, ages 41-74 years, disease duration of 1.5-4.75 years; 2 females, ages 58-74 years, disease duration of 3-5.75 years) and from 6 control individuals with no pathological evidence of neurological disease (5 males, ages 38-82 years; 1 females, age 63 years) were collected at the University of California San Diego using informed consent and protocols approved by the Human Research Protection Program of the University of California San Diego. *Postmortem* time intervals ranged from 3 to 8.5 h (mean = 5.3 h).

*Quantitative real-time polymerase chain reaction*

Mice were sacrificed using an overdose of Nembutal (10 mg/kg; Ceva chemicals, Hornsby, NSW, Australia). Lumbar spinal cords were collected, flash-frozen in liquid nitrogen and maintained at −80 °C until further use.

Total RNA was isolated from mouse lumbar spinal cords using the Tripure isolation reagent (Roche, Mannheim, Germany) according to the manufacturer's instructions. Total RNA concentration was measured with the ND-1000 Spectrophotometer (NanoDrop, Wilmington, DE, USA). For cDNA synthesis 1 µg of total RNA was reverse transcribed using the SuperScript® III First-Strand Synthesis System kit (Invitrogen, Carlsbad, CA, USA) with oligo-dT and random hexamer primers.

Subsequently, quantitative PCR (qPCR) was performed in a volume of 10 µl using Taqman Fast Universal PCR Master Mix 2X (Applied Biosystems, Carlsbad, CA, USA), TaqMan gene expression assays 20X (Applied Biosystems, Carlsbad, CA, USA) and 4 µl of a 1/15 dilution of cDNA template. Following

TaqMan gene expression 20X assays with FAM dye (Thermo Fisher Scientific, Waltham, MA, USA) were used: *Notch-1* (Mm00627185_m1), *Notch-2* (Mm00803077_m1), *Notch-3* (Mm01345646_m1), *Notch-4* (Mm00440525_m1), *Jagged-1* (Mm00496902_m1, for standard gene expression analysis), *Jagged-1* (Mm00496904_m1, for recombination efficiency analysis), *Jagged-2* (Mm01325629_m1), *Dll-1* (Mm01279269_m1), *Dll-3* (Mm00432854_m1), *Dll-4* (Mm00444619_m1), *F3/Contactin-1* (Mm00514374_m1), *NB3/Contactin-6* (Mm00516899_m1), *Rbpjk* (Mm00770450_m1), *Maml-1* (Mm00614627_m1), *Maml-2* (Mm00620617_m1), *Maml-3* (Mm01294189_m1), *Hes-1* (Mm01342805_m1), *Hes-5* (Mm00439311_g1), *Hes-7* (Mm00473576_m1), *Hey-1* (Mm00468865_m1), *Hey-2* (Mm00469280_m1), *Hey-L* (Mm00516555_m1), *Hprt* (Mm00446968_m1), *Gapdh* (Mm99999915_g1) and *Polr2a* (Mm00839502_m1).

Thermal cycling was performed on a ViiA™ 7 Real-Time PCR System (Applied Biosystems, Carlsbad, CA, USA). All samples were run in triplicate and only samples with at least two replicates within the range of 0.5 quantification cycle values (Cq) were included. Reference genes used for normalization were determined by geNorm analysis. The optimal number of reference genes in our experimental situation was two (geNorm V < 0.15). Biogazelle qBase+ 2.6 Software was used for raw data analysis, quality control and quantification of the calibrated normalized relative gene expression. Scaling was done to the average of the control group.

*Western blot*

Mice were sacrificed using an overdose of Nembutal (10 mg/kg; Ceva chemicals, Hornsby, NSW, Australia) and lumbar spinal cords were dissected. Samples were collected in lysis matrix D tubes (MP Biomedicals, Santa Ana, CA, USA), flash-frozen in liquid nitrogen and maintained at −80 °C until further use.

Tissues were homogenized in RIPA buffer (50mM Tris-HCl, 150mM NaCl, 1 vol % NP-40, 0.5%Na-deoxycholate and 0.1 % SDS) supplemented with Complete™ protease inhibitor cocktail (Roche, Mannheim, Germany) using a rapidly oscillating MagNa Lyser instrument (Roche, Mannheim, Germany), incubated on ice for 1 h and subsequently centrifuged at 4°C for 20 min at a speed of 20000g. Supernatans was collected and protein concentrations were determined using the Micro BCA protein assay kit (Thermo Scientific, Waltham, MA, USA) according to the manufacturer's instructions.

Forty micrograms of total protein lysate together with Pierce™ lane marker reducing sample buffer 5X (Thermo Fisher Scientific, Waltham, MA, USA) were boiled for 5 min at 95°C and subsequently loaded on a 7.5% (for large proteins) or 12% (for small proteins) fresh Sodium Dodecyl Sulphate polyacrylamide (SDS-PAGE) gel. Electrophoresis was performed using a Mini- PROTEAN® Tetra Vertical Electrophoresis Cell (Bio-Rad, Hercules, CA, USA) at 90 V for 1 h. Samples were transferred on Immobilon-P polyvinyldifluoride (PVDF) transfer membrane with 0.45 µm pore size (Millipore, Bedford, MA, USA) using a semi-dry blotting apparatus (TE70XP, Hoefer, San Francisco, CA, USA) with 20% methanol containing blotting buffer for 1 h 45 min at 180 mA. The membranes were blocked with 5% skimmed milk (Bio-Rad, Hercules, CA, USA) in Tris Buffered Saline with 0.1% Tween-20 (TBST) for 1 h at room temperature (RT). Following primary antibodies diluted in Tris Buffered Saline with 0.1% Tween-20 (TBST) were used: rabbit anti-NOTCH-1 (Cell Signaling Technology, D1E11, RRID: AB_2153354, 1:1000 in TBST with 5% BSA, overnight at 4°C), rabbit anti-NOTCH-2 (Cell Signaling Technology, D76A6, RRID: AB_10693319, 1:1000 in TBST with 5% BSA, 2 h at room temperature (RT)), rabbit anti-JAGGED-1 (Cell Signaling Technology, 28H8, RRID: AB_10693295, 1:1000 in TBST with 5% BSA, overnight at 4°C), rabbit anti-RBPjk (Cell Signaling Technology, D10A4, RRID: AB_2665555, 1:1000 in TBST, 1 h at RT), rabbit anti-Cleaved NOTCH-1 (Val1744) (Cell Signaling Technology, D3B8, RRID: AB_2153348, 1:1000 in TBST with 5% BSA, overnight at 4°C), mouse anti-GAPDH (Ambion, AM4300, RRID: AB_437392, 1:5000 in TBST, 1 h at RT) and mouse anti-alpha TUBULIN (Sigma-Aldrich, T6199, RRID: AB_477583, 1:5000 in TBST, 1 h at RT). Membranes were washed three times 5 min in TBST and subsequently incubated with the corresponding HRP-conjugated secondary antibodies (Dako,

Glostrup, Denmark, 1:5000 in TBST, 1 h at RT). After washing, protein bands were visualized using enhanced chemiluminescent substrate (ECL): SuperSignal™ West Femto Maximum Sensitivity ECL Substrate (for NOTCH-1, NOTCH-2, JAGGED-1, RBPjk and Cleaved NOTCH-1 (NICD-1); Thermo Fisher Scientific, Waltham, MA, USA) or Pierce™ ECL Western Blotting Substrate (for GAPDH and alpha-TUBULIN; Thermo Fisher Scientific, Waltham, MA, USA). Membranes were scanned using a LAS4000 Biomolecular imager (GE Healthcare, Little Chalfont, UK). Western blots were analyzed and quantified using ImageQuant TL software (GE Healthcare, Little Chalfont, UK). Protein levels were normalized to GAPDH and alpha-TUBULIN.

*Immunofluorescence and immunohistochemistry*

Mice were sacrificed using an overdose of Nembutal (10 mg/kg; Ceva Chemicals, Hornsby, NSW, Australia) and transcardially perfused with ice-cold PBS 1X (Sigma-Aldrich) followed by 4% paraformaldehyde (PFA, Sigma-Aldrich). After dissection of the lumbar spinal cords, the samples were post-fixed in 4% PFA for 2 h on ice, dehydrated by overnight incubation in a 30% sucrose solution at 4°C, embedded in Optimal Cutting Temperature (O.C.T.) compound mounting medium for cryotomy (VWR, Radnor, PA, USA) and stored at -80°C until further processing. Twenty micrometer-thick cryosections were cut from O.C.T. embedded mouse lumbar spinal cords on a Thermo Scientific cryostat (Thermo Scientific, Waltham, MA, USA) and collected on SuperFrost® Plus adhesion slides (VWR, Radnor, PA, USA). Sections were washed in PBS containing 0.1% Triton X-100 (PBST) and blocked with 10% normal donkey serum (Sigma-Aldrich) in PBST for 1 h at RT. Sections were then incubated with the following primary antibodies in PBST with 10% normal donkey serum: goat anti-JAGGED-1 (Santa Cruz Biotechnology, C-20 sc-6011, RRID: AB_649689, 1:50, overnight at 4°C), mouse anti-NeuN (Millipore, MAB377, RRID: AB_2298772, 1:200, 1 h at RT), mouse anti-GFAP (Sigma-Aldrich, G3893, RRID: AB_477010, 1:200, 1 h at RT), rabbit anti-IBA-1 (Wako Chemicals, 019-19741, RRID: AB_839504, 1:200, 1 h at RT), rat anti-F4/80 clone CI:A3-1 (BioRad, MCA497, RRID: AB_2098196, 1:500, overnight

at 4°C) and mouse anti-CC1 (Abcam, ab16794, RRID: AB_443473, 1:100, 2 h at RT). After three washes with PBST, sections were incubated with donkey Alexa-555 or Alexa-488 conjugated secondary antibodies (Invitrogen, 1:500, 1 h at RT). Sections were mounted using ProLong® Gold Antifade Mountant with DAPI (Thermo Fisher Scientific, Molecular probes, Waltham, MA, USA).

For the Jagged-1 staining, the standard staining protocol was preceded by a pre-treatment with 0.5 % SDS (Sigma-Aldrich) in PBS for maximally 5 min followed by washing with PBST, blocking with 10% normal donkey serum and incubation with goat anti-JAGGED-1 (Santa Cruz Biotechnology, C-20 sc-6011, RRID: AB_649689, 1:50, overnight at 4°C) and the corresponding secondary antibody, as described above. The specificity of the goat anti-JAGGED-1 (Santa Cruz Biotechnology, C-20, 1:50) was evaluated by overnight pre-incubation with 6 µg of following JAGGED-1 neutralizing peptides: sc-6011 P blocking peptide (Santa Cruz Biotechnology, Dallas, Texas, USA) or Jagged-1 recombinant protein antigen NBP1-90208PEP (Novus Biologicals, Abingdon, England), respectively.

For the NICD-1 staining, sections were permeabilized with PBST and immersed in Sodium-Citrate buffer (10mM Sodium Citrate, pH6, 0.01% Tween20) for 30 min at 96°C followed by 20 min cooldown at 4°C for antigen retrieval. Endogenous peroxidases were inactivated with 3% $H_2O_2$ in methanol (30 min, at RT). After blocking for 1 h with 3% BSA in TBS (150mM Tris pH7.5, 150mM NaCl), sections were incubated with rabbit anti-NICD-1 (Val1744) (Cell Signaling Technology, D3B8, RRID: AB_2153348, 1:100 in TBS with 0.1% Tween20 and 3% BSA, overnight at 4°C). After incubation with biotinylated donkey anti-rabbit secondary antibody (Jackson ImmunoResearch 711-065-152, West Grove, PA, USA) for 1 h at RT, the signal intensity was amplified using the TSA biotin signal amplification detection kit (NEL700A001KT, Perkin Elmer, Waltham, MA, USA) according to the manufacturer's recommendations and visualized with streptavidin-Alexa-488 (Jackson ImmunoResearch 016-540-084, West Grove, PA, USA). Sections were mounted with MOWIOL (Sigma-Aldrich) supplemented with DAPI.

Thionin staining was used to visualize (motor) neurons, as described before (175). In summary, sections were fixed for 1 minute in 100% ethanol, washed twice for 15 s in $dH_2O$ and stained for 45 s in 2X

Thionin. After washing again twice for 15 s in $dH_2O$, sections were dehydrated in 70%, 90% and 100% ethanol (30 s each), cleared for 1 minute with Histoclear solution and mounted with Pertex mounting medium (Histolab, Västra Frölunda, Sweden). The area of the neuronal cell bodies and the ventral horn was measured and the number of motor neurons was normalized to the area of the ventral horn.

For the human JAGGED-1 staining on formalin-fixed paraffin embedded lumbar spinal cord samples from sALS patients and from control persons, sections (6 µm) were deparaffinized and rehydrated by subsequent immersion in xylene (2 times, 10 min; VWR, Radnor, PA, USA), 100% ethanol (2 times, 1 minute), 95% ethanol (1 minute), 70% ethanol (2 min), 50% ethanol (1 minute) and $H_2O$ (5 min). Antigen retrieval was performed with sodium-citrate buffer (10mM sodium citrate, pH6, 0.01% Tween20) supplemented with 0.1% SDS (Sigma-Aldrich) for 40 min at 96°C followed by 20 min cooldown at 4°C. Endogenous peroxidases were inactivated by 30 min incubation in 3% $H_2O_2$ in PBS supplemented with 50% methanol. Blocking with 10% NDS in PBST for 1 h at RT was followed by incubation with goat anti-JAGGED-1 (Santa Cruz Biotechnology, C-20 sc-6011, RRID: AB_649689, 1:50 in PBST with 10% NDS, overnight at 4°C) and with biotinylated donkey anti-goat secondary antibody (Jackson ImmunoResearch 705-067-003, 1:300 in PBST, 1 h at RT). Subsequently, sections were incubated with streptavidin-HRP (Perkin Elmer TSA kit, NEL700A001KT, 1:100 in PBST, 30 min) according to the manufacturer's instruction. After incubation with Tris-HCl (50 mM Tris, pH 7.5; 2 times, 5 min), staining was revealed using 3,3'-diaminobenzidine (DAB, SK-4100, Vector Laboratories, Burlingame, CA) as a substrate. Sections were counterstained with Harris's hematoxylin (VWR, Radnor, PA, USA; 159 380 025), dehydrated and mounted.

For the human NICD-1 staining, the sections were deparaffinized and rehydrated as described above. The NICD-1 staining procedure was performed as described for the NICD-1 staining on mouse cryosections with the following differences to the protocol: antigen retrieval was performed with TE buffer (10 mM Trizma base, 1 mM EDTA, pH9, 0.005% Tween20) and the tyramide amplification was followed by incubation with streptavidin-HRP (Perkin Elmer TSA kit, NEL700A001KT, 1:100 in TBS with

0.1% Tween20 and 3% BSA, 30 min). The staining was revealed using 3,3'-diaminobenzidine (DAB, SK-4100, Vector Laboratories, Burlingame, CA) as a substrate and the sections were dehydrated and mounted. For proper visualization of NICD-1, no hematoxylin counterstaining was performed in combination with the NICD-1 staining.

The human GFAP staining was performed on the BOND RX stainer (Leica Biosystems, Wetzlar, Germany) with the Bond™ Polymer Refine Detection Protocol (Leica Biosystems Wetzlar, Germany; DS9800) according to the manufacturer's instructions. The following primary antibody was used: FLEX Polyclonal Rabbit Anti-Glial Fibrillary Acidic Protein (Dako, Ready-To-Use Autostainer solution). Afterwards, sections were mounted in the Leica CV5030 Fully Automated Glass Coverslipper (Leica Biosystems Wetzlar, Germany).

Fluorescent images were taken on an Axio Imager.M1 microscope equipped with an AxioCam MRc5 camera or an AxioCam MRm camera (Zeiss, Jena, Germany). Confocal images were taken on a Leica TCS SP8 confocal laser scanning microscope (Leica Microsystems, Wetzlar, Germany). Bright-field images were taken on a Leica DM2000 LED microscope equipped with a DFC7000 digital camera (Leica Microsystems, Wetzlar, Germany). Several images (5 to 10) of the ventral horn region were taken per sample and image analysis and quantification was performed in a blinded manner using freeware ImageJ and AxioVision SE64 software.

*Evaluation of disease progression in mice: motor performance, nerve conduction, bodyweight, disease onset and endpoint determination*

Motor performance was assessed twice a week from the age of 60 days onwards by the hanging wire and rotarod performance tests, as previously described (176). For the hanging wire test, mice were placed on a grid and turned upside down for maximum 60 s. The time mice could hang was registered

as a measure for motor performance. For the rotarod performance test, mice were placed on a rotarod (Ugo Basile, Varese, Italy) rotating at 15 rpm for 5 min (fixed rotarod test) or rotating from 4 to 40 rpm in 5 min (accelerated rotarod test). Each animal was given three consecutive trials on the fixed rotarod and three consecutive trials on the accelerated rotarod with a 1 minute resting interval between the fixed and the accelerated rotarod test. The average time a mouse could spend on the rotarod was used as a measure of motor performance. Before starting the actual rotarod test at the age of 60 days, mice were trained at the age of 50 days for 4 days in a row.

Innervation and nerve conduction studies were performed using a ultra pro S100 EMG monitoring set-up (Natus Neurology, Pleasanton, CA, USA) with Synergy software (Acertys, Aartselaar, Belgium), according to the protocol described previously (177). In summary, to measure compound muscle action potentials (CMAP), mice were anesthetized with 3% isoflurane and subdermal 0.4-mm electrodes (Technomed Europe, Maastricht, The Netherlands) were placed at the level of the sciatic notch for stimulation and at the gastrocnemius muscle for recording. CMAPs were measured at supramaximal stimulation. For *Jagged-1*$^{lox/lox}$ *Cx30-CreER SOD1*$^{G93A}$ mice, *Jagged-1*$^{lox/-}$ *Cx30-CreER SOD1*$^{G93A}$ mice and their littermate control *SOD1*$^{G93A}$ mice, the CMAP amplitudes were normalized to the CMAP amplitude measured at the age of 50 days, because their CMAP amplitudes measured at 50 days of age (this is before the tamoxifen-induced inactivation of Jagged-1) were not identical.

Bodyweight was measured twice a week starting from the age of 60 days as a generalized parameter to follow disease progression.

Disease onset was defined the day when a mouse was not able to hold on for 60 s on the hanging grid test anymore, except for the mice with ubiquitous inactivation of Jagged-1 and their littermate controls where disease onset was determined as the time when bodyweight reached the maximum, since they were not able to perform the hanging wire test.

End stage was determined as the time point when paralyzed mice could no longer turn themselves within 10 s when placed on their side. At that moment, mice were sacrificed using an overdose of Nembutal (10 mg/kg; Ceva Chemicals, Hornsby, NSW, Australia). Survival was defined as the time from birth to end stage. Disease duration was defined as the period between disease onset and end stage.

Of note, the number of mice per group is often unbalanced in these experiments due to the complexity of the triple transgenic crosses.

*Statistical analysis*

GraphPad Prism 5 software (Graphad Software, La Jolla, CA, USA) was used for all statistical analysis. Unpaired t-test, Mann-Whitney U-test, one- and two-way ANOVA with *post hoc* analysis and Log-rank Mantel-Cox test were performed as specified in the figure legends. Normality was evaluated with the Shapiro-Wilk normality test. Quantitative data are presented as mean ± SEM. P-values smaller than 0.05 were considered statistically significant.

# PART 1: CHARACTERIZATION OF THE NOTCH SIGNALING PATHWAY IN ALS

**The work presented in part 1 is published in:**

**Nonneman A**, Criem N, Lewandowski SA, Nuyts R, Thal DR, Pfrieger F, Ravits J, Van Damme P, Zwijsen A, Van Den Bosch L, Robberecht W. Astrocyte-derived Jagged-1 mitigates deleterious Notch signaling in amyotrophic lateral sclerosis. Neurobiol Disease. 2018;119:26-40.

## 1. Introduction

In ALS, motor neuron degeneration is not only arising through cell intrinsic mechanisms, but different types of glial cells, including microglia, astrocytes and oligodendroglial cells, are known to actively contribute to the degeneration of the motor neurons as well (41).

The Notch signaling pathway is a critical mediator of cell-cell interactions (98, 99) and has been described to play an important role in several processes that are relevant to the pathogenesis of ALS, including axonal outgrowth and retraction (144-148), neuromuscular junction maturation (150), microgliosis (128, 132, 139, 151), astrocytosis (140, 157, 159, 160), proliferation and differentiation of oligodendrocyte precursor cells into mature oligodendrocytes (133, 162, 167, 168), and cell death (137, 171). In addition, abnormal Notch signaling has been linked to neurodegenerative diseases (109), such as Alzheimer's disease (125, 126), multiple sclerosis (127-129), spinal muscular atrophy (130), prion disease (131, 178) and ischemic stroke (132).

Based on this knowledge, ***we hypothesize the Notch signaling pathway to be involved in the pathogenesis of ALS***.

The aim of the current study was to characterize the different components of the Notch signaling pathway, including the different Notch receptors, ligands, co-factors and downstream targets, in the affected lumbar spinal cord of *SOD1$^{G93A}$* mice, the best-characterized mouse model for ALS, and also in the affected lumbar spinal cord of sALS patients.

# 2. Results

## 2.1 Characterization of the Notch signaling pathway in an ALS mouse model

### *Key mediators of the Notch signaling pathway show increased expression in the affected lumbar spinal cord of SOD1$^{G93A}$ mice*

We first examined the expression, both on the mRNA and protein level, of the Notch receptors (Notch-1, -2, -3 and -4), the ligands (Jagged-1 and -2; Delta-like-1, -3 and -4) and the transcription cofactors (RBPjk and Mastermind-like-1, -2 and - 3) of the canonical Notch signaling pathway in the lumbar spinal cord of the *SOD1$^{G93A}$* mouse. In addition, two non-canonical ligands (F3/Contactin-1 and NB3/Contactin-6) were studied for completeness. Lumbar spinal cords of age-matched non-transgenic mice and of age-matched *SOD1$^{WT}$* mice were used as controls.

Quantitative PCR showed that the mRNA expression of the Notch receptors increases with disease progression (Figure 7A). Until day 60, the mRNA expression levels of all four Notch receptors were unaltered compared to age-matched control *SOD1$^{WT}$* mice and non-transgenic mice. However, during disease (125 days and 150 days), a significant upregulation of all Notch receptors in the affected lumbar spinal cord was observed, whereas their expression in control *SOD1$^{WT}$* spinal cords remained unchanged (Figure 7A).

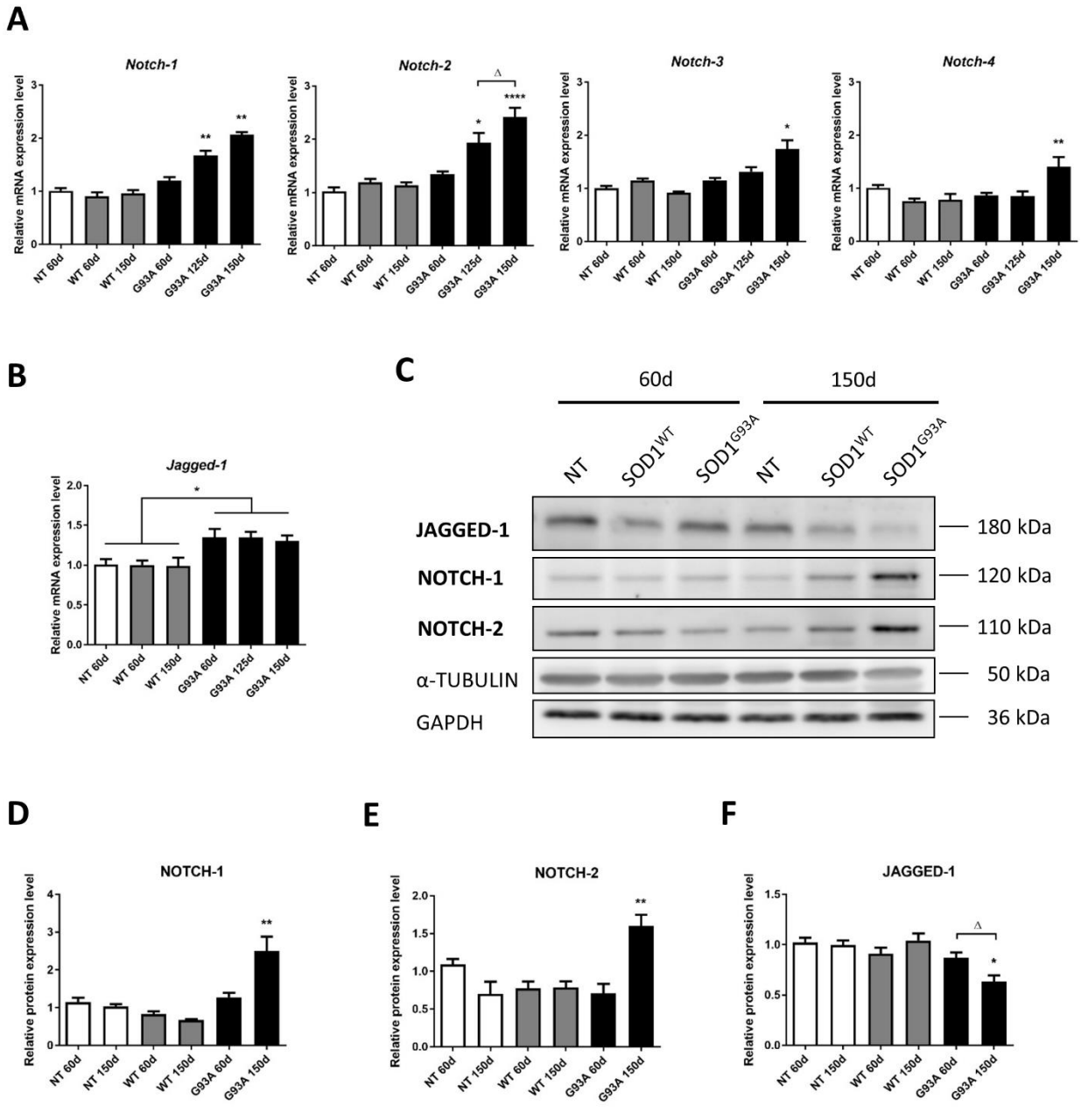


***Figure 7: The Notch receptors and the ligand Jagged-1 are more abundantly expressed in the affected lumbar spinal cord of SOD1$^{G93A}$ mice compared to control mice.*** *mRNA levels of (A) the Notch receptors and (B) the ligand Jagged-1 in the affected lumbar spinal cord of SOD1$^{G93A}$ mice (G93A) at different disease stages (60d = asymptomatic stage; 125d = symptomatic stage; 150d = end stage), determined by qRT-PCR. Lumbar spinal cords of age-matched SOD1$^{WT}$ mice (WT) and non-transgenic mice (NT) were used as controls. Expression data are normalized to Hprt and Gapdh and scaled to NT 60d. (C) Western Blot analysis showing NOTCH-1, NOTCH-2 and JAGGED-1 in the affected lumbar spinal cord of SOD1$^{G93A}$ mice (G93A) at different disease stages (60d = asymptomatic stage; 150d = end stage). Lumbar spinal cords of age-matched SOD1$^{WT}$ mice (WT) and non-transgenic mice (NT) were used as controls. α-TUBULIN and GAPDH were used for loading controls. (D, E and F) Protein levels of indicated proteins determined by densitometric analysis of the Western Blots shown in (C). One-way ANOVA with Tukey's posthoc analysis: *p<0.05, **p<0.01, ****p<0.0001 with all other groups, except when indicated differently, and Δ p=0.06 indicates a tendency, n=6 mice per group for qRT-PCR and n=3 mice per group for western Blot. Data represent mean ± SEM.*

Similarly, the mRNA expression of the canonical Notch ligand *Jagged-1* was increased significantly in *SOD1$^{G93A}$* lumbar spinal cord (Figure 7B). Interestingly, this increase was already observed at the age of 60 days, well before disease onset and did not further increase with disease progression (Figure 7B). The expression of other canonical (Figure 8A) and non-canonical ligands (Figure 8B) was not significantly changed.

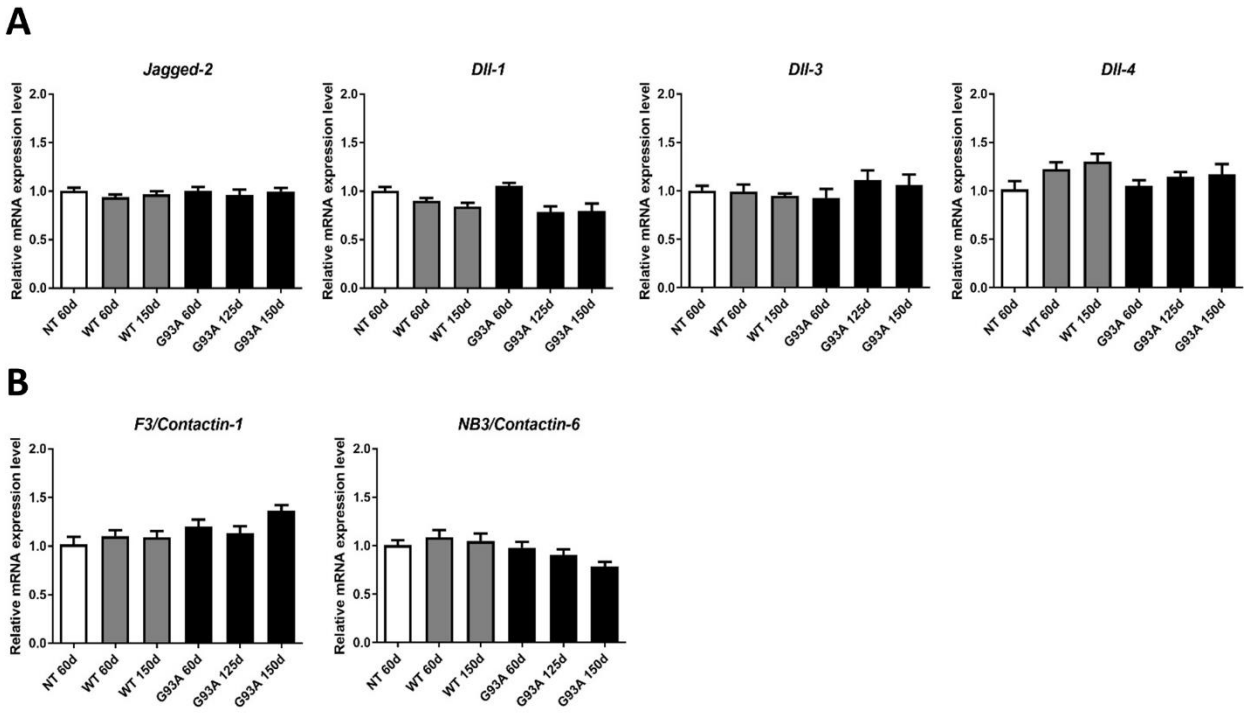


***Figure 8: The mRNA expression of the Notch ligands other than Jagged-1 are not upregulated in the affected lumbar spinal cord of SOD1$^{G93A}$ mice compared to control mice.*** *The mRNA levels of (A) the canonical Notch ligands other than Jagged-1 and (B) the non-canonical Notch ligands in the affected lumbar spinal cord of SOD1$^{G93A}$ mice (G93A) at different disease stages (60d = asymptomatic stage; 125d = symptomatic stage; 150d = end stage), determined by qRT-PCR. Lumbar spinal cords of age-matched SOD1$^{WT}$ mice (WT) and non-transgenic mice (NT) were used as controls. Expression data are normalized to Hprt and Gapdh and scaled to NT 60d. Data represent mean ± SEM, n=6 mice per group.*

We next studied the expression of these factors at the protein level. We focused on the proteins NOTCH-1 and NOTCH-2, because their mRNA increase was most prominent during disease progression (Figure 7A). In agreement with the mRNA data, Western blot analysis showed a significant increase of the levels of the processed forms of the receptor proteins NOTCH-1 (molecular weight of 120 kDa,

Figure 7C-D) and NOTCH-2 (molecular weight of 110 kDa, Figure 7C and E) in lumbar spinal cords of end stage *SOD1$^{G93A}$* mice (150 days) compared to asymptomatic *SOD1$^{G93A}$* mice (60 days) and age-matched control *SOD1$^{WT}$* or non-transgenic mice. In contrast to its increased mRNA levels, the protein expression of full-length JAGGED-1 (molecular weight of 180 kDa) was significantly reduced in the spinal cord from end stage *SOD1$^{G93A}$* mice compared to asymptomatic *SOD1$^{G93A}$* mice (60 days), and compared to age-matched control *SOD1$^{WT}$* or non-transgenic mice (Figure 7C and F), which potentially might indicate increased JAGGED-1 processing (cleavage, endocytosis and degradation) after signal transduction (179-183).

### *The Notch signaling pathway is more activated in the lumbar spinal cord of SOD1$^{G93A}$ mice*

The mRNA and protein expression profiles described above suggest that the Notch signaling pathway is aberrantly activated in the spinal cord of *SOD1$^{G93A}$* mice. To test this, we evaluated Notch receptor cleavage, the expression of key-components of the downstream transcription activation complex and the expression of Notch target genes.

NICD-1 was readily detectable by immunohistochemical staining using tyramide signal amplification, although it was undetectable using Western blot. To quantify Notch-1 activation in a cell-specific way, we evaluated the number of NICD-1 positive cells in the lumbar spinal cord ventral horn. The specificity of the NICD-1 staining was evaluated by staining the spinal cord of *Notch-1$^{lox/lox}$ CAGG-CreER* mice (Figure 9A-B), in which Notch-1 mRNA expression is reduced with approximately 90% upon tamoxifen administration (Figure 9C), resulting in an almost complete abolishment of the nuclear NICD-1 staining in the spinal cord ventral horn (Figure 9A-B).

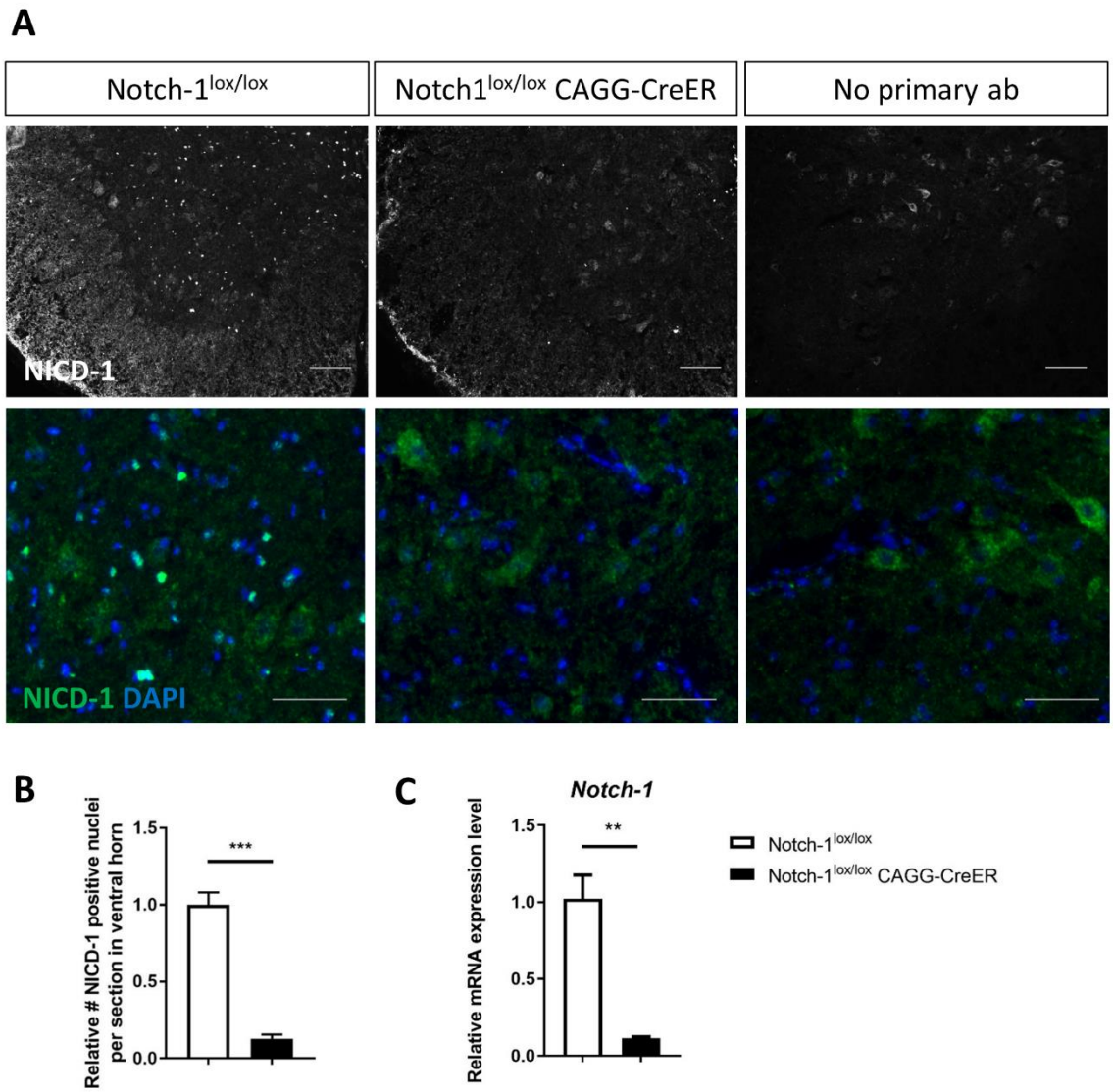


***Figure 9: Evaluation of the specificity of the antibody against NICD-1.*** *(A-B) Immunofluorescent staining of NICD-1 in the lumbar spinal cord of Notch-1$^{lox/lox}$ CAGG-CreER mice and control Notch-1$^{lox/lox}$ mice upon tamoxifen administration. (A) The upper panels show an overview of the NICD-1 staining (white dots) in the lumbar spinal cord ventral horn. The lower panels are higher magnification images to show co-staining of NICD-1 (green) in DAPI-positive nuclei (blue). The 'No primary ab' condition shows the background staining in the absence of incubation with the NICD-1 antibody. Scale bar is 100 µm (upper panels) and 50 µm (lower panels). (B) Relative quantification of the number of NICD-1 positive nuclei per section in the ventral horn of lumbar spinal cord. (C) The Notch-1 mRNA expression level in the spinal cord of Notch-1$^{lox/lox}$ CAGG-CreER mice and Notch-1$^{lox/lox}$ control mice after tamoxifen administration was determined by qRT-PCR for Notch-1. Expression data are normalized to Polr2a and Hprt. Unpaired t-test: **p<0.01, ***p<0.001, n=3 mice per group. Data represent mean ± SEM.*

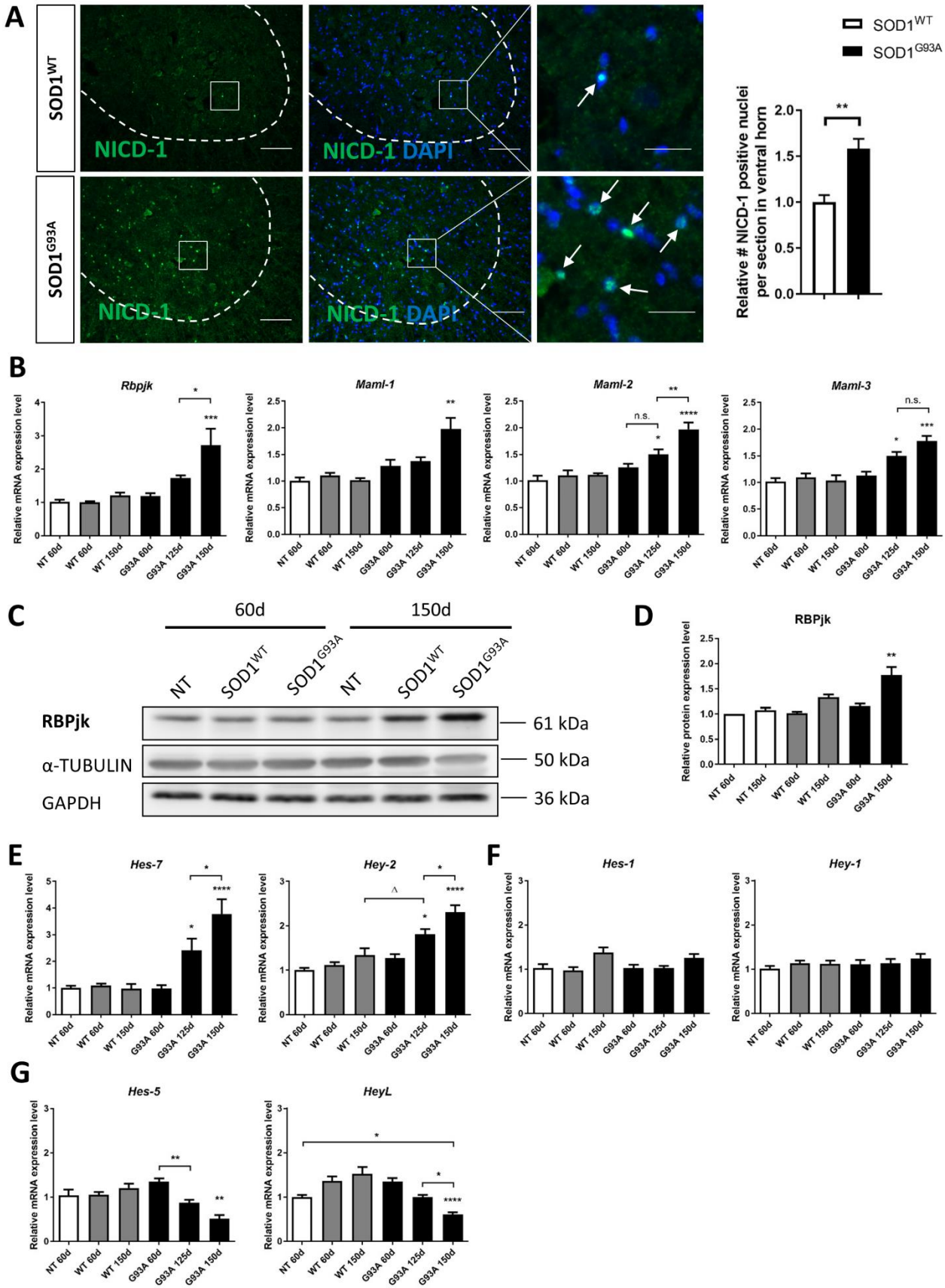


***Figure 10: Notch signaling is more active in the affected lumbar spinal cord of SOD1$^{G93A}$ mice compared to control mice.*** *(A) Representative image of the NICD-1 staining in the lumbar spinal cord of symptomatic SOD1$^{G93A}$ mice at the age of 130 days and age-matched SOD1$^{WT}$ mice, and quantification of the relative number of NICD-1*

*positive nuclei counted per section in the ventral horn. Nuclei are stained with DAPI. Higher magnification images of the boxed area are shown in the right panels. The arrows indicate the NICD-1 positive DAPI positive nuclei. Scale bar is 100 µm (left and middle panels) and 25 µm (right panels with higher magnification). Unpaired t-test: **p<0.01, n=4 mice per group. (B) mRNA levels of the co-factors, necessary to form the transcription activation complex, Rbpjk and the different isoforms of Maml, in the affected lumbar spinal cord of SOD1$^{G93A}$ mice (G93A) at different disease stages (60d = asymptomatic stage; 125d = symptomatic stage; 150d = end stage), determined by qRT-PCR. Lumbar spinal cords of age-matched SOD1$^{WT}$ mice (WT) and non-transgenic mice (NT) were used as controls. Expression data are normalized to Hprt and Gapdh and scaled to NT 60d. (C and D) Western Blot analysis of RBPjk and its quantification by densitometric analysis in the affected lumbar spinal cord of SOD1$^{G93A}$ mice (G93A) at different disease stages (60d = asymptomatic stage; 150d = end stage). Lumbar spinal cords of age-matched SOD1$^{WT}$ mice (WT) and non-transgenic mice (NT) were used as controls. α-TUBULIN and GAPDH were used as loading controls. (E-G) mRNA levels of the Notch target genes Hes-1, Hes-5, Hes-7, Hey-1, Hey-2 and Hey-L in the affected lumbar spinal cord of SOD1$^{G93A}$ mice (G93A) during disease progression (60d = asymptomatic stage; 125d = symptomatic stage; 150d = end stage), determined by qRT-PCR. Lumbar spinal cords of age-matched SOD1$^{WT}$ mice (WT) and non-transgenic mice (NT) were used as controls. Expression data are normalized to Hprt and Gapdh and scaled to NT 60d. One-way ANOVA with Tukey's posthoc analysis: *p<0.05, **p<0.01, ***p<0.001, ****p<0.0001 with all other groups, except when indicated differently, and Δ p=0.062 indicates a tendency, n=6 mice per group (for qRT-PCR) and n=3 mice per group (for Western Blot). Data represent mean ± SEM.*

In the affected lumbar spinal cord ventral horn of symptomatic SOD1$^{G931}$ mice, nuclear NICD-1 staining was present in a significantly higher number of cells when compared to age-matched control *SOD1$^{WT}$* mice (Figure 10A). Unfortunately, the lack of specific antibodies precludes the study of NICD-2.

We next evaluated the expression levels of Rbpjk and Maml. These co-factors form the transcription-activation complex together with NICD and contribute to enhanced Notch signaling activation when expressed at high-level (184, 185). A significant upregulation of *Rbpjk* and all three isoforms of *Maml* (*Maml-1, Maml-2, Maml-3)* was evident during disease progression, when compared to age-matched control *SOD1$^{WT}$* mice or non-transgenic mice (Figure 10B). In agreement with the mRNA data, the protein expression of RBPjk was increased as well (Figure 10C-D).

We next quantified the mRNA expression of the *Hes* and *Hey* downstream target genes of Notch, of which the expression levels are differentially affected upon activation of Notch signaling (186-189). Indeed, *Hes-7* and *Hey-2* expression levels were significantly enhanced during disease progression (Figure 10E), while levels of *Hes-1* and *Hey-1* remained unchanged (Figure 10F), and *Hes-5* and *Hey-L*

expression levels were decreased (Figure 10G). This pattern of changes of target gene expression is known to occur upon Notch signaling activation (186-189).

Overall, our data suggest that the Notch signaling pathway is overactive in the lumbar spinal cord of ALS mice compared to controls.

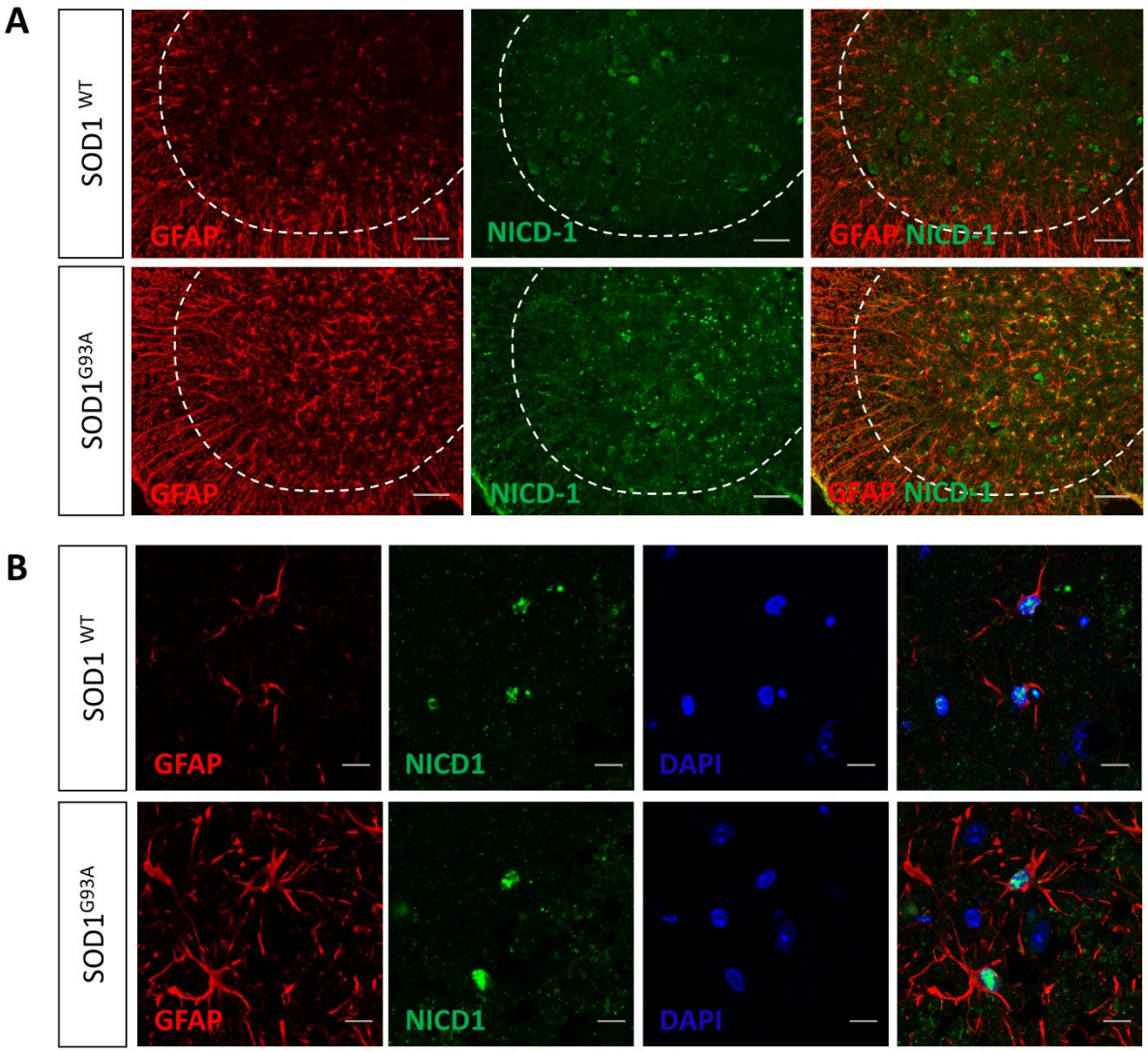


***Figure 10: NICD-1 is abundantly expressed by reactive astrocytes in the affected lumbar spinal cord ventral horn of symptomatic SOD1$^{G93A}$ mice.*** *(A) Immunofluorescent staining of NICD-1 and the astrocytic marker GFAP in the lumbar spinal cord ventral horn (marked by the white dotted line) of from symptomatic SOD1$^{G93A}$ mice at the age of 130 days and age-matched control SOD1$^{WT}$ mice show that more GFAP-positive astrocytes are NICD-1 positive in the symptomatic SOD1$^{G93A}$ mice, when compared to age-matched SOD1$^{WT}$ mice. Scale bar is 100 µm. (B) Confocal images of the immunofluorescent staining of NICD-1, the astrocytic marker GFAP and the nuclear marker DAPI show that NICD-1 is expressed in the DAPI+ nuclei of GFAP+ astrocytes, both in resting astrocytes of SOD1$^{WT}$ mice and in diseased, reactive astrocytes of symptomatic SOD1$^{G93A}$ mice. Scale bar is 10 µm.*

### *Neurons and astrocytes are cell types involved in Notch signaling in SOD1$^{G93A}$ mice*

To investigate which cell types of the spinal cord mediate Notch signaling, we determined the cellular localization of NICD-1 and JAGGED-1 using double staining for these proteins and different neuronal and glial cell type markers.

In the spinal cord ventral horn of both *SOD1$^{G93A}$* mice at the age of 130 days (symptomatic stage) and age-matched control *SOD1$^{WT}$* mice, NICD-1 was found in nuclei of GFAP-positive astrocytes, and more NICD-1 positive astrocytes were observed in the ventral horn of symptomatic *SOD1$^{G93A}$* mice when compared to control *SOD1$^{WT}$* mice (Figure 11A-B).

No NICD-1 signal was observed in NeuN-positive neurons (Figure 12A and D), and only some of the CC1-positive oligodendrocytes and the F4-80-positive reactive microglia are positive for NICD-1 (Figure 12B-D). However as described before (190), the levels of NICD-1 in oligodendrocytes and microglia are considered negligible.

***Figure 12: NICD-1 is not detected in neurons, but present at negligible levels in some oligodendrocytes and reactive microglia in the affected lumbar spinal cord ventral horn of symptomatic SOD1$^{G93A}$ mice.*** *Immunofluorescent co-staining of NICD-1 and the neuronal marker NeuN (A), the oligodendroglial marker CC1 (B) and the reactive microglial marker F4-80 (C) in the lumbar spinal cord ventral horn from symptomatic SOD1$^{G93A}$ mice at the age of 130 days and age-matched SOD1$^{WT}$ mice. (A) These overview images of the entire ventral horn region (marked by the white dotted line) show that NICD-1 is not expressed in the nucleus of NeuN-positive neurons, both in SOD1$^{WT}$ mice and in symptomatic SOD1$^{G93A}$ mice. Of note, the cytoplasmic neuronal signal observed with the NICD-1 antibody is background signal, as was shown with the "no primary antibody" control condition in figure 9A. (B-C) The overview images of the co-staining of NICD-1 with the oligodendrocytic marker CC1 and reactive microglial marker F4-80 show that some oligodendrocytes and reactive microglia in the ventral horn of symptomatic SOD1$^{G93A}$ mice have a positive nuclear NICD-1 staining. The white arrows indicate co-localization. Scale bar is 100 µm. (D) Quantification of the percentage of the NICD-1 positive cells in the lumbar spinal cord ventral horn that are positive for the markers GFAP, NeuN, F4-80 and CC1, respectively. NB=not determined, since the marker F4-80 is only expressed by reactive microglia and no other antibodies against microglial markers were compatible with the NICD-1 immunofluorescent staining. Data represent mean ± SEM, n=3-4 mice per group.*

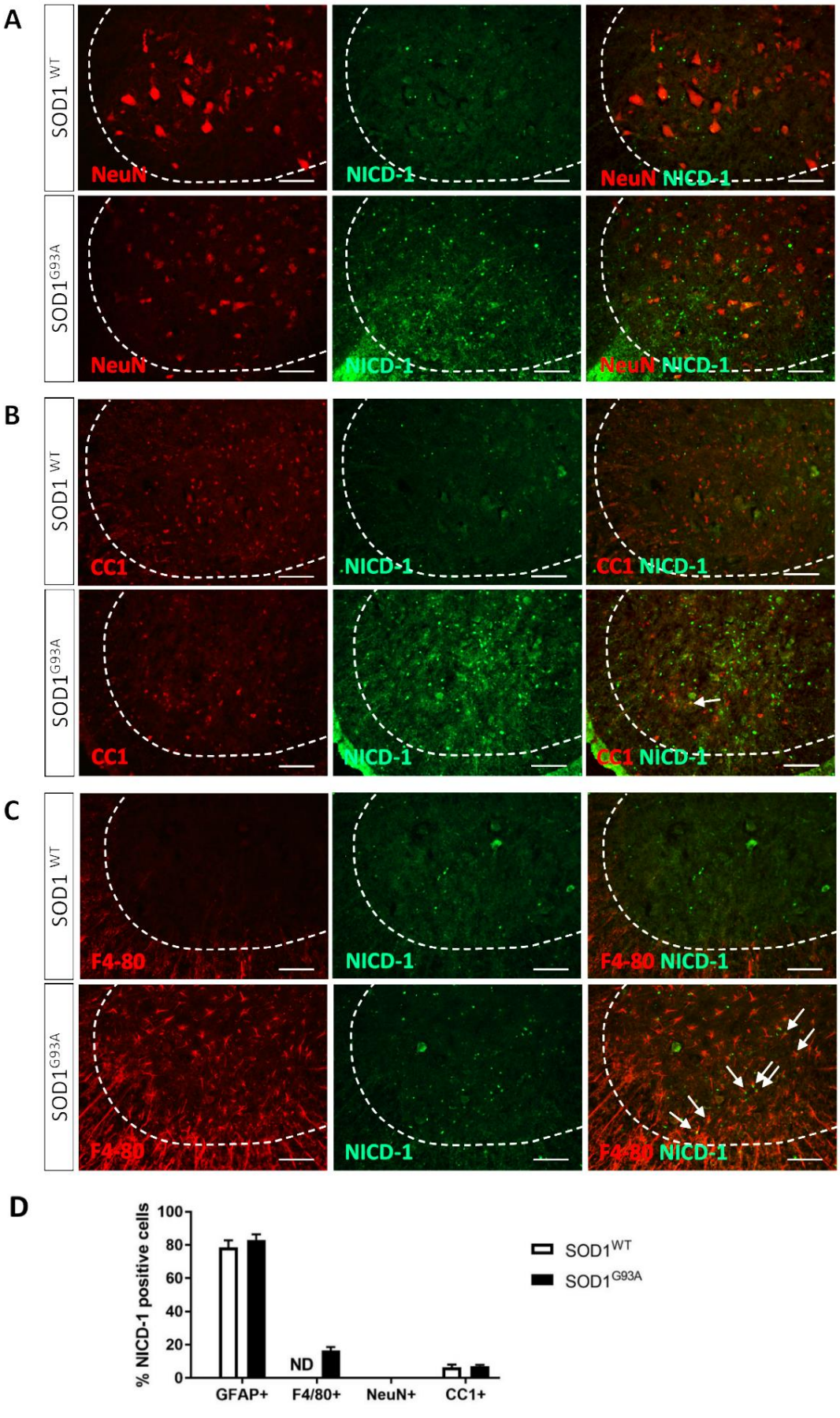
A
SOD1 WT
NeuN
NICD-1
NeuN NICD-1
SOD1G93A
NeuN
NICD-1
NeuN NICD-1
B
SOD1 WT
CC1
NICD-1
CC1 NICD-1
SOD1G93A
CC1
NICD-1
CC1 NICD-1
C
SOD1 WT
F4-80
NICD-1
F4-80 NICD-1
SOD1G93A
F4-80
NICD-1
F4-80 NICD-1
D
% NICD-1 positive cells
100
80
60
40
20
0
ND
GFAP+
F4/80+
NeuN+
CC1+
SOD1WT
SOD1G93A

JAGGED-1 expression was clearly identifiable in NeuN-positive (motor) neurons, both in the *SOD1*$^{WT}$ and *SOD1*$^{G93A}$ mouse spinal cord (Figure 13A). Interestingly, after disease onset, JAGGED-1 was abundantly expressed in GFAP-positive reactive astrocytes in symptomatic *SOD1*$^{G93A}$ mice at the age of 130 days (Figure 13B), while never observed in astrocytes of non-transgenic or *SOD1*$^{WT}$ mice.

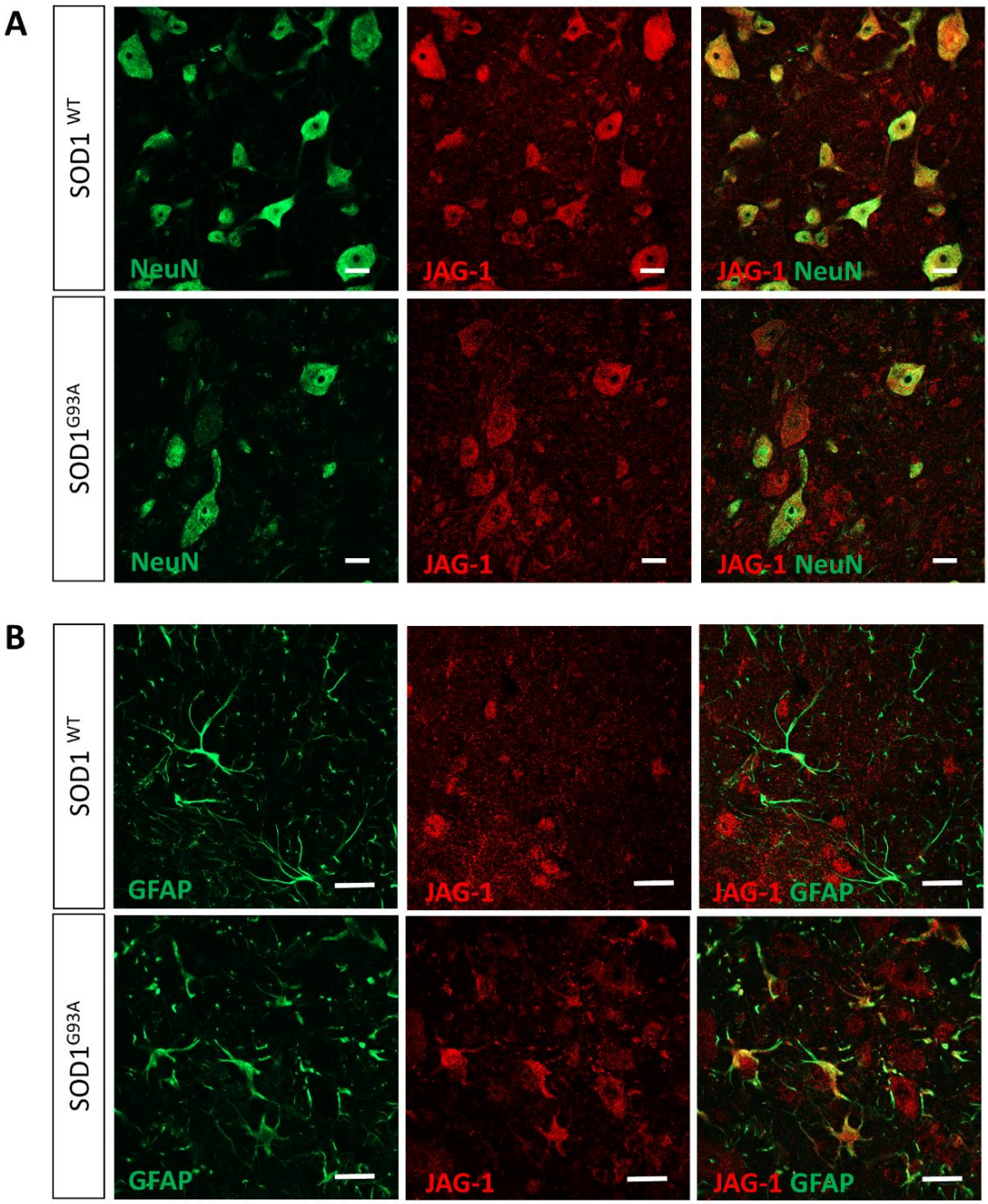


***Figure 13: Jagged-1 is expressed by (motor) neurons and reactive astrocytes in the affected lumbar spinal cord of SOD1$^{G93A}$ mice.*** *Confocal images of the immunofluorescent staining of JAGGED-1 in the ventral horn of the lumbar spinal cord from symptomatic SOD1$^{G93A}$ mice at the age of 130 days and age-matched SOD1$^{WT}$ mice in combination with (A) the neuronal marker NeuN and (B) the astrocytic marker GFAP. Scale bar is 20µm.*

The typical staining pattern of JAGGED-1 disappeared after pre-incubation of the JAGGED-1 antibody with two different neutralizing JAGGED-1 peptides, sc-6011 P (Santa Cruz Biotechnology) and NBP1-90208 PEP (Novus Biologicals), demonstrating the specificity of the antibody (Figure 14).

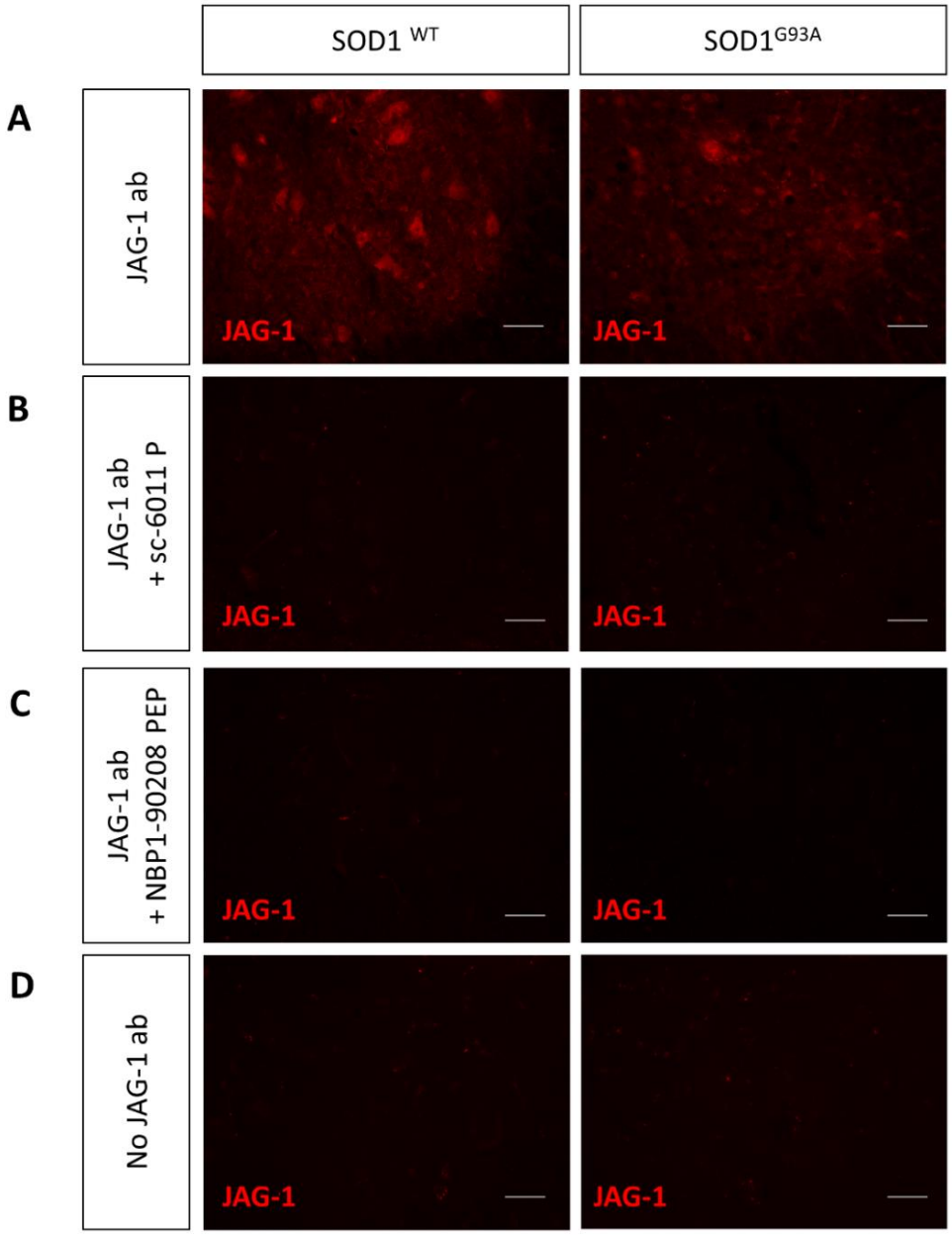


***Figure 14: Evaluation of the specificity of the antibody against JAGGED-1 with neutralizing JAGGED-1 peptides.*** *The specificity of the JAGGED-1 immunofluorescent staining in the lumbar spinal cord ventral horn from symptomatic $SOD1^{G93A}$ mice at the age of 130 days and age-matched $SOD1^{WT}$ mice was evaluated by comparing the following staining conditions: incubation (A) with anti-JAG-1 antibody, (B) with anti-JAG-1 antibody that was pre-incubated with the sc-6011 P neutralizing JAGGED-1 peptide, (C) with anti-JAG-1 antibody that was pre-incubated with the NBP1-90208 PEP neutralizing JAGGED-1 peptide and (D) without anti-JAG-1 antibody. Scale bar is 50 µm.*

Together these data suggest that the prominently increased Notch signaling activation in the spinal cord of *SOD1*$^{G93A}$ mice is astrocytic in nature, as well as the disease-associated JAGGED-1 expression.

## 2.2 Characterization of the Notch signaling pathway in sALS patients

To evaluate whether our findings concerning the Notch signaling pathway in the spinal cord of *SOD1*$^{G93A}$ mice are translatable to ALS patients, we investigated the Notch signaling pathway in *post-mortem* spinal cords from sALS patients and compared them to spinal cords from control individuals.

### *Key mediators of the Notch signaling pathway are more abundantly expressed and the Notch signaling pathway is more activated in the affected lumbar spinal cord of sALS patients*

From publicly available data (www.ncbi.nlm.nih.gov/geo, accession number GSE18920) (174) we retrieved the mRNA expression of *NOTCH-1*, *NOTCH-2* and *JAGGED-1* in human lumbar spinal cord motor neurons (obtained using laser capture microdissection) and in the remaining anterior horn (devoid of motor neurons) from 12 sALS patients and 8 control individuals. Increased mRNA expression of *NOTCH-1*, *NOTCH-2* and *JAGGED-1* was found in sALS spinal cords, both in the motor neuron fraction (Figure 15A), and in the remaining anterior horn fraction (Figure 15B).

We then evaluated the Notch signaling activation status by studying the mRNA expression profiles of the co-factors *RBPjk* and *MAML*, and the Notch target genes. In the motor neuron fraction of sALS patients, a significant increase in mRNA expression of the co-factor *MAML-2* and the Notch target genes *HES-1* and *HEY-2* was observed when compared to human control motor neurons (Figure 15A). In the remaining anterior horn fraction, the mRNA expression of *HES-1* and *HEY-2* tended to be increased as well, but to a lesser degree than in the motor neuron fraction (Figure 15B).

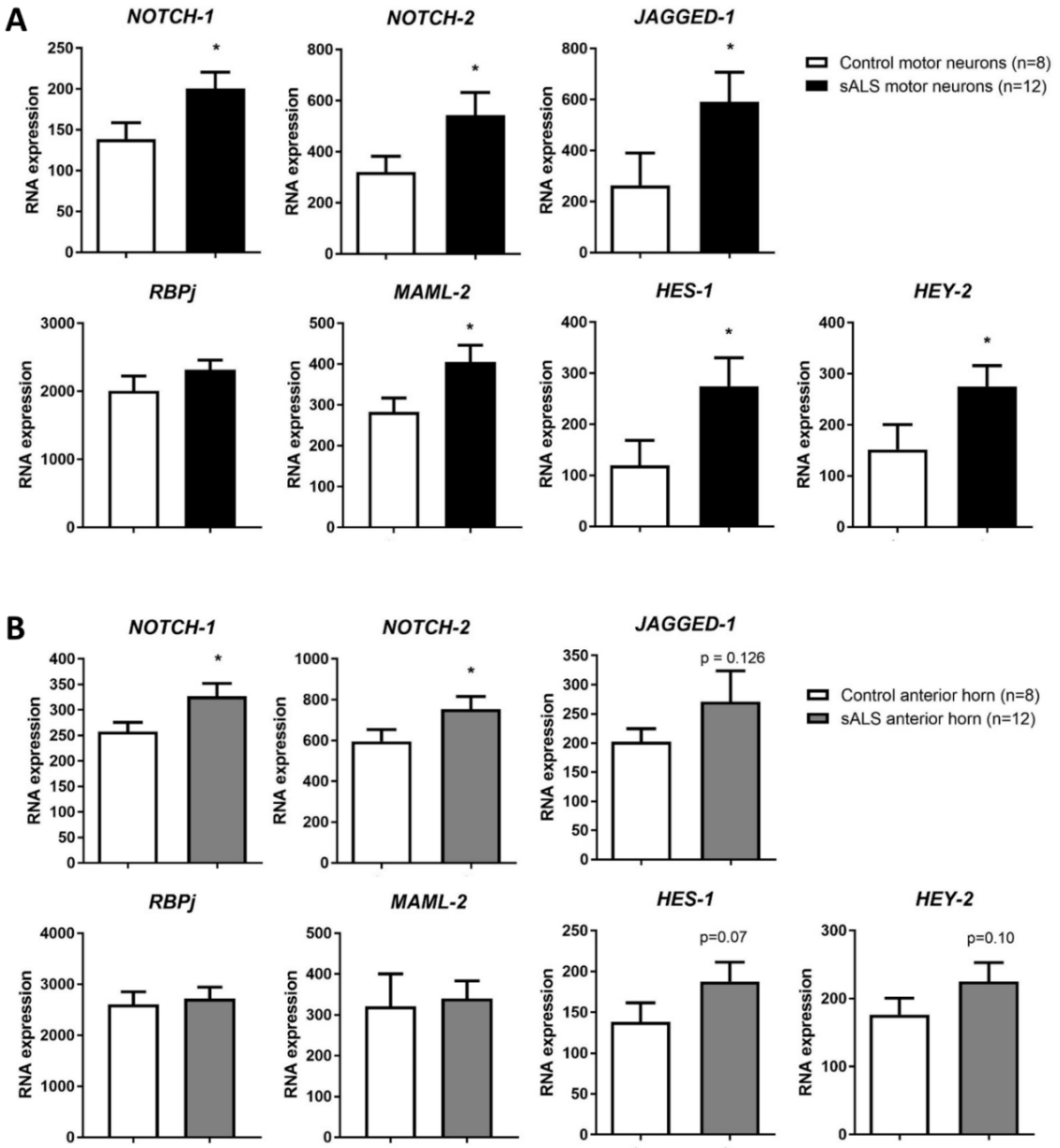


***Figure 15: Several key mediators of Notch signaling are more abundantly expressed and the Notch signaling pathway is more activated in post mortem lumbar spinal cord of sALS patients compared to controls.*** *RNA expression of different components of the Notch signaling pathway retrieved from a publicly available data set from a whole-genome exon splicing array (www.ncbi.nlm.nih.gov/geo, accession number GSE18920) performed on (A) motor neurons isolated by laser capture microdissection and (B) the remaining anterior horn glial fraction from spinal cords of 12 sporadic ALS patients (sALS) and 8 control individuals. RNA expression data were calculated based on summarized probe intensities. Unpaired t-test: *p<0.05, data represent mean ± SEM.*

The RNA expression of all other components of the Notch signaling pathway did not show consistent changes as shown in figure 16, except for the non-canonical ligand F3/Contactin-1 that was more abundantly expressed in both the sALS patient spinal cord motor neuron fraction and the anterior horn fraction, when compared to the fractions from control individuals.

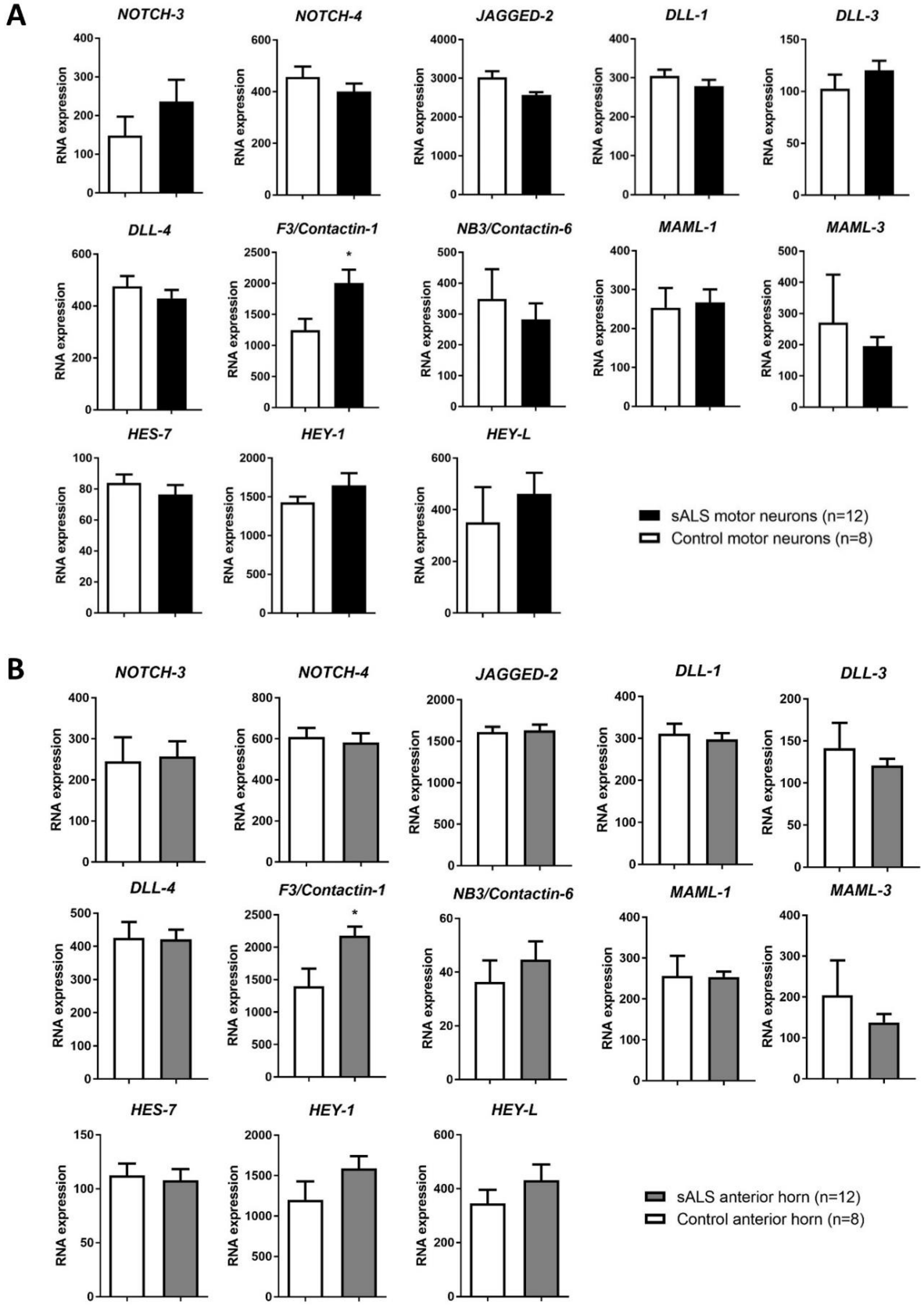


***Figure 16: RNA expression level of additional components of the Notch signaling pathway in post mortem spinal cord tissue from sALS patients and controls.*** *Analysis of additional Notch related genes from the publicly available data set from a whole-genome exon splicing array (www.ncbi.nlm.nih.gov/geo, accession number GSE18920) performed on (A) motor neurons and (B) the remaining anterior horn glial fraction from spinal cords of 12 sporadic ALS patients (sALS) and 8 controls. HES-5 was not found in this data set. RNA expression data were calculated based on summarized probe intensities. Unpaired t-test: *p<0.05, data represent mean ± SEM.*

The purity of the motor neuron fraction and the remaining anterior horn glial fraction and the presence of reactive astrocytosis and microgliosis in the sALS samples compared to the control samples, were analyzed by evaluating the expression of the motor neuronal marker choline acetyltransferase (*ChAT*) and the glial markers glial fibrillary acidic protein (*GFAP*) for astrocytes and ionized calcium-binding adapter molecule-1 (*IBA-1*) for microglia (Figure 17).

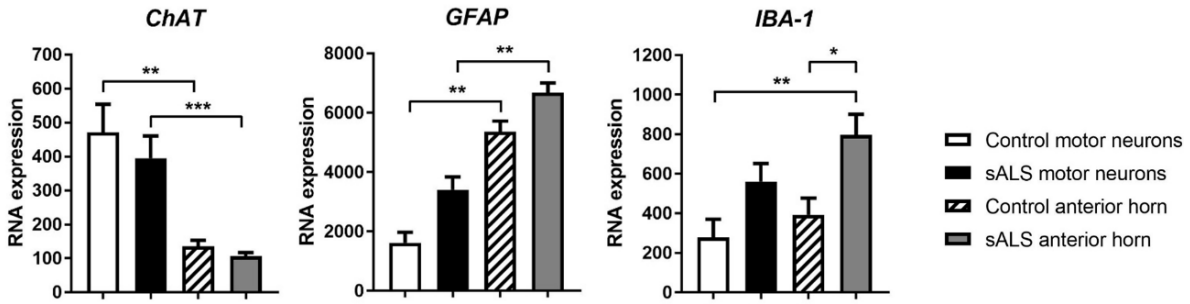


***Figure 17: Motor neuron and glial markers analyzed to evaluate the purity of the motor neuron fraction and the remaining anterior horn fraction.*** *From a publicly available whole-genome exon splicing array data set (www.ncbi.nlm.nih.gov/geo, accession number GSE18920) performed on motor neurons and the remaining anterior horn glial fraction from spinal cords of 12 sporadic ALS patients (sALS) and 8 controls, the neuronal marker ChAT and glial markers GFAP and IBA-1 were analysed to evaluate the purity of the motor neuron fraction and the anterior horn glial fraction. One-way ANOVA with Tukey's posthoc analysis: *p<0.05, **p<0.01, ***p<0.001 compared to motor neuron fraction, or compared to the group indicated. Data represent mean ± SEM.*

## *Neurons and astrocytes are cell types involved in Notch signaling in sALS patients*

We next examined the cellular localization of JAGGED-1 and NICD-1 in post-mortem spinal cord of sALS patients and control individuals (Figure 18). In both ALS and control spinal cord, JAGGED-1 was faintly expressed in (motor) neurons (Figure 18A). Interestingly and in agreement with what we observed in the *SOD1*$^{G93A}$ mouse model we observed JAGGED-1 to be expressed by reactive astrocytes in sALS lumbar spinal cords, while JAGGED-1 was absent in resting astrocytes in lumbar spinal cord samples from control individuals (Figure 18A, C). NICD-1 could not be detected in the lumbar spinal cord ventral horn of control individuals (Figure 18B). However, in the lumbar spinal cord ventral horn of sALS

patients NICD-1 was prominently present in the reactive astrocytes (Figure 18B-C). We observed this astrocytic JAGGED-1 and NICD-1 staining pattern in 5 out of 6 sALS patient lumbar spinal cords (PMI=3-6 h). No staining signal was observed in the sALS patient sample with the longest postmortem time interval (PMI=8.5 h).

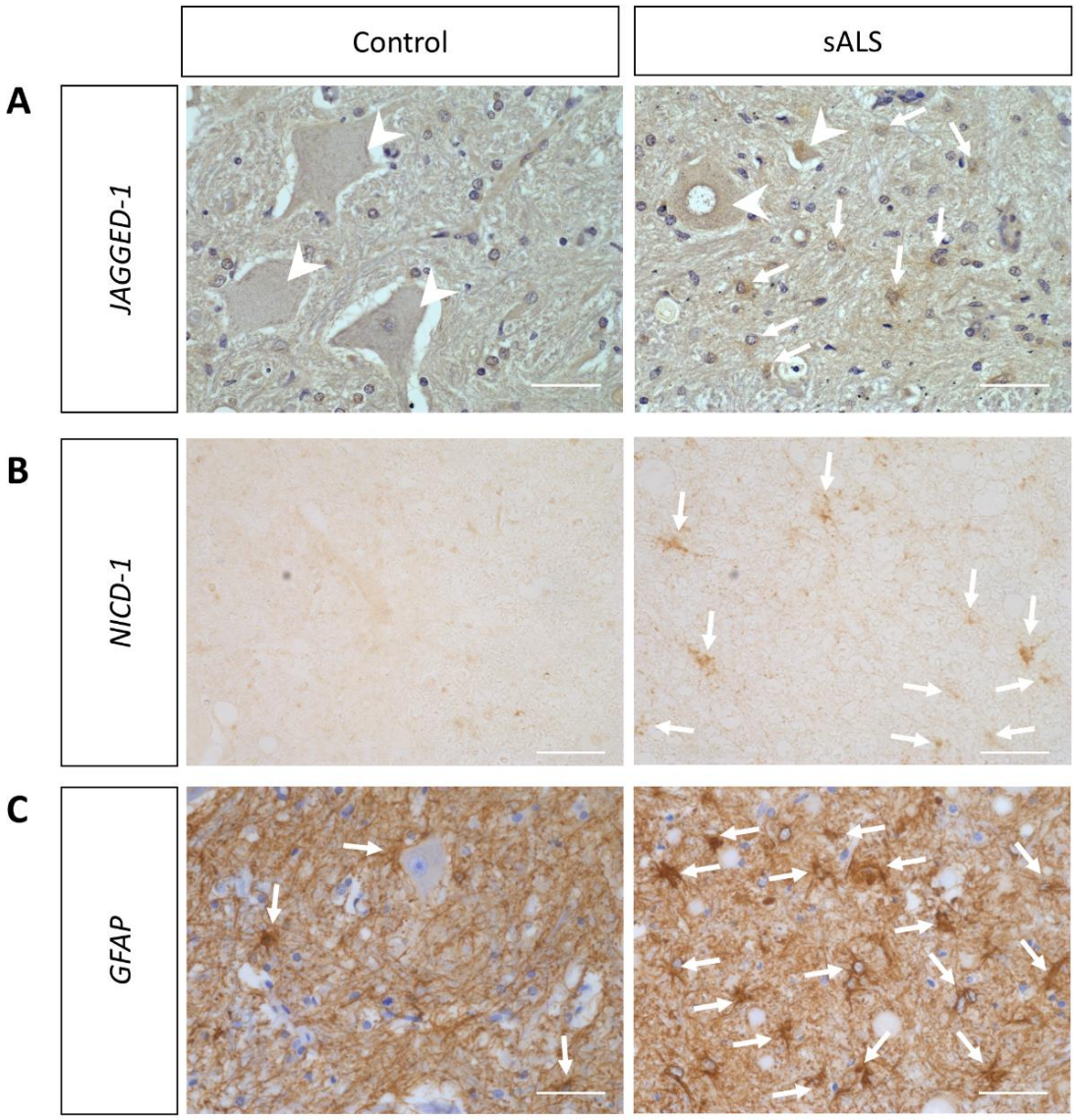


***Figure 18: JAGGED-1 is expressed in (motor) neurons and reactive astrocytes in post mortem spinal cord from sALS patients, and NICD-1 is expressed in reactive astrocytes only.*** *Representative images of the immuno-histochemical staining of (A) JAGGED-1, (B) NICD-1 and (C) GFAP in the ventral horn of post mortem human spinal cords from control individuals (left) and sALS patients (right). Arrowheads indicate the faint JAGGED-1 expression in (motor) neurons and the arrows indicate the pronounced JAGGED-1, NICD-1 and GFAP expression in the reactive astrocytes. Scale bar is 50 µm and n=6 individuals per group.*

Together, the data obtained from sALS patients are in full agreement with our findings from the *SOD1*$^{G93A}$ mouse model and confirm the increased Notch signaling activation and the aberrant cellular localization of JAGGED-1 and NICD-1 in reactive astrocytes in sALS spinal cord.

# 3. Discussion

The Notch signaling pathway, as a critical mediator of cell-cell interactions (98, 99), is an underestimated target in the study of the non-cell autonomous component of the pathogenesis of ALS and other neurodegenerative diseases. This is mainly due to its complexity and the limited knowledge about its role in the adult CNS (108).

In this part of the thesis, I characterized the Notch signaling pathway in ALS, by using *postmortem* sALS patient samples and the *SOD1*$^{G93A}$ mouse model. The Notch receptors Notch-1 and Notch-2, and the canonical ligand Jagged-1 are suggested to be important players, since they are most prominently upregulated in the context of ALS. Our data show that the Notch signaling pathway is abnormally active in the affected lumbar spinal cord of both sALS patients and *SOD1*$^{G93A}$ mice. In addition, we showed that astrocytes, which are generally known to actively contribute to the pathogenesis of ALS (191), are an important cell type in the context of abnormally active Notch signaling in ALS. First because, in both *SOD1*$^{G93A}$ mice and sALS patients, the active signaling fragment NICD-1 is prominently present in astrocytes and significantly more reactive astrocytes were positive for NICD-1 in the affected ALS spinal cord. Second, because the disease-associated aberrant expression of the ligand JAGGED-1 was also observed in reactive astrocytes, while never observed in resting astrocytes from *SOD1*$^{WT}$ mice and healthy control individuals.

Overall, our data described in this Notch signaling pathway characterization study show a signature of increased Notch signaling activation that is associated with ALS disease progression. The major strength of this study is the translational validity of our findings from the mouse model to the patients.

Specifically, we observed that in the affected lumbar spinal cord of both the *SOD1*$^{G93A}$ mice and the sALS patients the same key players of the Notch signaling pathway were upregulated, the Notch pathway was found to be aberrantly active and the astrocytes were shown to be involved in this overactive signaling.

# PART 2: MODULATION OF NOTCH SIGNALING IN AN ALS MOUSE MODEL

**The work presented in part 2 is partially published in:**

**Nonneman A**, Criem N, Lewandowski SA, Nuyts R, Thal DR, Pfrieger F, Ravits J, Van Damme P, Zwijsen A, Van Den Bosch L, Robberecht W. Astrocyte-derived Jagged-1 mitigates deleterious Notch signaling in amyotrophic lateral sclerosis. Neurobiol Disease. 2018;119:26-40.

## 1. Introduction

In the first part of this thesis entitled '*Characterization of the Notch signaling pathway in ALS*', we observed a signature of overactive Notch signaling in the affected lumbar spinal cord of both sALS patients and the *SOD1*$^{G93A}$ mouse model. Therefore, we were interested to investigate the role of increased Notch signaling activation in the pathogenesis of ALS by genetically interfering with this pathway in the *SOD1*$^{G93A}$ mouse model. Loss of Notch signaling by using constitutive knockout mice can cause severe embryonic phenotypes and early lethality (112-116, 192). However, the availability of inducible Cre-loxP targeting technology made it possible to choose the timing and the tissue type in which Notch signaling is modulated and allows to investigate the role of Notch signaling in adulthood and in adult-onset disease models (108, 117).

The aim of the current study was to inactivate the Notch signaling pathway in the *SOD1*$^{G93A}$ mouse model and evaluate the effect of this manipulation on disease, to unravel the role of increased Notch signaling activation in ALS pathogenesis. Since the canonical ligand Jagged-1 and the Notch receptors (mainly Notch-1 and Notch-2) are associated with increased Notch signaling activation observed in ALS, both ligand-based and receptor-based modulation approaches were of interest.

# 2. Results

## 2.1 A ligand-based modulation approach

In this study, we investigated whether interfering with the Notch signaling system may affect motor neuron degeneration in the ALS mouse model. We first focused on the modulation of the ligand Jagged-1, since Jagged-1 is the only canonical ligand showing increased mRNA expression levels in the spinal cord of both *SOD1$^{G93A}$* mice and sALS patients. In addition, we found that besides its expression in (motor) neurons, Jagged-1 is ectopically expressed in the reactive ALS-astrocytes in the lumbar spinal cord ventral horn, while below detection level in resting, healthy control astrocytes. Consequently, we were interested to study ubiquitous, as well as astrocyte-specific inactivation of Jagged-1 and evaluate its effect on disease in the *SOD1$^{G93A}$* mouse model.

### *Ubiquitous inactivation of Jagged-1 in the SOD1$^{G93A}$ mouse model*

To obtain ubiquitous Jagged-1 inactivation, we crossbred *Jagged-1$^{lox/lox}$* mice with *CAGG-CreER* mice and *SOD1$^{G93A}$* mice. In these transgenic mice, exon 4 of the ligand Jagged-1 is deleted ubiquitously by Cre-mediated excision upon administration of tamoxifen (Tx) at the age of 60 days (asymptomatic). This modified allele gives rise to a truncated, non-functional JAGGED-1 protein lacking the Notch receptor-binding domain (193). Recombination efficiency was on average 41 ± 3% in *SOD1$^{G93A}$* mice with heterozygous ubiquitous Jagged-1 inactivation (*Jagged-1$^{lox/-}$ CAGG-CreER SOD1$^{G93A}$*) and 89 ± 2% in *SOD1$^{G93A}$* mice with homozygous ubiquitous Jagged-1 inactivation (*Jagged-1$^{lox/lox}$ CAGG-CreER SOD1$^{G93A}$* mice), when compared to control *SOD1$^{G93A}$* mice (Figure 19).

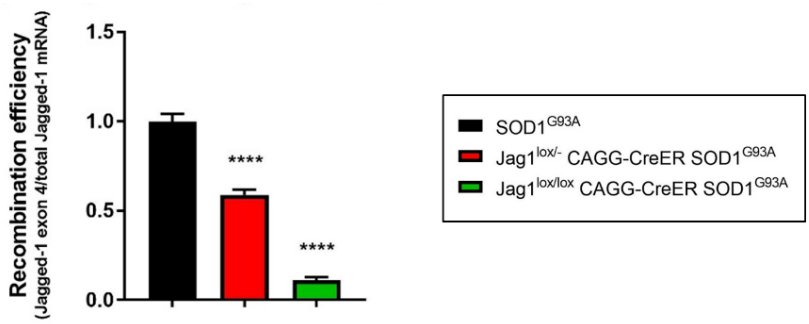


***Figure 19: Efficiency of ubiquitously induced Jagged-1 inactivation.*** *Recombination efficiency in spinal cord of Jagged-1$^{lox/lox}$ CAGG-CreER mice, Jagged-1$^{lox/-}$ CAGG-CreER mice and Jagged-1$^{lox/lox}$ control mice after tamoxifen administration, determined by qRT-PCR for exon 4 of Jagged-1 and for total Jagged-1 expression. Hprt and Gapdh were used for normalization (determined by geNorm analysis). One-way ANOVA with Bonferroni's posthoc analysis: ****p<0.0001, n=6 mice per group. All mice received tamoxifen at 60 days of age. Mean ± SEM.*

We observed that homozygous ubiquitous inactivation of Jagged-1 in *SOD1$^{G93A}$* mice (*Jagged-1$^{lox/lox}$ CAGG-CreER SOD1$^{G93A}$* + tamoxifen) had a clear beneficial effect on disease onset with a delay in onset of on average 10%, or 12 days, compared to control *SOD1$^{G93A}$* mice (*SOD1$^{G93A}$* + tamoxifen) (Figure 20A). This effect was mainly carried by the female mice, as female *SOD1$^{G93A}$* mice with homozygous Jagged-1 inactivation had a significant delay in disease onset of on average 17%, or 20 days (Figure 20B). Only a trend for a difference was evident in males (Figure 20C).

Because of this gender-based differential effect, we further studied female and male mice separately. Interestingly, homozygous ubiquitous inactivation of Jagged-1 in female *SOD1$^{G93A}$* mice (*Jagged-1$^{lox/lox}$ CAGG-CreER SOD1$^{G93A}$* + tamoxifen) showed also a significant benefit on survival of approximately 10%, or 15 days, compared to control female ALS mice (*SOD1$^{G93A}$* + tamoxifen) (Figure 20D). This benefit was not observed in the male homozygous Jagged-1 inactivated *SOD1$^{G93A}$* mice (Figure 20E). Disease duration was not altered in the female population (Figure 20F), suggesting that the longer survival can be explained by a delayed disease onset. In the male population we observed a clear trend towards a shorter disease duration (Figure 20G), supporting the trend for a later onset without an effect on survival described above.

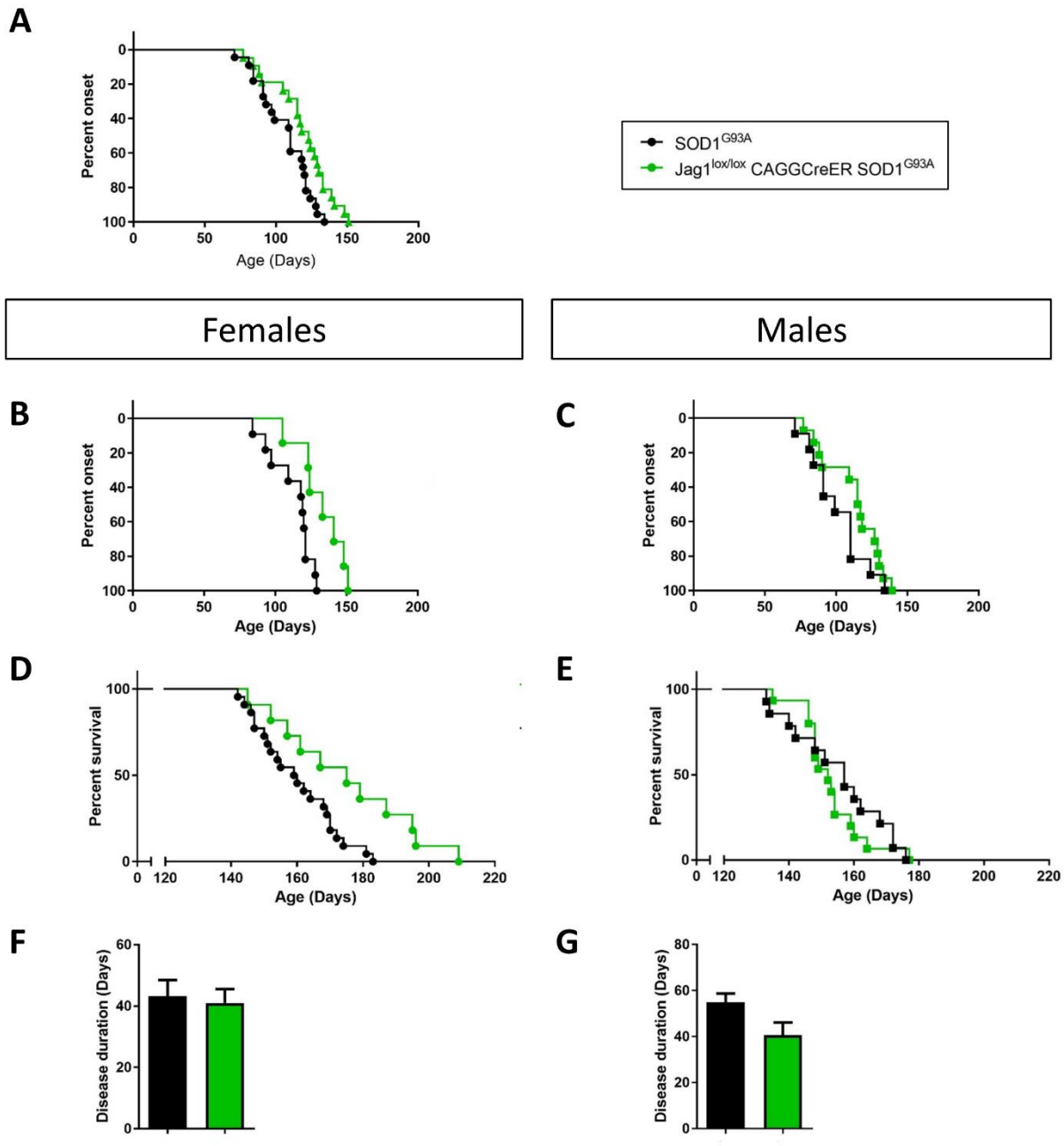


***Figure 20: Homozygous ubiquitous inactivation of Jagged-1 in female SOD1$^{G93A}$ mice improves disease outcome.*** *(A) Onset analysis determined by peak of bodyweight in Jagged-1$^{lox/lox}$ CAGG-CreER SOD1$^{G93A}$ mice (n=21) and control SOD1$^{G93A}$ mice (n=22): 119 ± 5 days compared to 107 ± 4 days, Log-rank Mantel-Cox test: *p<0.05. (B) Onset analysis of female Jagged-1$^{lox/lox}$ CAGG-CreER SOD1$^{G93A}$ mice (n=7) and female control SOD1$^{G93A}$ mice (n=11): 132 ± 6 days compared to 113 ± 5 days, Log-rank Mantel-Cox test: **p<0.01. (C) Onset analysis of male Jagged-1$^{lox/lox}$ CAGG-CreER SOD1$^{G93A}$ mice (n=14) and male control SOD1$^{G93A}$ mice (n=11): 112 ± 5 days compared to 101 ± 6 days, Log-rank Mantel-Cox test: p>0.05. (D) Survival analysis in female Jagged-1$^{lox/lox}$ CAGG-CreER SOD1$^{G93A}$ mice (n=11) and female control SOD1$^{G93A}$ mice (n=22): 175 ± 6 days compared to 160 ± 3 days, Log-rank Mantel-Cox test: *p<0.05. (E) Survival analysis in male Jagged-1$^{lox/lox}$ CAGG-CreER SOD1$^{G93A}$ mice (n=15) and male control SOD1$^{G93A}$ mice (n=14): 153 ± 3 days compared to 155 ± 4 days, Log-rank Mantel-Cox test: p>0.05. (F) Disease duration in female Jagged-1$^{lox/lox}$ CAGG-CreER SOD1$^{G93A}$ mice (n=7) and female control SOD1$^{G93A}$ mice (n=11): 41 ± 5 days compared to 43 ± 5 days, unpaired t-test: p>0.05. (G) Disease duration in male Jagged-1$^{lox/lox}$ CAGG-CreER SOD1$^{G93A}$ mice (n=14) and male control SOD1$^{G93A}$ mice (n=11): 41 ± 6 days compared to 55 ± 4 days, unpaired t-test: p=0.057. All mice received tamoxifen at the age of 60 days. Data represent mean ± SEM.*

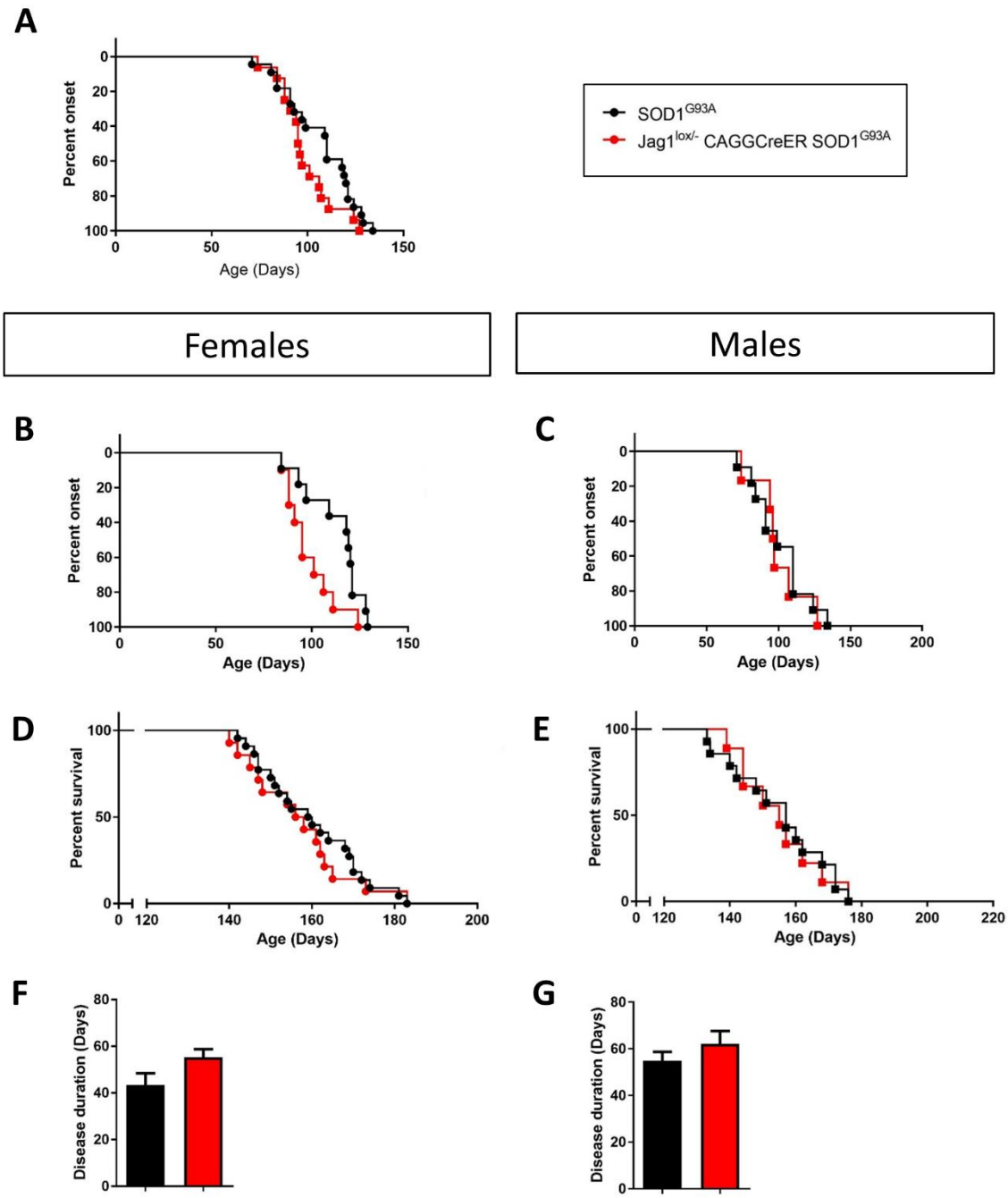


***Figure 21: Heterozygous inactivation of Jagged-1 in SOD1$^{G93A}$ mice does not alter the course of disease compared to control SOD1$^{G93A}$ mice.*** *(A) Onset analysis determined by peak of bodyweight in Jagged-1$^{lox/-}$ CAGG-CreER SOD1$^{G93A}$ mice (n=16) and control SOD1$^{G93A}$ mice (n=22): 99 ± 4 days compared to 107 ± 4 days, Log-rank Mantel-Cox test: p>0.05. (B) Onset analysis of female Jagged-1$^{lox/-}$ CAGG-CreER SOD1$^{G93A}$ mice (n=10) and female control SOD1$^{G93A}$ mice (n=11): 98 ± 4 days compared to 113 ± 5 days, Log-rank Mantel-Cox test: *p<0.05. (C) Onset analysis of male Jagged-1$^{lox/-}$ CAGG-CreER SOD1$^{G93A}$ mice (n=6) and male control SOD1$^{G93A}$ mice (n=11): 99 ± 7 days compared to 101 ± 6 days, Log-rank Mantel-Cox test: p>0.05. (D) Survival analysis in female Jagged-1$^{lox/-}$ CAGG-CreER SOD1$^{G93A}$ mice (n=14) and female control SOD1$^{G93A}$ mice (n=22): 157 ± 3 days compared to 160 ± 3 days, Log-rank Mantel-Cox test: p>0.05. (E) Survival analysis in male Jagged-1$^{lox/-}$ CAGG-CreER SOD1$^{G93A}$ mice (n=9) and male control SOD1$^{G93A}$ mice (n=14): 155 ± 4 days compared to 155 ± 4 days, Log-rank Mantel-Cox test: p>0.05. (F) Disease duration in female Jagged-1$^{lox/-}$ CAGG-CreER SOD1$^{G93A}$ mice (n=10) and female control SOD1$^{G93A}$ mice (n=11): 55 ± 4 days compared to 43 ± 5 days, unpaired t-test: p>0.05. (G) Disease duration in male Jagged-1$^{lox/-}$ CAGG-CreER SOD1$^{G93A}$ mice (n=6) and male control SOD1$^{G93A}$ mice (n=11): 62 ± 5 days compared to 55 ± 4 days, unpaired t-test: p>0.05. All mice received tamoxifen at the age of 60 days. Data represent mean ± SEM.*

The onset, survival and disease duration of the *SOD1$^{G93A}$* mice with heterozygous inactivation of Jagged-1 (*Jagged-1$^{lox/-}$ CAGG-CreER SOD1$^{G93A}$* + tamoxifen), both females and males, was not different from control *SOD1$^{G93A}$* mice (*SOD1$^{G93A}$* + tamoxifen) (Figure 21).

We evaluated whether the difference in the effect of Jagged-1 inactivation between male and female mice was due to a difference in Jagged-1 expression, or a difference in excision efficiency of the floxed exon 4 of the *Jagged-1* gene, but none of this was the case (Figure 22A). We also evaluated whether the gender effect was due to differences in the expression level of human *SOD1* that is overexpressed in our *SOD1$^{G93A}$* mouse model, but could not detect any differences between the groups (Figure 22B). The exact reason for the gender-dependent effect remains unknown.

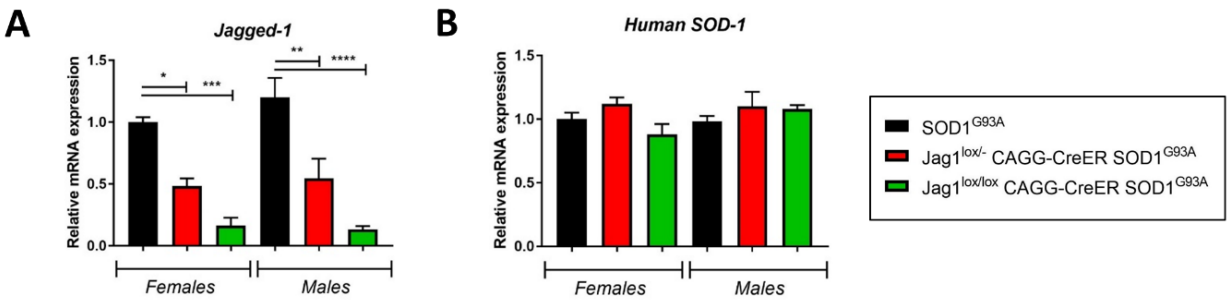


***Figure 22: Jagged-1 expression, recombination efficiency and human SOD1 expression was not different in female mice compared to male mice.*** *(A) Jagged-1 expression and recombination efficiency in female and male Jagged-1$^{lox/lox}$ CAGG-CreER SOD1$^{G93A}$ mice, Jagged-1$^{lox/-}$ CAGG-CreER SOD1$^{G93A}$ mice and control SOD1$^{G93A}$ mice was determined by qRT-PCR. (B) The expression of human SOD-1 mRNA levels was assessed by qRT-PCR in female and male Jagged-1$^{lox/lox}$ CAGG-CreER SOD1$^{G93A}$ mice, Jagged-1$^{lox/-}$ CAGG-CreER SOD1$^{G93A}$ mice and control SOD1$^{G93A}$ mice. One-way ANOVA with Bonferroni's posthoc analysis: * p<0.05, ** p<0.01, *** p<0.001, n=3 mice per group. All mice received tamoxifen at the age of 60 days. Data represent mean ± SEM.*

Measurements of bodyweight during disease progression, as a general parameter to determine wellbeing of the mice, showed that weight loss became apparent at approximately 120 days in female control *SOD1$^{G93A}$* mice, while the bodyweight of female *SOD1$^{G93A}$* mice with homozygous Jagged-1 inactivation was steady state much longer (Figure 23). Male *SOD1$^{G93A}$* mice with homozygous Jagged-

1 inactivation showed the same degree of weight loss compared to male control *SOD1$^{G93A}$* mice (Figure 23).

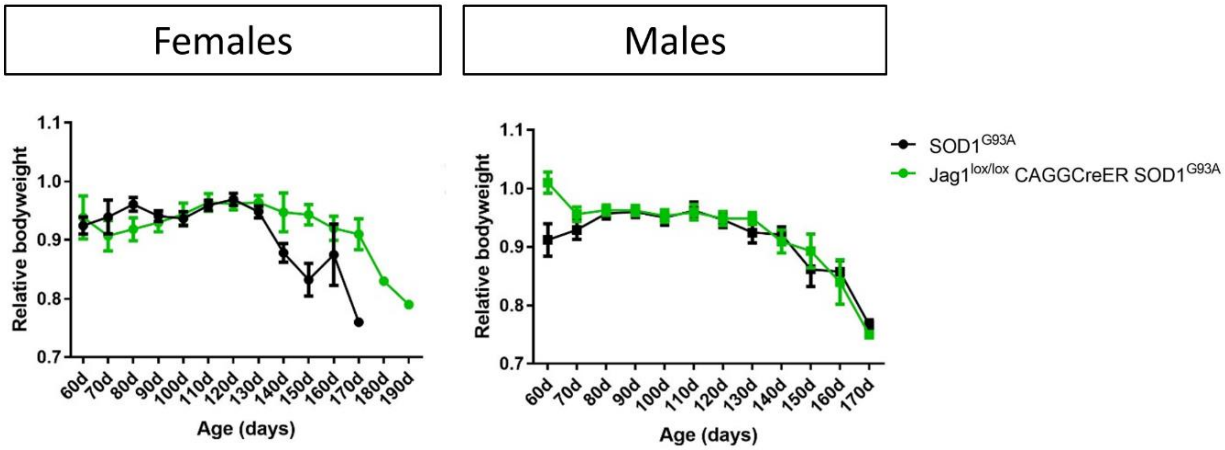


***Figure 23: Homozygous ubiquitous inactivation of Jagged-1 reduces bodyweight loss in female SOD1$^{G93A}$ mice, but not in male mice.*** *Bodyweight follow-up during disease progression (determined as weight relative to the maximal weight) in (A) female Jagged-1$^{lox/lox}$ CAGG-CreER SOD1$^{G93A}$ mice (n=7) and female control SOD1$^{G93A}$ mice (n=11) and (B) male Jagged-1$^{lox/lox}$ CAGG-CreER SOD1$^{G93A}$ mice (n=14) and male control SOD1$^{G93A}$ mice (n=11). Two-way ANOVA: for age is ***p<0.001 and for genotype is ** p<0.01 (females) or p>0.05 (males). Data represent mean ± SEM. All mice received tamoxifen at the age of 60 days.*

To evaluate motor performance in the ubiquitous Jagged-1 inactivation mice, we could not use the classical hanging grid test, because ubiquitous homozygous inactivation of Jagged-1 in mice without *SOD1$^{G93A}$* at the age of 60 days resulted approximately one month later into posture alterations (Figure 24A), mainly of the vertebral column, that significantly impaired their performance on the hanging grid test (Figure 24B). An extensive number of publications explains the involvement of Notch signaling in homeostasis of bone and skeletal health (194), but no clear bone phenotype became apparent by taking X-ray scans of these mice (Figure 24C). Instead of the hanging grid test, we only used the rotarod test to evaluate motor performance, as the Jagged-1 inactivation mice without *SOD1$^{G93A}$* (*Jagged-1$^{lox/lox}$ CAGG-CreER* + tamoxifen) performed normal on the latter test (Figure 24D), albeit the test obviously required a greater effort of the Jagged-1 inactivation mice due to the posture alterations. In addition, these mice also lose hair (Figure 24A), which makes them look smaller, but no difference in bodyweight was detected in homozygous ubiquitous Jagged-1 inactivation mice (*Jagged-1$^{lox/lox}$ CAGG-CreER* +

tamoxifen) compared to control mice (*Jagged-1*$^{lox/lox}$ + tamoxifen) (Figure 24E). Heterozygous Jagged-1 inactivation mice (*Jagged-1*$^{lox/-}$ *CAGG-CreER* + tamoxifen) did not develop a phenotype and performed like the control mice (*Jagged-1*$^{lox/lox}$ + tamoxifen).

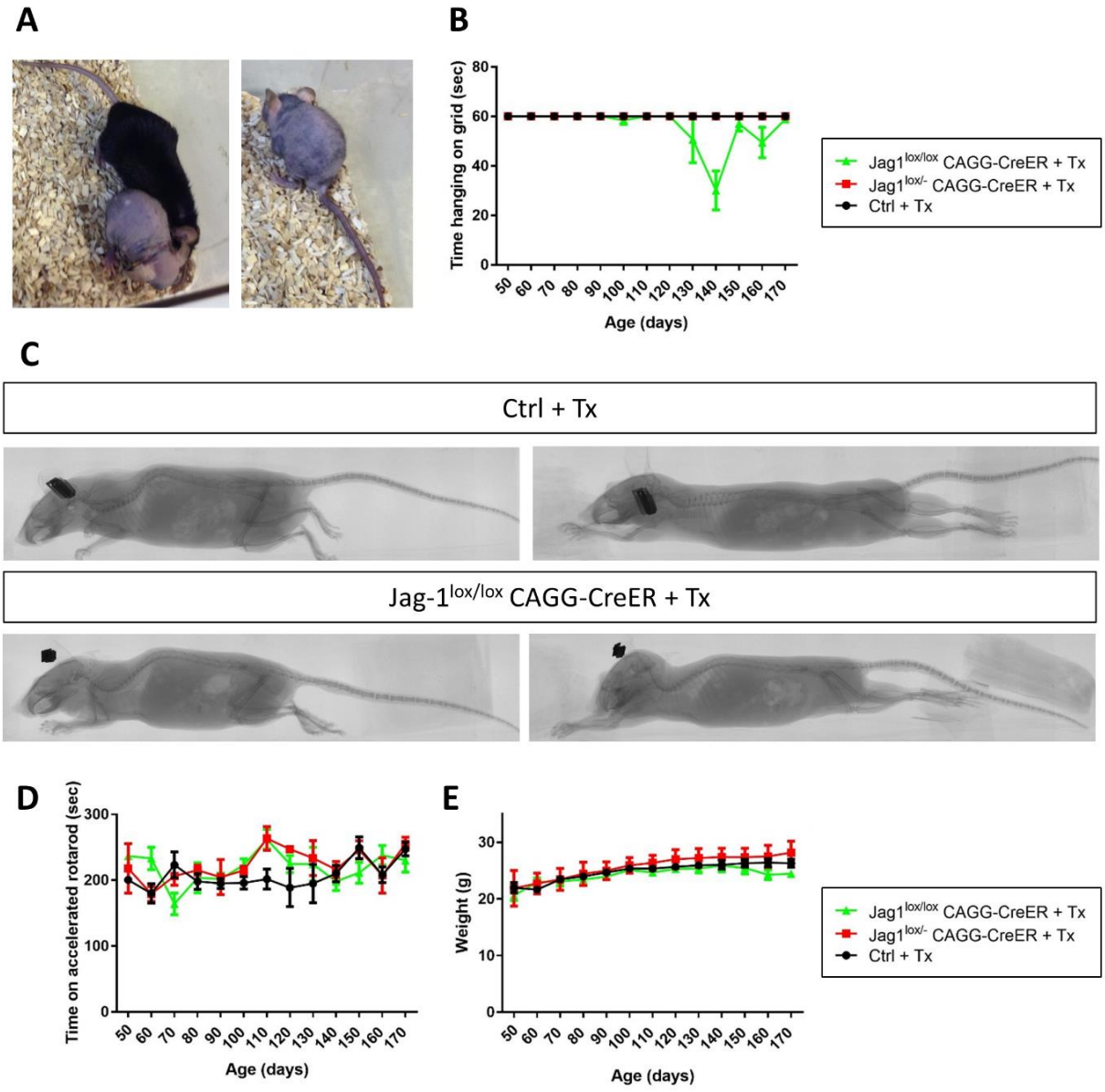


***Figure 24: Phenotyping of mice with ubiquitous inactivation of Jagged-1, but without SOD1$^{G93A}$.*** *(A) Representative image of the appearance of Jagged-1*$^{lox/lox}$ *CAGG-CreER mice and control Jagged-1*$^{lox/lox}$ *mice. (B) Performance on the hanging grid test over time of Jagged-1*$^{lox/lox}$ *CAGG-CreER mice (n=5), Jagged-1*$^{lox/-}$ *CAGG-CreER mice (n=3) and Jagged-1*$^{lox/lox}$ *control mice (n=7). (C) Representative image of X-ray scans of Jagged-1*$^{lox/lox}$ *CAGG-CreER mice and control Jagged-1*$^{lox/lox}$ *mice in a position at rest (left panels) and in a stretched position (right panels). (D) Performance on the accelerated rotarod test of Jagged-1*$^{lox/lox}$ *CAGG-CreER mice (n=5), Jagged-1*$^{lox/-}$ *CAGG-CreER mice (n=3) and Jagged-1*$^{lox/lox}$ *control mice (n=7) and (E) follow-up of bodyweight over time. All mice received tamoxifen at the age of 60 days. Data represent mean ± SEM.*

When evaluating the rotarod test in *SOD1$^{G93A}$* mice with Jagged-1 inactivation and control *SOD1$^{G93A}$* mice, we observed for the female *SOD1$^{G93A}$* mice with homozygous ubiquitous Jagged-1 inactivation a trend towards improved performance on fixed rotarod (Figure 25A) and significantly improved performance on accelerated rotarod (Figure 25C). These results might be an underestimation of the improved motor performance because the deformities observed in the homozygous ubiquitous Jagged-1 inactivation *SOD1$^{G93A}$* mice can reduce the beneficial effect. No significant difference in rotarod performance was observed in male mice (Figure 25B and D).

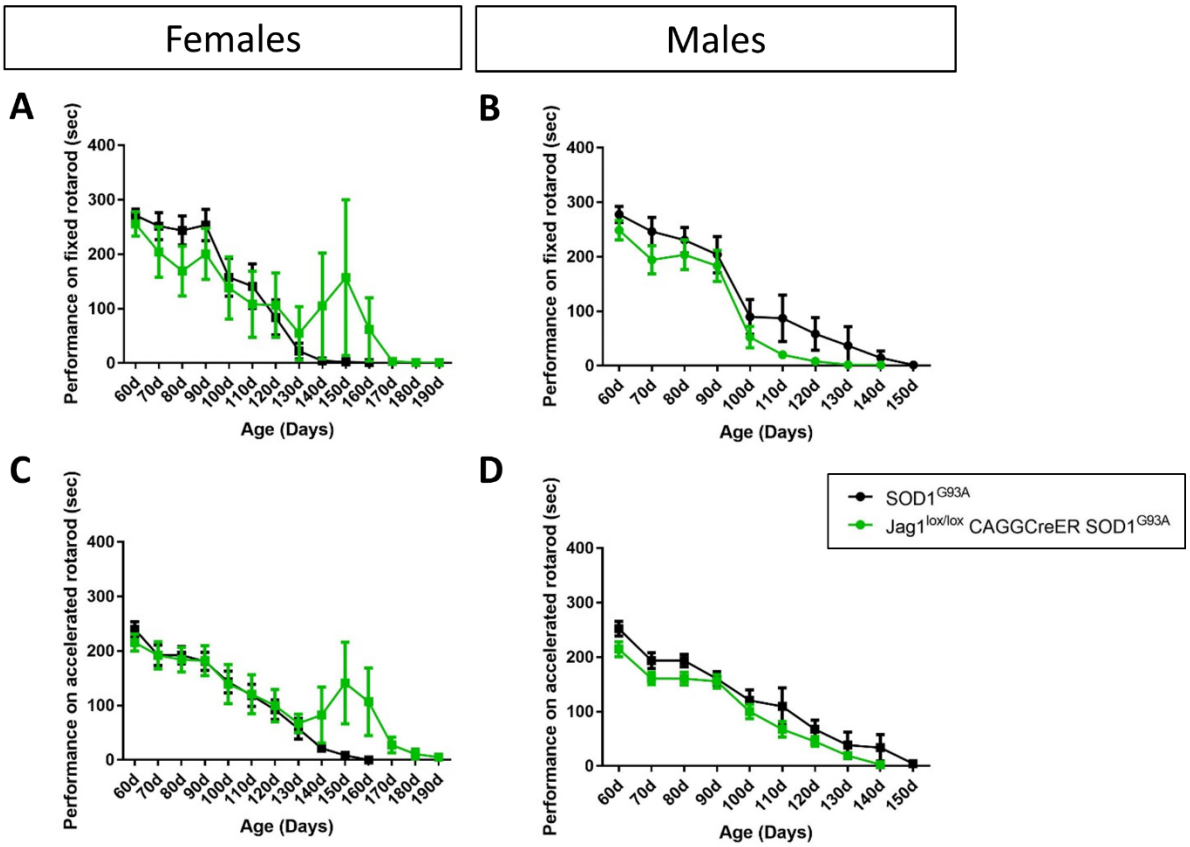


***Figure 25: Homozygous ubiquitous inactivation of Jagged-1 improves motor performance in female SOD1$^{G93A}$ mice.*** *Motor performance of (A and C) female Jagged-1$^{lox/lox}$ CAGG-CreER SOD1$^{G93A}$ mice (n=6) and female control SOD1$^{G93A}$ mice (n=10) and (B and D) male Jagged-1$^{lox/lox}$ CAGG-CreER SOD1$^{G93A}$ mice (n=13) and male control SOD1$^{G93A}$ mice (n=8) evaluated by means of (A and B) the fixed rotarod test (Two-way ANOVA: **** p<0.0001 for age and p>0.05 for genotype) and (C and D) the accelerated rotarod test. (Two-way ANOVA: **** p<0.0001 for age and *p<0.05 for genotype (for females). Data represent mean ± SEM. All mice received tamoxifen at the age of 60 days.*

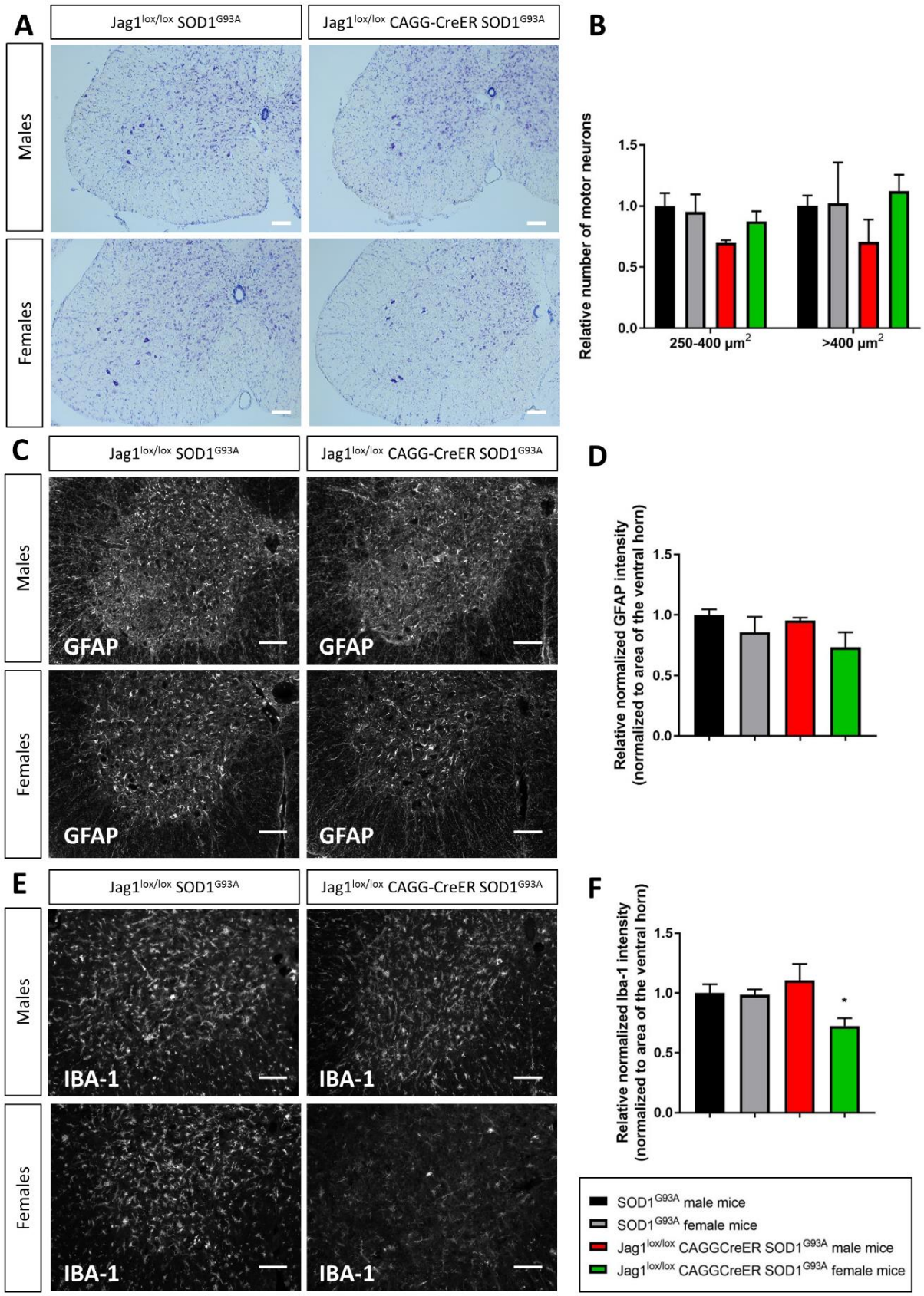


***Figure 26: Homozygous ubiquitous inactivation of Jagged-1 does not reduce motor neuron loss and reactive astrogliosis, but it reduces reactive microgliosis in female SOD1$^{G93A}$ mice.*** *(A-B) Representative images of the thionin staining in the spinal cord of male (n=3 mice per group) and female (n=4 mice per group) Jagged-1$^{lox/lox}$ CAGG-CreER SOD1$^{G93A}$ mice and control SOD1$^{G93A}$ mice at the age of 130 days was used to quantify the number*

*of small motor neurons (with a cell body area of 250-400 µm$^2$) and large motor neurons (with a cell body area above 400µm$^2$) shown in (B). Scale bar is 100 µm. Two-way ANOVA with Holm-Sidak's multiple comparison test: p>0.05. (C-F) Representative images of the immunofluorescent staining of the astrocytic marker GFAP (C) and the microglial marker IBA-1 (E) and their quantification (D and F) in lumbar spinal cord ventral horn of symptomatic male (n=3 mice per group) and female (n=4 mice per group) Jagged-1$^{lox/lox}$ CAGG-CreER SOD1$^{G93A}$ mice and control SOD1$^{G93A}$ mice, both at the age of 130 days. Scale bar is 100 µm. One-way ANOVA with Tukey's multiple comparison test: *p<0.05. Data represent mean ± SEM. All mice received tamoxifen at the age of 60 days.*

Quantification of the number of motor neurons at the age of 130 days revealed that both the number of small motor neurons (cell body area of 250-400 µm$^2$) and the number of large motor neurons (cell body area greater than 400µm$^2$) were not significantly different between female and male *SOD1$^{G93A}$* mice with and without ubiquitous Jagged-1 inactivation (Figure 26A-B).

In addition, we investigated the reactive astrogliosis and microgliosis by immunofluorescent staining for the markers GFAP and IBA-1 respectively. Quantification of the GFAP- and IBA-1 immunoreactivity in the lumbar spinal cord of female *SOD1$^{G93A}$* mice with ubiquitous Jagged-1 inactivation revealed no effect on reactive astrogliosis compared to all other groups (Figure 26C-D). However, we detected a significant reduction of reactive microgliosis, reflected by a decrease of IBA-1 immunoreactivity (Figure 26E-F).

These data show that homozygous ubiquitous inactivation of Jagged-1 can delay disease onset, improve motor performance, reduce gliosis, and consequently prolong survival in *SOD1$^{G93A}$* mice. This difference was gender-dependent, being more obvious in female animals.

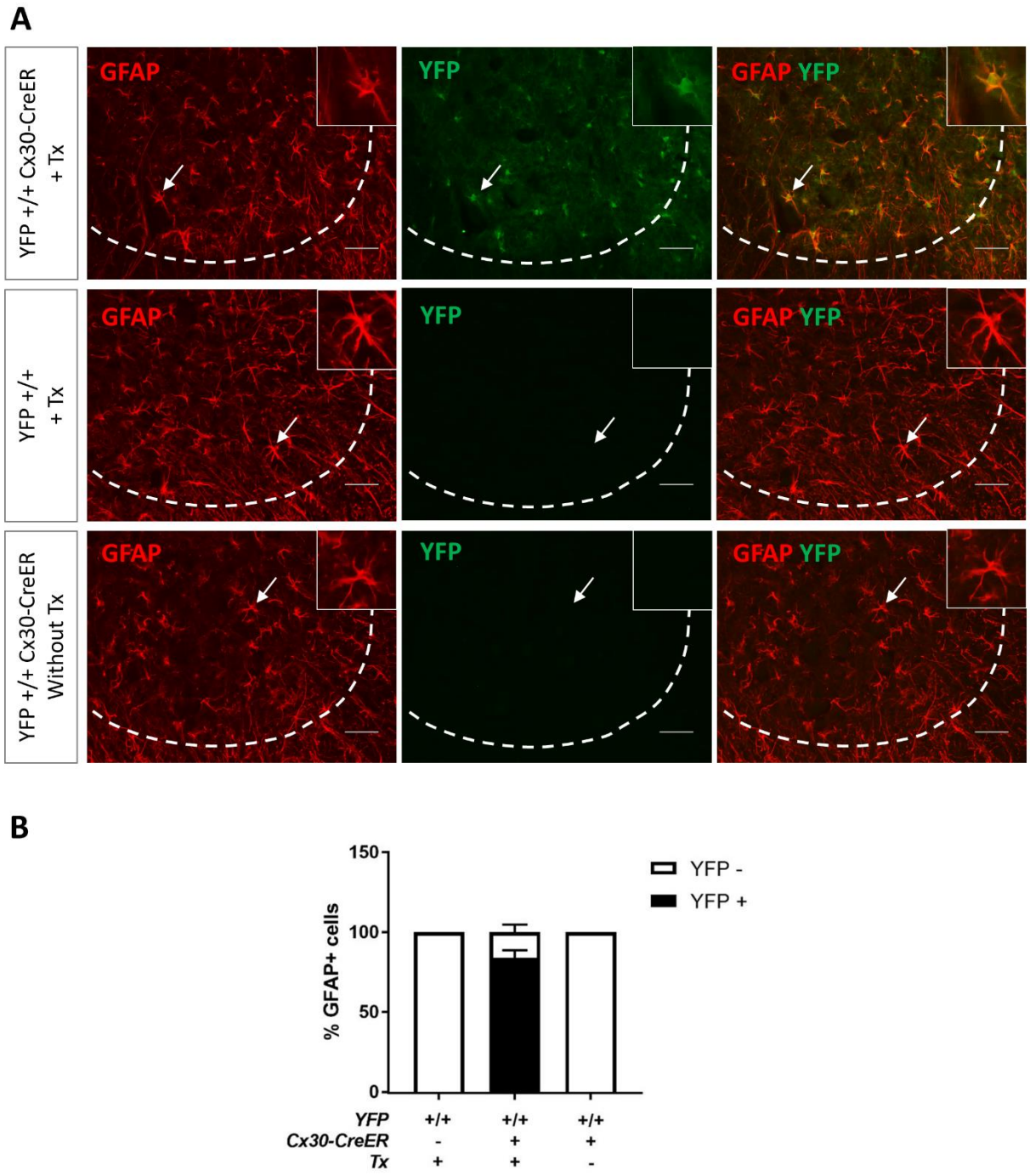


***Figure 27: Cx30-CreER induces highly efficient recombination specifically in astrocytes.*** *(A) Immuno-fluorescent staining of YFP (with an anti-GFP antibody) in combination with the astrocytic GFAP marker in the ventral horn of the lumbar spinal cord from Rosa-$^{lox}$STOP$^{lox}$-YFP Cx30-CreER mice (= YFP +/+ Cx30-CreER & Tx) and Rosa-$^{lox}$STOP$^{lox}$-YFP mice (= YFP +/+ & Tx), both receiving tamoxifen, and Rosa-$^{lox}$STOP$^{lox}$-YFP Cx30-CreER mice not receiving tamoxifen (= YFP +/+ Cx30-CreER & no Tx). The arrow indicates the astrocyte shown at a higher magnification in the upper right corner of each panel. Scale bar is 50 µm. (B) Quantification of the percentage of GFAP+ astrocytes expressing YFP, reflecting astrocyte-specific recombination in Rosa-$^{lox}$STOP$^{lox}$-YFP Cx30-CreER mice (= YFP +/+ Cx30-CreER & Tx) compared to controls (YFP +/+ & Tx and YFP +/+ Cx30-CreER & no Tx). Data represent mean ± SEM, n=3 mice per group. All mice received tamoxifen at the age of 60 days.*

### *Astrocyte-specific inactivation of Jagged-1 in the SOD1$^{G93A}$ mouse model*

To inactivate Jagged-1 specifically in astrocytes we crossbred *Jagged-1$^{lox/lox}$* mice with *Cx30-CreER* mice and *SOD1$^{G93A}$* mice. In these transgenic mice, exon 4 of the ligand Jagged-1 is deleted by Cre-mediated excision specifically in the astrocytes upon administration of tamoxifen (Tx) at the age of 60 days (asymptomatic), giving rise to a truncated non-functional JAGGED-1 protein lacking the Notch receptor binding domain as described above (193).

The specificity and efficiency of the astrocytic *Cx30-CreER* line (172, 173) was evaluated by crossbreeding *Cx30-CreER* mice to YFP reporter mice (*Rosa-$^{lox}$STOP$^{lox}$-YFP* mice), showing the expression of YFP upon tamoxifen induced Cre-mediated excision of the STOP-cassette. Immunofluorescent co-staining of YFP and GFAP in the spinal cord of *Rosa-$^{lox}$STOP$^{lox}$-YFP Cx30-CreER* mice after tamoxifen administration (*YFP+/+ Cx30-CreER* & Tx) revealed that YFP was only expressed in GFAP-positive astrocytes and that recombination took place in on average 84 ± 5% of all GFAP-positive astrocytes (Figure 27A-B). No recombination took place in the absence of tamoxifen (*YFP+/+ Cx30-CreER* & no Tx) or in the absence of *Cx30-CreER* (*YFP +/+* & Tx) (Figure 27A-B).

The offspring of the breeding of *Jagged-1$^{lox/lox}$* mice with *Cx30-CreER* mice and *SOD1$^{G93A}$* mice was treated with tamoxifen at the age of 60 days. This tamoxifen-induced deletion of exon 4 of *Jagged-1* in astrocytes resulted in a significant reduction of total spinal cord mRNA of *Jagged-1* containing exon 4 of on average 17.5 ± 3% in *Jagged-1$^{lox/lox}$ Cx30-CreER SOD1$^{G93A}$* mice and 9.2 ± 2% in *Jagged-1$^{lox/-}$ Cx30-CreER SOD1$^{G93A}$* mice when compared to control *SOD1$^{G93A}$* mice (*SOD1$^{G93A}$* + Tx) (Figure 28). The remaining expression of *Jagged-1* containing exon 4 thus largely came from non-astrocytic (mainly neuronal) cells.

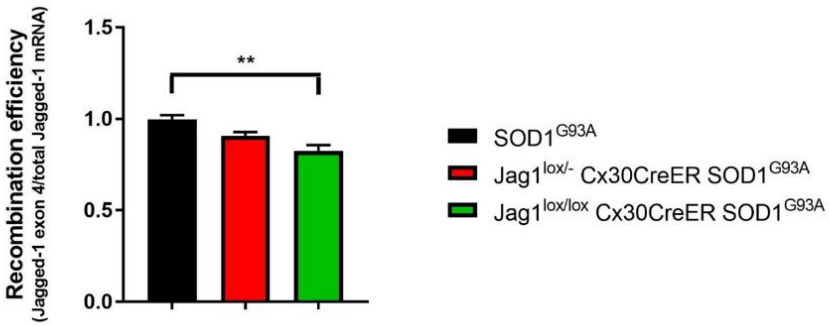


***Figure 28: Recombination efficiency of the astrocytic induced Jagged-1 inactivation.*** *Recombination efficiency in the spinal cord of Jagged-1$^{lox/lox}$ CAGG-CreER SOD1$^{G93A}$ mice and Jagged-1$^{lox/-}$ CAGG-CreER SOD1$^{G93A}$ mice compared to SOD1$^{G93A}$ control mice after tamoxifen administration was determined by qRT-PCR for exon 4 of Jagged-1 and normalized to the total Jagged-1 expression. Hprt and Gapdh were used as reference genes. One-way ANOVA with Bonferroni's posthoc analysis: **p<0.01, n=4 mice per group. Data represent mean ± SEM. All mice received tamoxifen at the age of 60 days.*

No gross phenotypical abnormalities were observed upon inactivation of Jagged-1 in double transgenic *Jagged-1$^{lox/lox}$ Cx30-CreER* mice (without *SOD1$^{G93A}$*) and *Jagged-1$^{lox/-}$ Cx30-CreER* mice (without *SOD1$^{G93A}$*), when compared to control *Jagged-1$^{lox/lox}$* mice.

Astrocytic homozygous inactivation of Jagged-1 in *SOD1$^{G93A}$* mice (*Jagged-1$^{lox/lox}$ Cx30-CreER SOD1$^{G93A}$* + Tx), had no effect on disease onset compared to control *SOD1$^{G93A}$* mice (*SOD1$^{G93A}$* + Tx) (Figure 29A), but accelerated disease after onset. Survival was significantly reduced with 18 days (Figure 29B) and consequently disease progression was hastened with an on average disease duration of 38 ± 5 days in *SOD1$^{G93A}$* mice with homozygous Jagged-1 inactivation (*Jagged-1$^{lox/lox}$ Cx30-CreER SOD1$^{G93A}$* + Tx) compared to 52 ± 3 days in control *SOD1$^{G93A}$* mice (Figure 29C).

Measurements of bodyweight during disease progression (Figure 29D) showed a significant enhancement of weight loss upon homozygous inactivation of Jagged-1 in astrocytes compared to control *SOD1$^{G93A}$* mice.

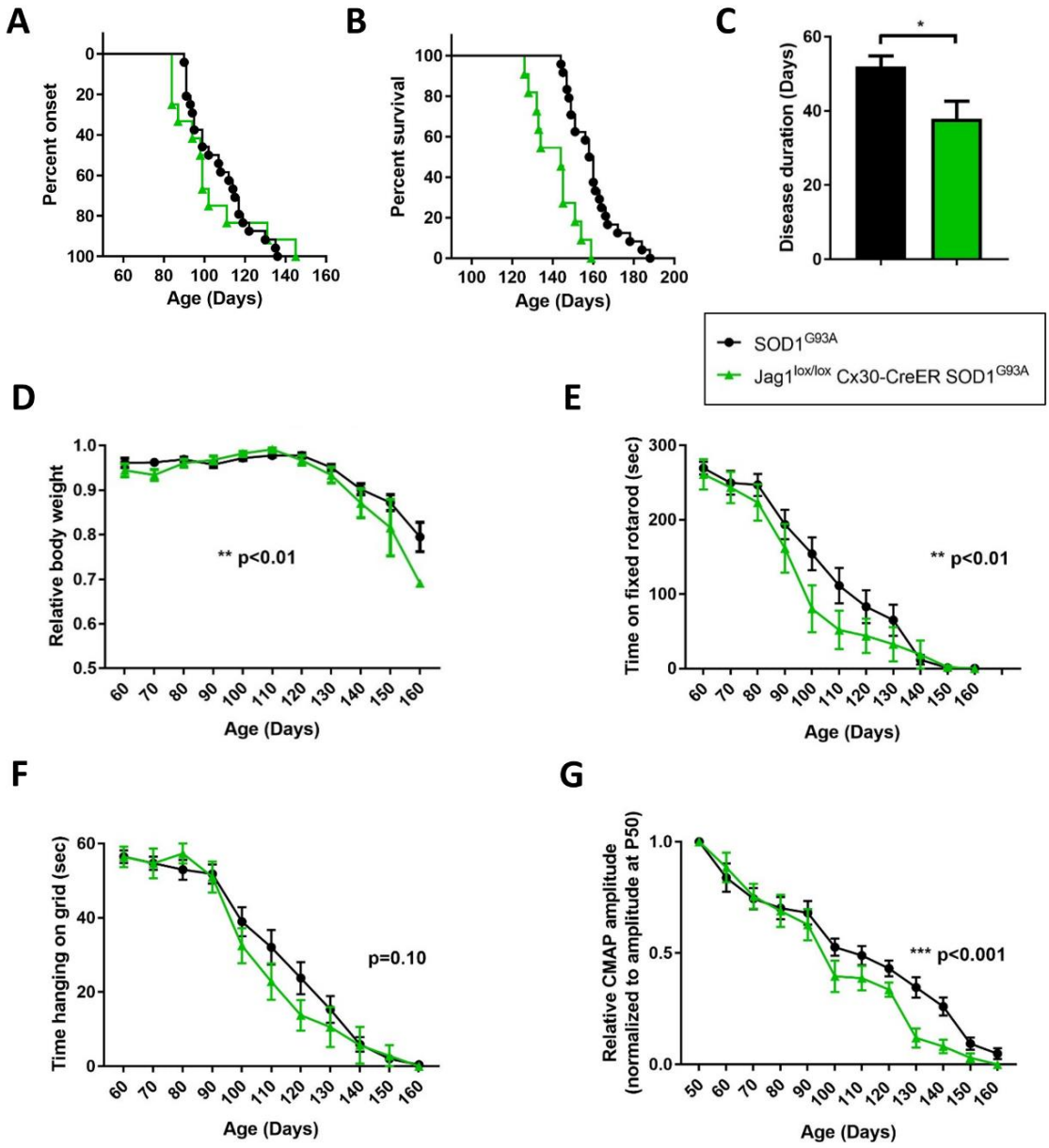


***Figure 29: Homozygous astrocyte-specific inactivation of JAGGED-1 in SOD1$^{G93A}$ mice aggravates disease progression.*** (A) Onset analysis determined by failure on the hanging grid test in *Jagged-1$^{lox/lox}$ Cx30-CreER SOD1$^{G93A}$* mice (102 ± 6 days, n=12) and control *SOD1$^{G93A}$* mice (107 ± 3 days, n=24). Log-rank Mantel-Cox test: p>0.05 (not significant). (B) Survival analysis in *Jagged-1$^{lox/lox}$ Cx30-CreER SOD1$^{G93A}$* mice (141 ± 3 days, n=11) and control *SOD1$^{G93A}$* mice (159 ± 3 days, n=24). Log-rank Mantel-Cox test: ****p<0.0001. (C) Disease duration in *Jagged-1$^{lox/lox}$ Cx30-CreER SOD1$^{G93A}$* mice (38 ± 5 days, n=11) and control *SOD1$^{G93A}$* mice (52 ± 3 days, n=23). Unpaired t-test: *p<0.05. (D) Follow-up of bodyweight during disease progression in *Jagged-1$^{lox/lox}$ Cx30-CreER SOD1$^{G93A}$* mice (n=12) and control *SOD1$^{G93A}$* mice (n=24). Two-way ANOVA: ****p<0.0001 for age and **p<0.01 for genotype. (E-F) Motor performance was determined during disease progression by means of (E) the fixed rotarod test (Two-way ANOVA: ****p<0.0001 for age and **p<0.01 for genotype) and (F) the hanging grid test (Two-way ANOVA: ****p<0.0001 for age and p=0.10 for genotype) in *Jagged-1$^{lox/lox}$ Cx30-CreER SOD1$^{G93A}$* mice (n=12) and control *SOD1$^{G93A}$* mice (n=25). (G) Innervation of the gastrocnemius muscle during the course of disease was determined by measuring CMAP amplitudes in *Jagged-1$^{lox/lox}$ Cx30-CreER SOD1$^{G93A}$* mice (n=12) and control *SOD1$^{G93A}$* mice (n=25). We normalized the CMAP amplitudes to the amplitude measured at the age of 50 days. Two-way ANOVA: ****p<0.0001 for age and ***p<0.001 for genotype. Data represent mean ± SEM. All mice received tamoxifen at the age of 60 days.

Motor performance was assessed by two classical tests, the fixed rotarod test (Figure 29E) and the hanging grid test (Figure 29F). We observed that *SOD1$^{G93A}$* mice with homozygous astrocyte-specific Jagged-1 inactivation perform significantly worse on the fixed rotarod tests compared to control *SOD1$^{G93A}$* mice (Figure 29E). With the hanging grid test, we could detect a clear tendency towards reduced performance (Figure 29F). Innervation of the gastrocnemius muscle was evaluated by measuring compound muscle action potentials (CMAP) at the level of the gastrocnemius muscle (Figure 29G). We observed that the CMAP amplitudes decreased significantly faster during disease progression, upon homozygous inactivation of Jagged-1 in astrocytes of *SOD1$^{G93A}$* mice, compared to control *SOD1$^{G93A}$* mice (Figure 29G). No difference in CMAP latencies was noticed (data not shown).

Heterozygous astrocytic inactivation of Jagged-1 in *SOD1$^{G93A}$* mice (*Jagged-1$^{lox/-}$ Cx30-CreER SOD1$^{G93A}$* + Tx) resulted in a more modest reduction of total spinal cord mRNA of *Jagged-1* containing exon 4 (on average 9.2 ± 2%) as expected (Figure 28) and did not affect disease onset (Figure 30A). Of interest, this limited Jagged-1 reduction shortened survival by on average 12 days compared to control *SOD1$^{G93A}$* mice (Figure 30B) and consequently a tendency towards a shorter disease duration was observed (Figure 30C). However, the evaluation of bodyweight loss, motor performance and muscle innervation over time did not reveal any differences between *Jagged-1$^{lox/-}$ Cx30-CreER SOD1$^{G93A}$* mice and control *SOD1$^{G93A}$* mice (Figure 30D-G).

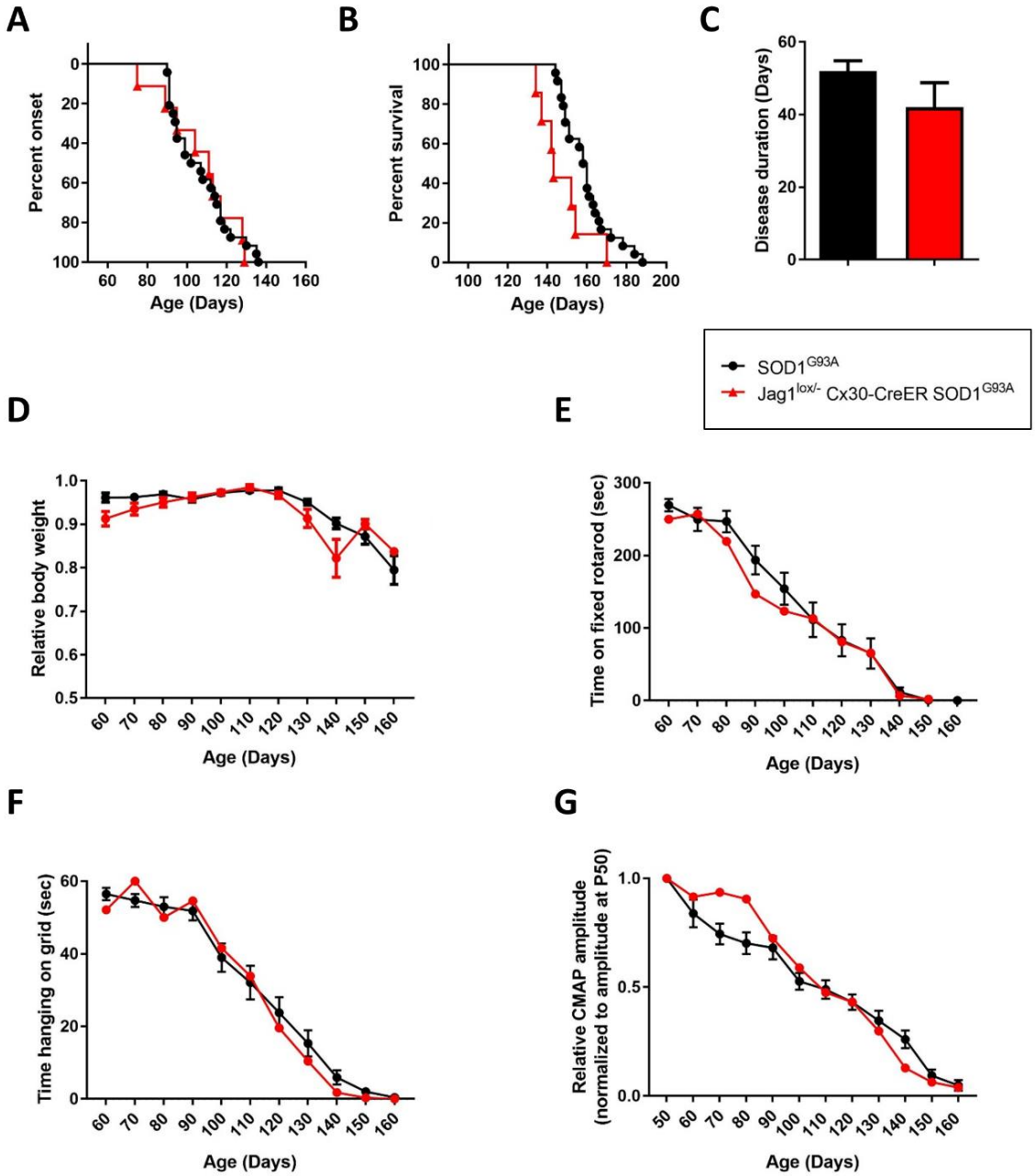


***Figure 30: Heterozygous astrocyte-specific inactivation of JAGGED-1 in SOD1$^{G93A}$ mice has no effect on disease progression.*** *(A) Onset analysis determined by failure on the hanging grid test in Jagged-1$^{lox/-}$ Cx30-CreER SOD1$^{G93A}$ mice (107 ± 6 days, n=9) and control SOD1$^{G93A}$ mice (107 ± 3 days, n=24). Log-rank Mantel-Cox test: p>0.05 (not significant). (B) Survival analysis in Jagged-1$^{lox/-}$ Cx30-CreER SOD1$^{G93A}$ mice (147 ± 5 days, n=7) and control SOD1$^{G93A}$ mice (159 ± 3 days, n=24). Log-rank Mantel-Cox test: *p<0.05. (C) Disease duration in Jagged-1$^{lox/-}$ Cx30-CreER SOD1$^{G93A}$ mice (42 ± 7 days, n=7) and control SOD1$^{G93A}$ mice (52 ± 3 days, n=23). Unpaired t-test: p=0.13. (D) Follow-up of bodyweight during disease progression in Jagged-1$^{lox/-}$ Cx30-CreER SOD1$^{G93A}$ mice (n=9) and control SOD1$^{G93A}$ mice (n=24). Two-way ANOVA: ****p<0.0001 for age and p>0.05 for genotype. (E-F) Motor performance was determined during disease progression by means of (E) the fixed rotarod test (Two-way ANOVA: ****p<0.0001 for age and p>0.05 for genotype) and (F) the hanging grid test (Two-way ANOVA: ****p<0.0001 for age and p>0.05 for genotype) in Jagged-1$^{lox/-}$ Cx30-CreER SOD1$^{G93A}$ mice (n=9) and control SOD1$^{G93A}$ mice (n=25). (G) Innervation of the gastrocnemius muscle during the course of disease was determined by measuring CMAP amplitudes in Jagged-1$^{lox/-}$ Cx30-CreER SOD1$^{G93A}$ mice (n=9) and control SOD1$^{G93A}$ mice (n=25). We normalized the CMAP amplitudes to the amplitude measured at the age of 50 days. Two-way ANOVA: ****p<0.0001 for age and p>0.05 for genotype. Data represent mean ± SEM. All mice received tamoxifen at the age of 60 days. The control SOD1$^{G93A}$ mice in these graphs are the same mice as in figure 29.*

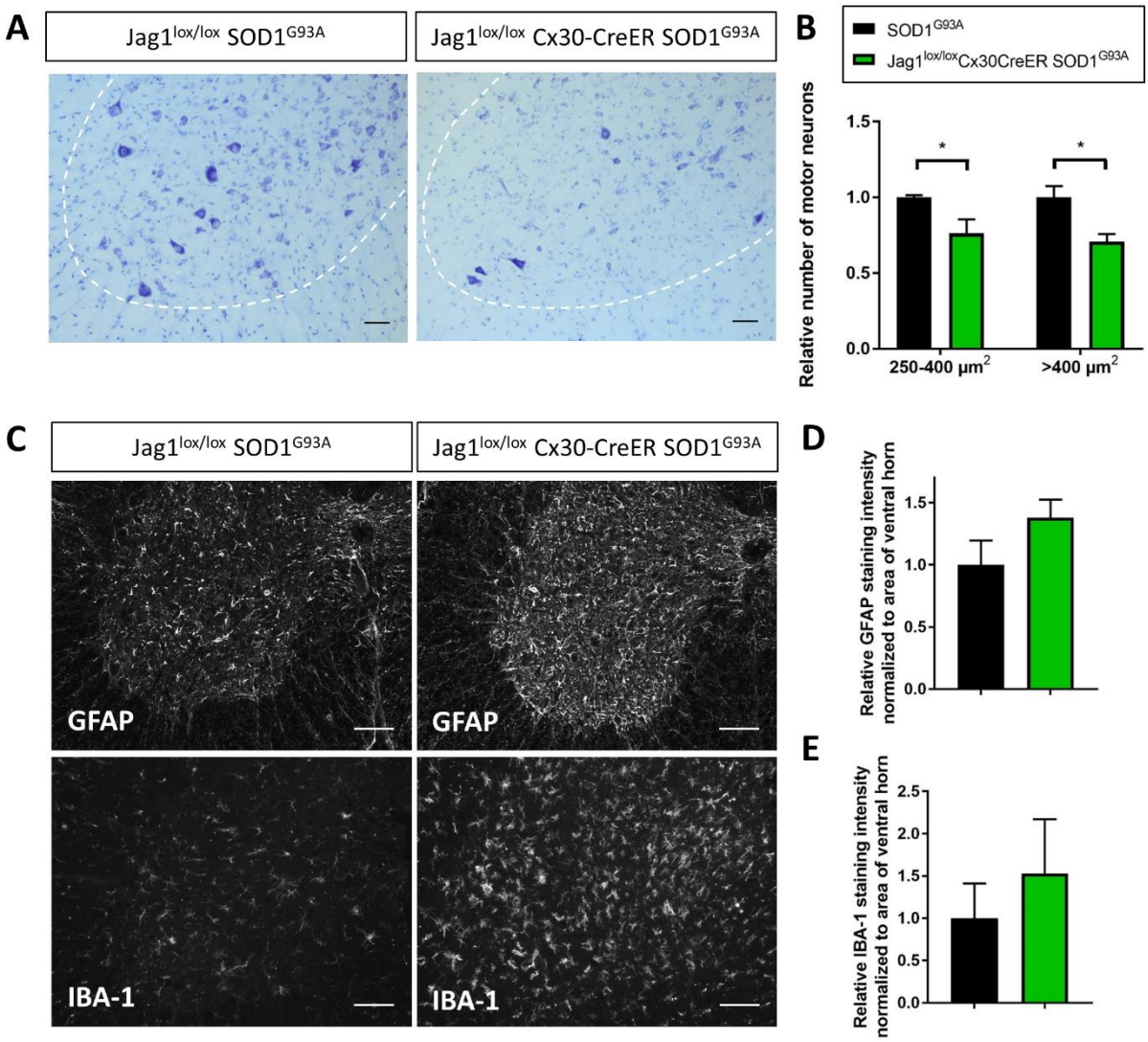


***Figure 31: Astrocyte-specific inactivation of JAGGED-1 in SOD1$^{G93A}$ mice aggravates motor neuron loss and gliosis.*** *(A-B) Thionin staining in the lumbar spinal cord ventral horn of Jagged-1$^{lox/lox}$ Cx30-CreER SOD1$^{G93A}$ mice (n=3) and control SOD1$^{G93A}$ mice (n=3) at the age of 130 days (scale bar is 50 µm) was used to quantify the number of small motor neurons (with a cell body area of 250-400 µm$^2$) and large motor neurons (with a cell body area above 400µm$^2$) shown in (B). One-way ANOVA with Holm-Sidak's multiple comparison test: *p<0.05. (C) Representative images of the immunofluorescent staining of the astrocytic marker GFAP (upper panels) and the microglial marker IBA-1 (lower panels) and (B-C) their quantification in lumbar spinal cord ventral horn of symptomatic Jagged-1$^{lox/lox}$ Cx30-CreER SOD1$^{G93A}$ mice (n=3) and control SOD1$^{G93A}$ mice (n=3), both at the age of 130 days. Scale bar is 100 µm. Unpaired t-test: p>0.05. Data represent mean ± SEM. All mice received tamoxifen at the age of 60 days.*

Quantification of the number of motor neurons revealed that the number of small motor neurons (cell body area of 250-400 µm$^2$) and large motor neurons (cell body area above 400µm$^2$) was significantly reduced in the lumbar spinal cord ventral horn of *Jagged-1$^{lox/lox}$ Cx30-CreER SOD1$^{G93A}$* mice at the age of 130 days, when compared to age-matched littermate control *SOD1$^{G93A}$* mice (Figure 31A-B). We

additionally investigated whether this enhanced disease severity was evident when quantifying reactive astrogliosis and microgliosis by staining for the markers GFAP and IBA-1, respectively (Figure 31C-E). Although not statistically significant, we observed a 38% increase in GFAP staining intensity and a 53% increase in IBA-1 staining in the lumbar spinal cord ventral horn of *Jagged-1$^{lox/lox}$ Cx30-CreER SOD1$^{G93A}$* mice at the age of 130 days compared to control *SOD1$^{G93A}$* mice (Figure 31C-E).

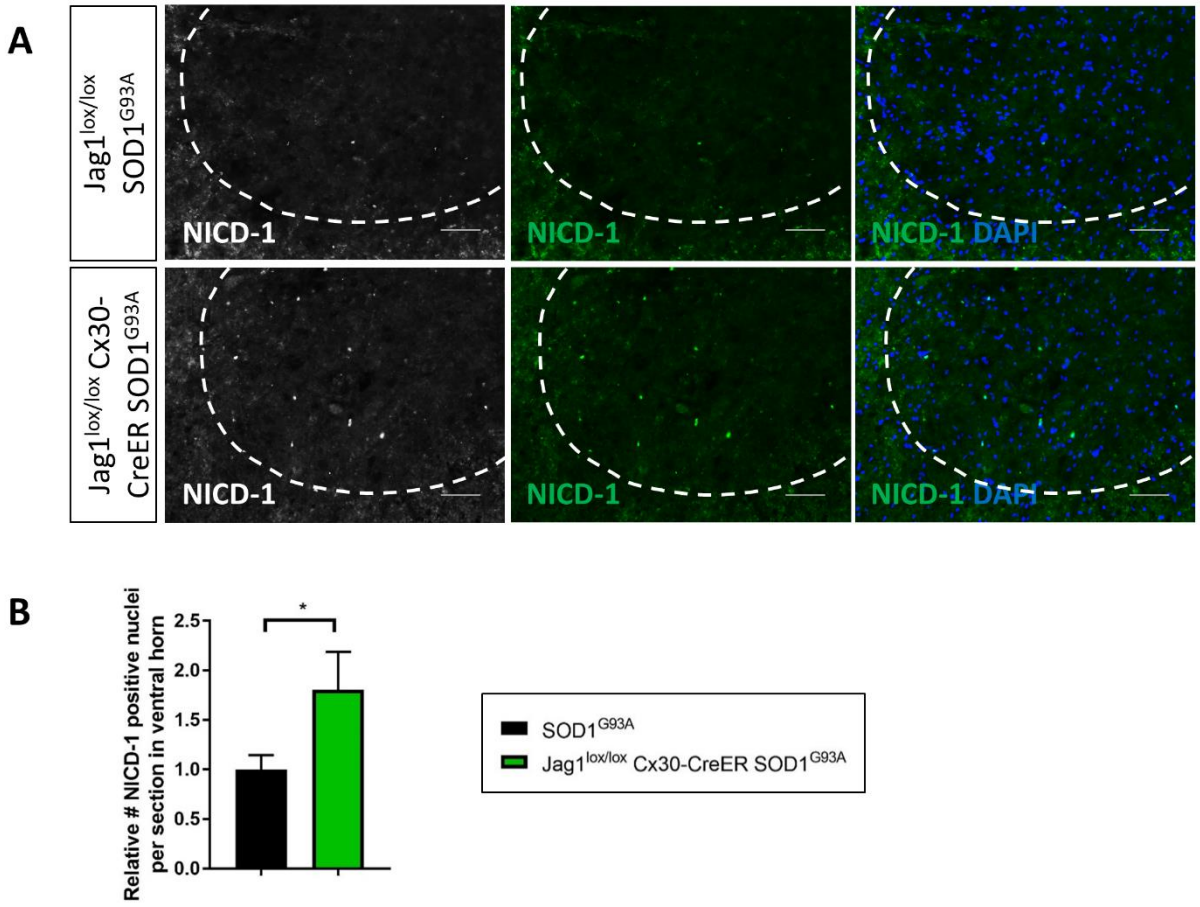


***Figure 32: Astrocyte-specific inactivation of JAGGED-1 in SOD1$^{G93A}$ mice enhances Notch signaling activation in lumbar spinal cord ventral horn.*** *(A) Representative image of the immunofluorescent staining of NICD-1 in the ventral horn of lumbar spinal cord of end stage Jagged-1$^{lox/lox}$ Cx30-CreER SOD1$^{G93A}$ mice (n=4) and end stage control SOD1$^{G93A}$ mice (n=4). Left and middle panels show the immunofluorescent staining of NICD-1 in white (for better visualization) and green. Right panel shows the overlay of NICD-1 with the DAPI stained nuclei and was used for the quantification of the NICD-1 positive nuclei shown in B. Scale bar is 50 µm. (B) Quantification of the number of NICD-1 positive nuclei per section in the lumbar spinal cord ventral horn. Unpaired t-test: *p<0.05. Data represent mean ± SEM. All mice received tamoxifen at the age of 60 days.*

We next evaluated the effect of astrocytic Jagged-1 inactivation on Notch signaling in this cell type. To this end, we stained for NICD-1 and quantified the number of NICD-1 positive nuclei in the lumbar spinal cord ventral horn of end stage *SOD1$^{G93A}$* mice and end stage *SOD1$^{G93A}$* mice with homozygous inactivation of Jagged-1 specifically in astrocytes (Figure 32A-B). We found the number of such NICD-1 positive nuclei to be significantly increased with 80% in *Jagged-1$^{lox/lox}$ Cx30-CreER SOD1$^{G93A}$* mice compared to control *SOD1$^{G93A}$* mice.

Together these data show that homozygous inactivation of Jagged-1 specifically in astrocytes of *SOD1$^{G93A}$* mice aggravates disease after onset, shortens survival and enhances Notch signaling activation, thereby suggesting a beneficial role for the ectopically expressed astrocytic Jagged-1 in ALS.

## 2.2 A receptor-based modulation approach

Next, we wanted to study Notch signaling inactivation in the *SOD1$^{G93A}$* mouse model via a receptor-based modulation approach and evaluate the effect of this manipulation on disease.

### *Ubiquitous deletion of RBPjk in the SOD1$^{G93A}$ mouse model, as a generalized method to inactivate the canonical signaling from all four Notch receptors*

As the Notch receptors Notch-1 and Notch-2 were found to be most prominently upregulated during disease in the spinal cord of the ALS mouse model and Notch-3 and Notch-4 show a moderate upregulation only at end stage (Figure 7A), we started by studying the effect of deleting RBPjk, a crucial co-factor for Notch signaling activation downstream of all four Notch receptors, as a generalized way to inhibit the signaling of all four Notch receptors at once. To obtain ubiquitous deletion of RBPjk we crossbred *RBPjk$^{lox/lox}$* mice with *CAGG-CreER* mice. In these transgenic mice, exons 6 and 7 of the

cofactor RBPjk were deleted ubiquitously by Cre-mediated excision upon administration of tamoxifen at the age of 60 days (asymptomatic). Recombination efficiency in the *RBPjk$^{lox/lox}$ CAGG-CreER* mice was on average 64 ± 5% (Figure 33).

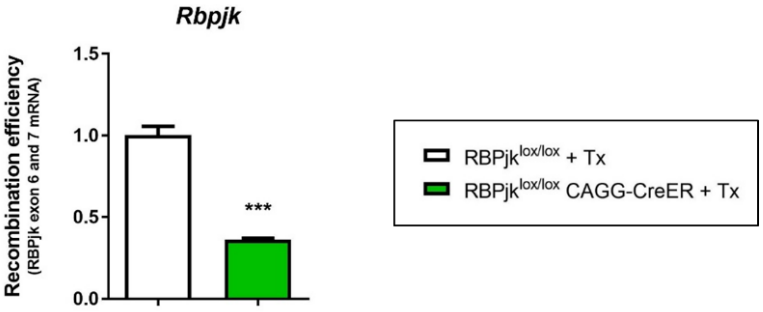


***Figure 33: Efficiency of the ubiquitously induced RBPjk deletion.*** *Recombination efficiency in the spinal cord of RPBjk$^{lox/lox}$ CAGG-CreER mice and RBPjk$^{lox/lox}$ control mice after tamoxifen administration was determined by qRT-PCR for exon 6 and 7 of RBPjk. Expression data are normalized to Polr2a and Gapdh (determined by geNorm analysis). Unpaired t-test: ***p<0.001 and n=3 mice per group. All mice received tamoxifen at the age of 60 days. Data represent mean ± SEM.*

However, homozygous ubiquitous deletion of RBPjk was found to result into early lethality (Figure 34) due to gastrointestinal toxicity. The early mortality was not ALS-related, but due to obstructions, perforation and bleedings of the gastrointestinal tract. Consequently, no data are available on disease onset and motor performance during disease progression in these mice.

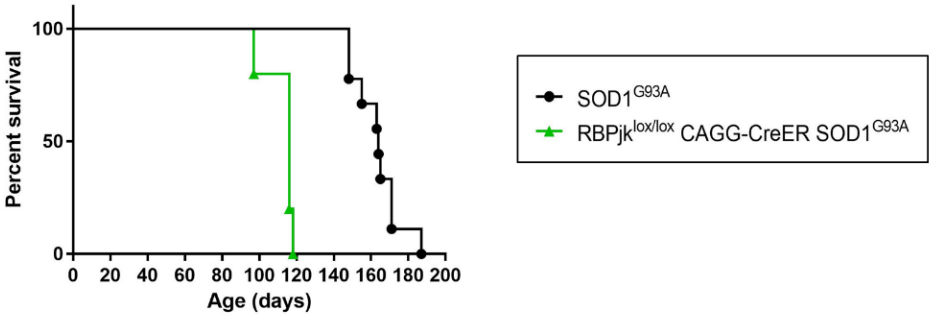


***Figure 34: Homozygous ubiquitously induced RBPjk deletion in the SOD1$^{G93A}$ mouse model results in early lethality, that is not ALS-related.*** *Survival analysis in RBPjk$^{lox/lox}$ CAGG-CreER SOD1$^{G93A}$ mice (113 ± 4 days, n=5) and control SOD1$^{G93A}$ mice (164 ± 4 days, n=9). Log-rank Mantel-Cox test: ****p<0.0001. Data represent mean ± SEM. All mice received tamoxifen at the age of 60 days.*

Heterozygous ubiquitous deletion of RBPjk did not result in early lethality, nor did it alter disease onset, survival, disease duration, or motor performance (Figure 35).

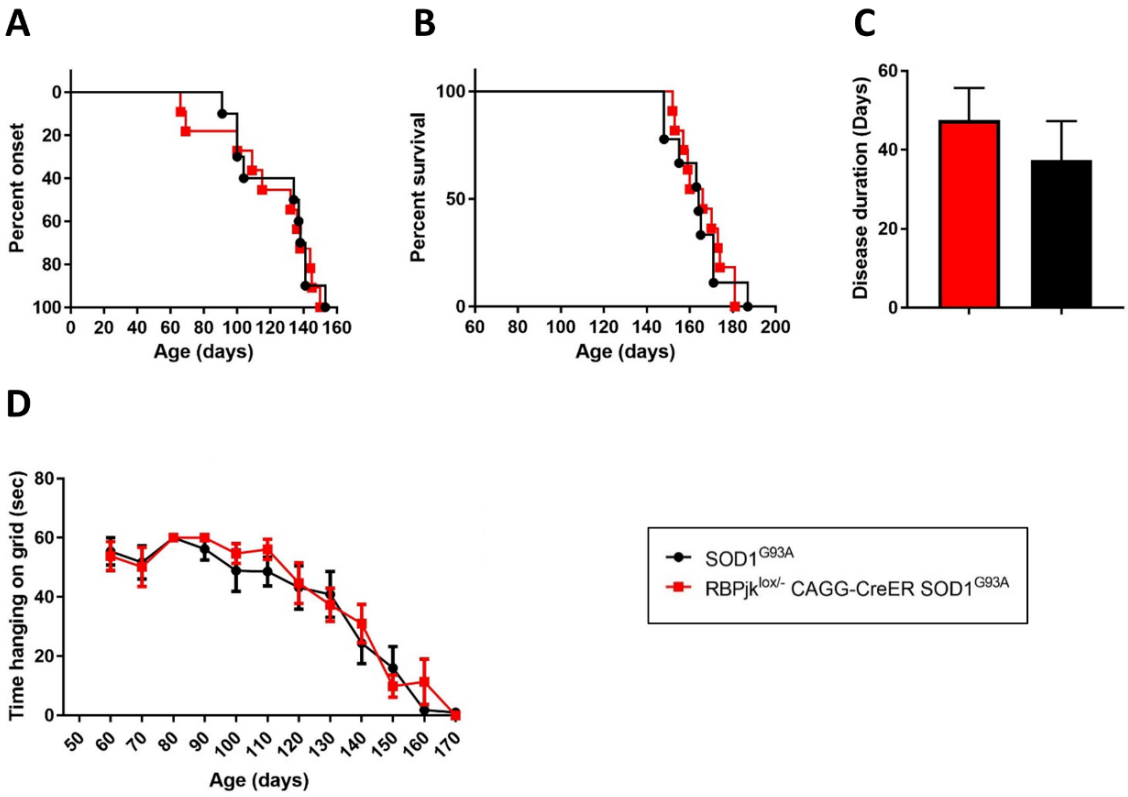


***Figure 35: Heterozygous ubiquitously induced RBPjk deletion in the SOD1$^{G93A}$ mouse model has no effect on disease.*** *(A) Onset analysis determined by failure on the hanging grid test in RBPjk$^{lox/-}$ CAGG-CreER SOD1$^{G93A}$ mice (119 ± 9 days, n=11) and control SOD1$^{G93A}$ mice (124 ± 7 days, n=10). Log-rank Mantel-Cox test: p>0.05. (B) Survival analysis in RBPjk$^{lox/-}$ CAGG-CreER SOD1$^{G93A}$ mice (166 ± 3 days, n=11) and control SOD1$^{G93A}$ mice (164 ± 4 days, n=9). Log-rank Mantel-Cox test: p>0.05. (C) Disease duration in RBPjk1$^{lox/-}$ CAGG-CreER SOD1$^{G93A}$ mice (47 ± 8 days, n=11) and control SOD1$^{G93A}$ mice (37 ± 10 days, n=9). One-way ANOVA with Bonferroni's posthoc analysis: p>0.05. (D) Motor performance was determined during disease progression by means of the hanging grid test (Two-way ANOVA: ****p<0.0001 for age and p>0.05 for genotype) in RBPjk$^{lox/-}$ CAGG-CreER SOD1$^{G93A}$ mice (n=11) and control SOD1$^{G93A}$ mice (n=12). Data represent mean ± SEM. All mice received tamoxifen at the age of 60 days.*

These data show that the generalized inhibition of Notch signaling by homozygous ubiquitous deletion of RBPjk is toxic and cannot be used to evaluate the effect of Notch signaling inactivation on disease in the SOD1$^{G93A}$ mouse model.

### *Ubiquitous deletion of Notch-1 in the SOD1$^{G93A}$ mouse model*

To avoid toxicity and early lethality related to the generalized Notch signaling inhibition-approach described, we decided to ubiquitously delete only the Notch-1 receptor. This because we showed in the first part '*Characterization of the Notch signaling pathway in ALS*' that the Notch-1 receptor is one of the two Notch receptors that are most prominently upregulated during disease in *SOD1$^{G93A}$* mouse spinal cords, as well as in *postmortem* spinal cords from ALS patients.

To this end, we crossbred *Notch-1$^{lox/lox}$* mice with *CAGG-CreER* mice. Upon administration of tamoxifen at the age of 60 days (asymptomatic) exon 1 of the Notch-1 receptor is deleted by Cre-mediated excision. Recombination efficiency obtained was on average 89 ± 1% in the *Notch-1$^{lox/lox}$ CAGG-CreER* mice and 38 ± 9% in *Notch-1$^{lox/-}$ CAGG-CreER* mice (Figure 36).

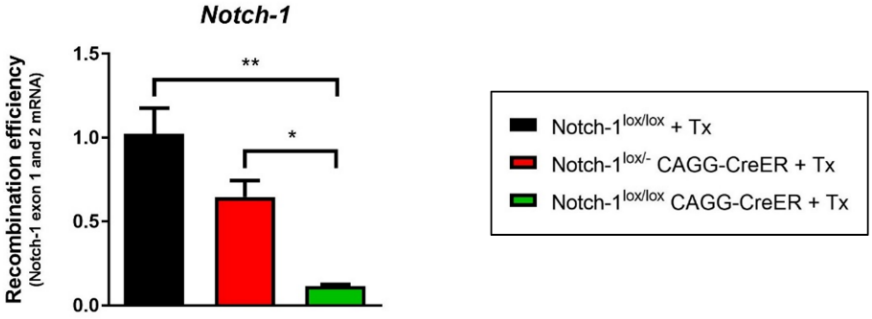


***Figure 36: Efficiency of the ubiquitously induced Notch-1 deletion.*** *Recombination efficiency in the spinal cord of Notch-1$^{lox/lox}$ CAGG-CreER mice, Notch-1$^{lox/-}$ CAGG-CreER mice and Notch-1$^{lox/lox}$ control mice after tamoxifen administration was determined by qRT-PCR for exon 1 of Notch-1. Expression data are normalized to Polr2a and Hprt (determined by geNorm analysis). One-way ANOVA with Bonferroni's posthoc analysis: *p<0.05, **p<0.01 and n=3 mice per group. All mice received tamoxifen at the age of 60 days. Data represent mean ± SEM.*

Despite the high recombination efficiency obtained, ubiquitous homozygous as well as heterozygous deletion of Notch-1 in the *SOD1$^{G93A}$* mice failed to show any beneficial effect on disease onset, survival or disease duration. No changes in bodyweight, nor improvement on motor performance tests or compound muscle action potential (CMAP) measurements were observed (Figure 37).

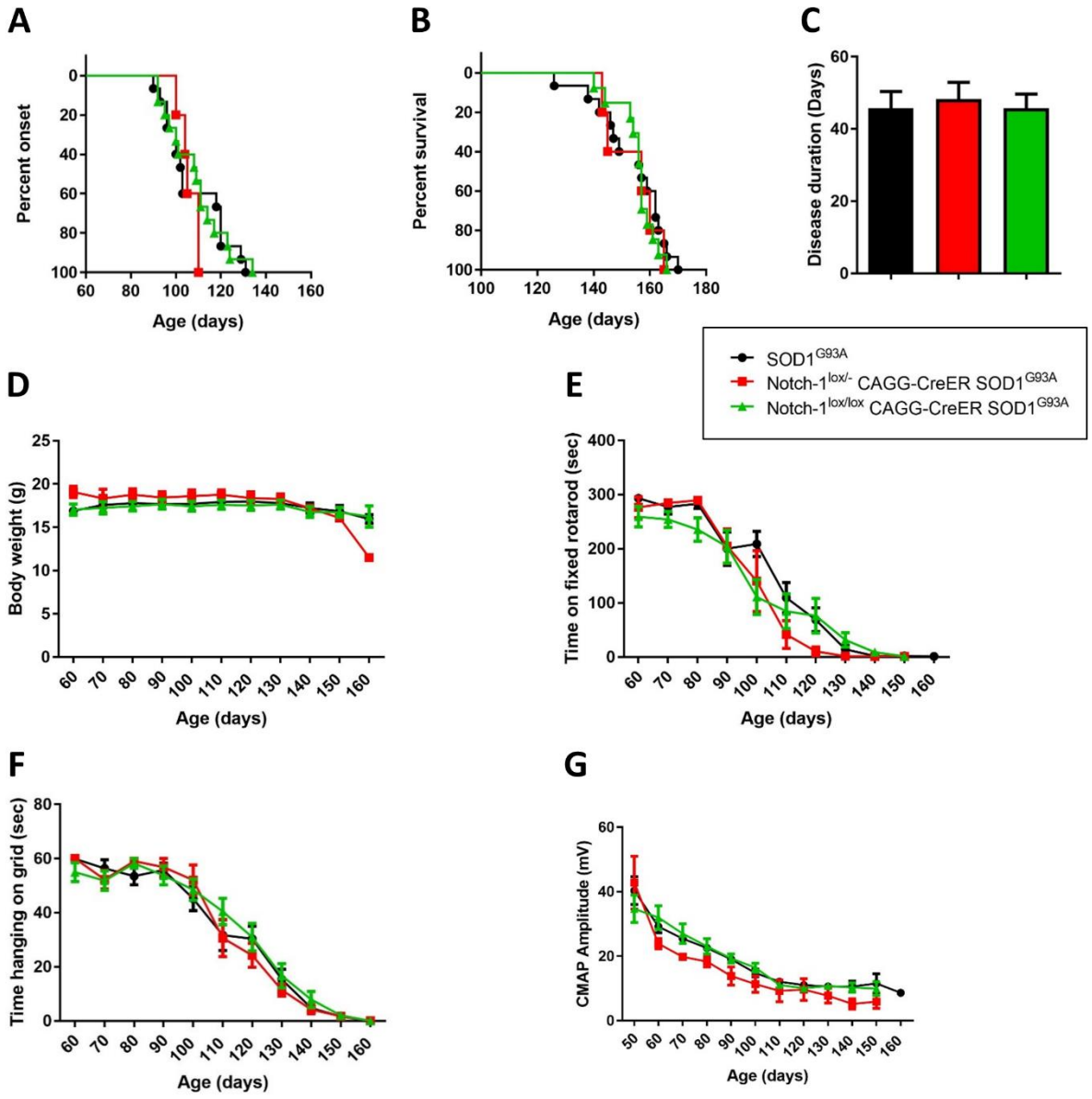


***Figure 37: Ubiquitously induced Notch-1 deletion does not alter disease in the SOD1$^{G93A}$ mouse model.*** *(A) Onset determined by failure on the hanging grid test in Notch-1$^{lox/lox}$ CAGG-CreER SOD1$^{G93A}$ mice (109 ± 3 days, n=15), Notch-1$^{lox/-}$ CAGG-CreER SOD1$^{G93A}$ mice (106 ± 2 days, n=5) and control SOD1$^{G93A}$ mice (108 ± 4 days, n=15). Log-rank Mantel-Cox test: p>0.05 (not significant). (B) Survival of Notch-1$^{lox/lox}$ CAGG-CreER SOD1$^{G93A}$ mice (156 ± 2 days, n=13), Notch-1$^{lox/-}$ CAGG-CreER SOD1$^{G93A}$ mice (154 ± 4 days, n=5) and control SOD1$^{G93A}$ mice (154 ± 3 days, n=15). Log-rank Mantel-Cox test: p>0.05 (not significant). (C) Disease duration in Notch-1$^{lox/lox}$ CAGG-CreER SOD1$^{G93A}$ mice (46 ± 4 days, n=13), Notch-1$^{lox/-}$ CAGG-CreER SOD1$^{G93A}$ mice (48 ± 5 days, n=5) and control SOD1$^{G93A}$ mice (46 ± 5 days, n=15). One-way ANOVA with Bonferroni's posthoc analysis: p>0.05. (D) Bodyweight during disease progression in Notch-1$^{lox/lox}$ CAGG-CreER SOD1$^{G93A}$ mice (n=15), Notch-1$^{lox/-}$ CAGG-CreER SOD1$^{G93A}$ mice (n=5) and control SOD1$^{G93A}$ mice (n=15). Two-way ANOVA: ****p<0.0001 for age, p>0.05 for genotype. (E-F) Motor performance determined during disease with (E) the fixed rotarod test (Two-way ANOVA: ****p<0.0001 for age, p>0.05 for genotype) and (F) the hanging grid test (Two-way ANOVA: ****p<0.0001 for age, p>0.05 for genotype) in Notch-1$^{lox/lox}$ CAGG-CreER SOD1$^{G93A}$ mice (n=15), Notch-1$^{lox/-}$ CAGG-CreER SOD1$^{G93A}$ mice (n=5) and control SOD1$^{G93A}$ mice (n=15). (G) Innervation of the gastrocnemius muscle during disease progression was evaluated by measuring CMAP amplitudes in Notch-1$^{lox/lox}$ CAGG-CreER SOD1$^{G93A}$ mice (n=15), Notch-1$^{lox/-}$ CAGG-CreER SOD1$^{G93A}$ mice (n=5) and control SOD1$^{G93A}$ mice (n=15). Two-way ANOVA: ****p<0.0001 for age, p>0.05 for genotype. Data represent mean ± SEM. All mice received tamoxifen at the age of 60 days.*

These data show that although the receptor Notch-1 is significantly upregulated during disease in the *SOD1*$^{G93A}$ mouse model, deletion of the Notch-1 receptor has no effect on disease.

# 3. Discussion

For decades the modulation of Notch signaling to study the effect on the adult CNS and adult-onset disease models has been difficult since constitutive knockout causes severe embryonic phenotypes and early lethality (112-116). However, the discovery of inducible Cre-loxP targeting technology changed the scene and made these kind of studies possible (108, 117).

In this part of the thesis, we studied the effects of Notch signaling inactivation on disease in the *SOD1*$^{G93A}$ mouse model for ALS, in order to unravel the role of increased Notch signaling activation in ALS pathogenesis. Since the canonical ligand Jagged-1 and the Notch receptors (mainly Notch-1 and Notch-2) are associated with increased Notch signaling activation observed in ALS, a ligand-based modulation approach and a receptor-based modulation approach were of interest.

Regarding the inactivation of the ligand Jagged-1, we first evaluated ubiquitous inactivation, since Jagged-1 was expressed in (motor) neurons and reactive diseased astrocytes. Ubiquitous inactivation of the ligand Jagged-1 resulted in a delay in disease onset, an extension of the survival and an improvement of the motor performance in female *SOD1*$^{G93A}$ mice. These effects however, were not observed in male *SOD1*$^{G93A}$ mice when inactivating Jagged-1. While motor neuron loss was not significantly altered upon ubiquitous Jagged-1 inactivation, reactive microgliosis was reduced in female mice. Secondly, we evaluated inactivation of Jagged-1 specifically in astrocytes and observed that, although no effect was observed in disease onset, disease progression was significantly aggravated after onset. In these mice, survival was reduced, and motor performance was impaired upon inactivation of Jagged-1 in the astrocytes. In addition, we observed that motor neuron loss and reactive

gliosis was aggravated in these mice and that activation of the Notch signaling pathway was further enhanced upon astrocytic Jagged-1 inactivation. These opposing results obtained when inactivating Jagged-1 ubiquitously and specifically in the astrocytes, suggest that the ectopic expression of the astrocytic Jagged-1 has protective effects, while (motor) neuronal Jagged-1 may have harmful effects in ALS. We did not study the effect of inactivation of Jagged-1 specifically in the (motor) neurons, but we will further elaborate on this aspect in the chapter '*Discussion and future perspectives*'.

For the receptor-based modulation approach, we first evaluated ubiquitous deletion of the down-stream co-factor RBPjk that mediated canonical signaling through all four Notch receptors. This generalized approach was of interest since we observed that both the receptors Notch-1 and Notch-2 were prominently upregulated during disease, whereas Notch-3 and Notch-4 only modestly at end stage. However, induction of homozygous ubiquitous deletion of RBPjk at the age of 60 days resulted in early lethality that was unrelated to ALS. Then, we evaluated ubiquitous deletion of specifically the Notch-1 receptor alone, but no effects on disease were observed upon deletion of the Notch-1 receptor in the *SOD1*$^{G93A}$ mouse model. These results suggest that either the influence of the Notch-2 receptor (and by extension Notch-3 and Notch-4) on disease is major, either interference with both the Notch-1 and the Notch-2 receptors (and by extension Notch-3 and Notch-4) is needed to be able to influence disease. We did not evaluate the effects of specifically deleting Notch-2, or a combination of Notch-1 and Notch-2.

Taken together, our data show that although the Notch signaling pathway is more active in the affected ALS spinal cord, interfering with this pathway as a therapeutic approach has to be done with a great deal of precision, in order to avoid and circumvent the harmful (side) effects.

# DISCUSSION & FUTURE PERSPECTIVES

**Part of this section is published in:**

**Nonneman A**, Criem N, Lewandowski SA, Nuyts R, Thal DR, Pfrieger F, Ravits J, Van Damme P, Zwijsen A, Van Den Bosch L, Robberecht W. Astrocyte-derived Jagged-1 mitigates deleterious Notch signaling in amyotrophic lateral sclerosis. Neurobiol Disease. 2018;119:26-40.

The Notch signaling pathway, as a critical mediator of cell-cell interactions (98, 99), is an underestimated target in the study of neurodegenerative diseases in general and more particularly in the non-cell autonomous component of the pathogenesis of ALS. This is due to the impressive complexity of the Notch signaling pathway and the limited knowledge about its role in the adult CNS (108).

In this study, we explored the contribution of Notch signaling to the pathogenesis of ALS, by studying *postmortem* sALS patient samples, the SOD1$^{G93A}$ mouse model and conditional knockout mice. Our data show that the Notch signaling pathway is abnormally active in the affected spinal cord of both sALS patients and *SOD1$^{G93A}$* mice and contributes to motor neuron degeneration and disease progression in the ALS mouse model. Several lines of evidence support this statement.

First, overactive Notch signaling was suggested by the prominent increase in the mRNA expression of the receptors Notch-1 and Notch-2, along with an increase in the expression of the processed (not full-length) forms of these Notch proteins, including an increase in the levels of the active signaling fragment NICD-1, in *SOD1$^{G93A}$* mice. In human sALS *postmortem* lumbar spinal cord, the mRNA expression level of these two Notch receptors was found to be increased as well. This was the case in both the motor neurons and the remaining non-motor neuron fraction. Overactive Notch signaling was

also suggested in sALS patients by the increase in the levels of the active signaling fragment NICD-1 in sALS *postmortem* lumbar spinal cord ventral horn, when compared to control individuals.

Second, the increased mRNA expression of the canonical ligand Jagged-1 in lumbar spinal cord of both sALS patients and *SOD1*$^{G93A}$ mice in combination with the decreased expression level of the full length form of the Jagged-1 protein in the spinal cord of *SOD1*$^{G93A}$ mice, suggests increased JAGGED-1 processing and turnover (cleavage, endocytosis and degradation) after signal transduction (179-183).

Furthermore, in lumbar spinal cord of *SOD1*$^{G93A}$ mice and sALS patients, several co-factors needed to form the transcription activation complex together with the active signaling fragment NICD, are upregulated. This observation suggests increased Notch signaling activation as well, because it is known from overexpression studies that increased levels of RBPjk or Mastermind-like 2 are sufficient to trigger Notch signaling activation (184, 185).

We visualized and quantified NICD-1, along with the expression levels of downstream Notch target genes to evaluate the activation status of the Notch signaling pathway. Significantly more astrocytes stained positive for NICD-1 in the lumbar spinal cord ventral horn of both *SOD1*$^{G93A}$ mice and sALS patients compared to controls, reflecting increased signaling activation. Surprisingly, we could not detect NICD-1 in neurons and only very few oligodendrocytes stained positive for NICD-1, despite the reported effects of Notch-1 in neurons (144-146, 148) and oligodendroglial cells (133, 162, 167, 168). Obviously, its level may be below the limit of detection by immunohistochemistry. These results are in agreement with publicly available data (more information can be found on https://web.stanford.edu/group/barres_lab/brain_rnaseq.html) (190). When looking at the Notch target genes in *SOD1*$^{G93A}$ mice compared to *SOD1*$^{WT}$ mice, a differential effect on target gene expression was observed, with enhanced expression of *Hes-7* and *Hey-2*, decreased expression of *Hes-5* and *Hey-L*, and unchanged *Hes-1* and *Hey-1* levels. This is known to occur upon Notch signaling activation, as they are subject to a rather complex system of regulation (186-189). The *Hes* and *Hey* genes described above are all direct Notch downstream targets, but they differ in the level of Notch activation required

for their transcription activation and their expression is known to correlate with different Notch ligands (186). In addition they also differ in mRNA stability (186), they can cross-regulate each other (186-189) and their expression can be influenced by other signaling pathways, such as Bmp, Wnt and Fgf signaling (186). In contrast, the increase in Notch signaling activation in the spinal cord of sALS patients is nicely reflected in the expression of the Notch target genes, with an upregulation of *HES-1* and *HEY-2*, while no changes were observed for *HES-7*, *HEY-1* and *HEY-L*. *HES-5* was not detected in the human dataset. The fact that the target genes are differentially expressed between the spinal cord of the ALS mouse model and sALS patients can be explained by interspecies-variability and possibly also by the observation that the non-canonical ligand *F3/CONTACTIN-1* is significantly upregulated in the motor neurons and the non-motor neuron fraction of sALS patient spinal cord samples, while this was not observed in the spinal cord of *SOD1*$^{G93A}$ mice.

Overall, the data obtained from the ALS mouse model and *postmortem* sALS patient samples clearly demonstrate a signature of overactive Notch signaling in the lumbar spinal cord.

In addition, astrocytes which are generally known to actively contribute to the pathogenesis of ALS (191), are an important cell type in the context of increased Notch signaling activation in ALS. This because we observed that the active signaling fragment NICD-1 is prominently present in astrocytes and significantly more reactive astrocytes were positive for NICD-1 in the affected spinal cord of both *SOD1*$^{G93A}$ mice and sALS patients, when compared to control spinal cords. An additional argument to claim that astrocytes are important in this context of increased Notch signaling activation in ALS is the disease-associated aberrant expression of the ligand JAGGED-1 in reactive astrocytes in the affected lumbar spinal cord of both *SOD1*$^{G93A}$ mice and sALS patients, while we could not observe JAGGED-1 in resting astrocytes from *SOD1*$^{WT}$ mice and healthy control individuals.

The major strength of this Notch signaling pathway characterization study is the translational validity of our findings from the mouse model to the patients. In affected lumbar spinal cord of both the *SOD1*$^{G93A}$ mice and the sALS patients, the same key players of the Notch signaling pathway are

upregulated, the Notch signaling pathway is more active and astrocytes are involved in this overactive signaling. In addition, it is important to mention that our finding regarding Notch signaling in the *SOD1*$^{G93A}$ mouse model are not only of relevance to patients with SOD1 mutations, which represent a minority of the patient population, but are applicable to the sALS patients as well, which represent the majority (~90%) of the ALS patients (3, 4, 13).

In order to unravel the role of increased Notch signaling activation in the pathogenesis of ALS, we studied the effects of Notch signaling inactivation on disease in the *SOD1*$^{G93A}$ mouse model.

Two observations encouraged us to study the role of Jagged-1 in the pathogenesis of ALS. First, Jagged-1 is the only canonical ligand showing increased mRNA expression levels in both SOD1$^{G93A}$ mice and sALS patients. Second, besides its expression in (motor) neurons, Jagged-1 is ectopically expressed in the reactive ALS-astrocytes localized in the lumbar spinal cord ventral horn of both sALS patients and *SOD1*$^{G93A}$ mice, while below detection level in resting, healthy control astrocytes. Consequently, we were interested to study the inactivation of Jagged-1 in a ubiquitous way, as well as specifically in the astrocytes to evaluate its effect on disease in the *SOD1*$^{G93A}$ mouse model.

Ubiquitous inactivation of Jagged-1 resulted in a delay in disease onset, a significant extension of survival and improved motor performance in female *SOD1*$^{G93A}$ mice. The latter beneficial effect on motor performance might be an underestimation of the improved motor performance because *SOD1*$^{G93A}$ mice with homozygous ubiquitous Jagged-1 inactivation develop posture alterations, mainly of the vertebral column, starting approximately 1 month after tamoxifen-induced inactivation of Jagged-1. An extensive amount of publications explains the involvement of Notch signaling in homeostasis of bone and muscle tissue. Notch signaling regulates the differentiation and function of osteoblasts and osteoclasts and as a consequence it controls bone remodeling (194). However, no clear bone phenotype was observed when taking X-ray scans of these mice. Notch signaling also plays a crucial role in skeletal muscle development and regeneration (195-197), suggesting another possible explanation for the posture alterations in the mice with ubiquitous homozygous inactivation of Jagged-

1. Further investigation of the cause of this phenotype was beyond the scope of this study. The beneficial effect of ubiquitous Jagged-1 inactivation was only observed in female *SOD1*$^{G93A}$ mice, but not in male *SOD1*$^{G93A}$ mice. This was surprising, since the Jagged-1 gene is not located on the X-chromosome, no gender differences in the expression of Jagged-1 and in the recombination efficiency were observed and the human mutant SOD1 expression level was equal between male and female *SOD1*$^{G93A}$ mice. The exact reason is unknown up to now, but we can only speculate that this is due to gender differences in the CNS, gender differences in the disease phenotypes and gender differences in the ability to respond to and repair damage, that were all reported in ALS, both in patients and in the *SOD1*$^{G93A}$ mouse model (198). In the *SOD1*$^{G93A}$ mouse model, disease starts earlier in male mice than in female *SOD1*$^{G93A}$ mice. Estrogen was found to be responsible for protecting the female *SOD1*$^{G93A}$ mice (199). Examples of differences between the CNS of males and females relevant to ALS are the following: gender differences have been reported in the axons of the corticospinal tract (200), in the excitability of the motor axons (201), in muscle fibers and motor units (202) and in the ability to repair damage (203).

In contrast, when inactivating Jagged-1 specifically in astrocytes, disease was aggravated substantially by affecting disease duration rather than disease onset, which is in agreement with the hypothesis that reactive astrocytes affect disease progression rather than disease onset (57, 80). Interestingly, the worsening of disease upon astrocyte-specific inactivation of Jagged-1, both behaviorally and pathologically, was accompanied by enhanced Notch activation.

This finding of increased Notch signaling activation together with the opposing results when inactivating Jagged-1 ubiquitously or specifically in the astrocytes, can be explained by our model depicted in figure 38 and figure 39, that is based on the fact that the Notch signaling pathway only can get activated by a ligand positioned in *trans* (i.e. on another cell) (204), while it is inhibited by a ligand positioned in *cis* (i.e. on the same cell) (104). We suggest that the overactive Notch signaling in astrocytes, possibly activated by neuronal *trans*-Jagged-1, is detrimental to the motor neuronal system

and contributes to the pathogenesis of ALS; reactive astrocytes attempt to mitigate this detrimental *trans*-activation of the Notch signaling pathway by overexpressing Jagged-1 in order to mediate cis-inhibition (see model in figure 38).

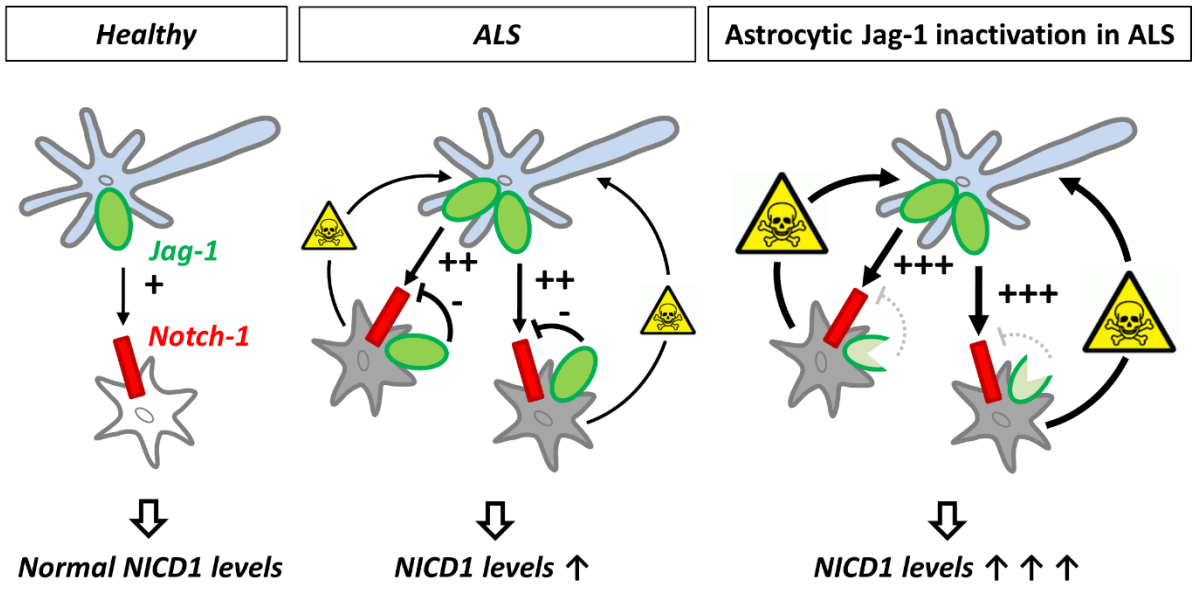


***Figure 38: Jagged-1-mediated Notch signaling in ALS pathogenesis: a hypothetical model.*** *Model describing our hypothesis about the role of Jagged-1 expressed on reactive astrocytes in ALS. In healthy spinal cord (left panel), Jagged-1 is expressed on (motor) neurons and Notch-1 on some astrocytes, resulting into basal levels of NICD-1, reflecting normal Notch signaling activation (indicated by "+"). In ALS affected spinal cord (middle panel), Jagged-1 is expressed on (motor) neurons and more astrocytes express Notch-1, resulting into an increase in the number of NICD-1 positive astrocytes, reflecting enhanced Notch signaling activation (indicated by "++") that is harmful for motor neurons in ALS. Remarkably, reactive ALS astrocytes overexpress Jagged-1 as well. Ligands expressed on the same cell as the Notch receptor act inhibitory on Notch signaling activation, a mechanism called cis-inhibition. Consequently, we believe that the astrocytic Jagged-1 mediates cis-inhibition (indicated by "-") as an attempt to reduce the enhanced Notch signaling activation in ALS, but it is not enough to reduce Notch signaling activation to normal healthy levels. In ALS affected spinal cord upon astrocyte-specific Jagged-1 inactivation (right panel), the cis-inhibitory rescue mechanism is removed. Consequently, the Notch signaling pathway is activated even more (indicated by "+++") and disease is aggravated substantially.*

In order to confirm this model, it would be interesting to evaluate the effect of ubiquitous Jagged-1 inactivation on the NICD-1 levels, and to evaluate the effect of (motor) neuronal specific inactivation of Jagged-1 on disease in follow-up experiments. We hypothesize that ubiquitous Jagged-1 inactivation

has beneficial effects on disease in female *SOD1*$^{G93A}$ mice by lowering the NICD-1 levels and consequently generating a less toxic environment for the motor neurons (Figure 39, left panel). In addition, we believe that (motor) neuronal specific inactivation of Jagged-1 may have beneficial effects on disease as well, since the harmful Jagged-1 that is responsible for *trans*-activation of the Notch receptor is removed and consequently may lower the detrimental NICD-1 levels (Figure 39, right panel). Possibly this may lead to no or less compensatory ectopic Jagged-1 expression on astrocytes.

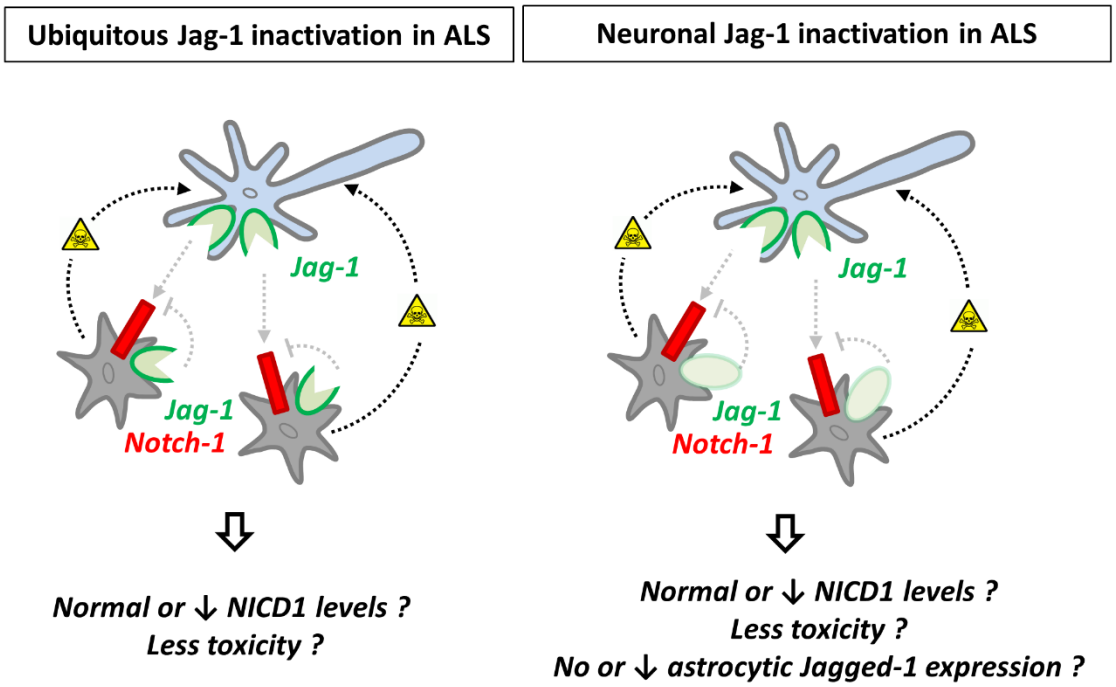


***Figure 39: Hypothetical model of action when inactivating Jagged-1 ubiquitously and specifically in the (motor) neurons.*** *Hypothetical model describing what may happen when Jagged-1 is inactivated ubiquitously (left panel) or specifically in the (motor) neurons (right panel). Ubiquitous Jagged-1 inactivation may lead to reduced Notch signaling activation and consequently may create a less toxic environment for the motor neurons. We hypothesize that neuronal specific Jagged-1 inactivation may also result into less Notch signaling activation and consequently into a less toxic environment for the motor neurons. In addition, we hypothesize that no or less compensatory ectopic Jagged-1 expression on astrocytes will be observed.*

The effect of ubiquitous deletion of RBPjk, as a generalized approach to inactivate the canonical signaling through all Notch receptors in the *SOD1*$^{G93A}$ mice, could not be studied due to severe side

effects and early lethality. Therefore, we focused on the deletion of the Notch-1 receptor alone. Surprisingly, despite the high recombination efficiency, ubiquitous deletion of Notch-1 in the *SOD1*$^{G93A}$ mouse model did not affect the course of disease in the ALS mouse model. These results suggest that either the role of the Notch-2 receptor (and by extension eventually Notch-3 and Notch-4) in the pathogenesis of ALS is more significant when compared to the contribution of the Notch-1 receptor, either interference with both the Notch-1 and the Notch-2 receptors (and by extension Notch-3 and Notch-4) is needed to be able to influence disease. We believe the latter is more plausible. Evaluating the effect of specifically deleting Notch-2 alone on disease, or the effect of deleting Notch-1 and Notch-2 together on disease, can be of interest for a follow-up study.

Altogether, this study shows that aberrant Notch signaling activation contributes to motor neuron degeneration in ALS and that exacerbation of Notch signaling by inactivation of the astrocytic Jagged-1 accelerates disease progression after onset, while ubiquitous Jagged-1 inactivation has a beneficial effect on disease onset and survival in female *SOD1*$^{G93A}$ mice. However, targeting only the Notch-1 receptor does not have any effect on disease, suggesting that other Notch receptors are involved as well. A similar detrimental effect of Notch on neurodegenerative diseases has been suggested before, in a mouse model of focal ischemic stroke showing a significant increase in Notch signaling activation (132). However, when the NICD levels were decreased, as in mice transgenic for antisense Notch and mice treated with γ-secretase inhibitors, smaller infarct sizes, reduced microglial activation and lymphocyte infiltration, and a better functional outcome were observed (132). This study suggests the involvement of Notch signaling in neuroinflammatory responses in other neurodegenerative diseases as well. Our data are also in agreement with findings in *Drosophila*, showing that loss-of-function mutations of Notch or of downstream Notch target genes extended the lifespan of TDP-43 transgenic flies (141). It should be noted, however, that they contrast with another study in *Drosophila*, in which increased Notch expression was found to suppress toxicity induced by the GR dipeptide repeat associated with C9ORF72 expansions (142).

Our results also add to the understanding of the role of astrocytes in the pathogenesis of ALS. It is generally accepted that astrocytes actively contribute to the progression of disease (57, 80), because they lose important neuroprotective functions and acquire toxic phenotypes (80). However, our results show that reactive ALS astrocytes also exert some protective functions, as they appear to sense the harmful Notch activation and respond by increasing their own Jagged-1 expression to reduce the detrimental Notch signaling activation through Jagged-1 mediated *cis*-inhibition. Interfering with this protective function of ALS astrocytes therefore worsens disease.

It is clear from our data that therapeutic approaches for neurodegenerative disorders that target Notch signaling, although certainly being promising, have to be considered with caution, given the pleiotropic action of Notch signaling and as the balance between *trans*-activation and *cis*-inhibition needs to be taken into account. Thus, targeting Notch signaling as a therapeutic option has to be done with a great deal of precision, in order to circumvent toxic side-effects and the harmful effects of interfering with feedback mechanisms (205).

# SUMMARY

Amyotrophic lateral sclerosis (ALS) is a devastating late-onset neurodegenerative disease that mainly affects motor neurons. In this disease, motor neuron degeneration is accompanied and aggravated by oligodendroglial pathology and the presence of reactive astrocytes and microglia.

In this PhD thesis, the role of the Notch signaling pathway in ALS was investigated, as this pathway is implicated in several processes that might contribute to the disease, including axonal retraction, microgliosis, astrocytosis, oligodendrocyte precursor cell proliferation and differentiation, and even cell death.

We observed abnormal activation of the Notch signaling pathway in the affected lumbar spinal cord of both *SOD1*$^{G93A}$ mice, a well-established mouse model of ALS, and patients with sporadic ALS (sALS). This increased Notch signaling activation was particularly evident in reactive astrocytes. In addition, we found that one of the main Notch ligands, namely Jagged-1, was ectopically expressed in reactive astrocytes in the spinal cord from ALS mice and patients, but it was not detected in resting astrocytes.

From Cre-lox mediated modulation experiments in the *SOD1*$^{G93A}$ mice using ligand-based inactivation approaches, we learned that astrocytic expression of the ligand Jagged-1 is beneficial, since removal further exacerbates Notch pathway activation and accelerates disease progression without affecting disease onset. Ubiquitous deletion of Jagged-1 is beneficial, at least for female SOD1$^{G93A}$ mice, since it delays disease onset and consequently extends survival in female SOD1$^{G93A}$ mice, but not in male SOD1$^{G93A}$ mice. From receptor-based deletion approaches, we learned that ubiquitous deletion of RBPjk, the co-factor crucial for canonical Notch signaling activation through all four Notch receptors, induces early lethality due to gastrointestinal toxicity, and ubiquitous deletion of only the Notch-1 receptor has no effect on the course of disease in the SOD1$^{G93A}$ mouse model, suggesting the importance of other Notch receptors.

Together, these data suggest that aberrant Notch signaling activation is involved in the pathogenesis of ALS, both in sALS patients and in the *SOD1*$^{G93A}$ mouse model, but plays a rather complex role that potentially consists of both harmful and protective functions. Given the pleiotropic functions of Notch signaling, interference with this pathway as a therapeutic approach must be considered with caution, to circumvent toxic side-effects and effects of disturbing the complex balance between the harmful *trans*-activation and the protective *cis*-inhibition.

# SAMENVATTING

Amyotrofische laterale sclerose (ALS) is een dodelijke neurodegeneratieve aandoening die pas op latere adulte leeftijd tot uiting komt en voornamelijk één specifieke populatie neuronen treft, namelijk de motorische zenuwcellen, ook motorneuronen genoemd. Bij deze ziekte gaat de motorneurondegeneratie gepaard met aantasting van de oligodendrogliale cellen, de astrocyten en de microglia, wat de ziekte dan ook verergert en het verloop versnelt.

In deze doctoraatsthesis werd de rol van de Notch signaalcascade in de pathogenese van ALS bestudeerd. Dit aangezien deze signaalcascade een belangrijke rol speelt bij verschillende processen waarvan geweten is dat ze bijdragen tot het ontstaan van ALS, waaronder axonale retractie, microgliose en astrocytose, het deelproces van oligodendrocyt precursor cellen en hun maturatie proces tot functionele oligodendrocyten, en deze signaalcascade speelt zelfs een rol bij celdood mechanismen.

In het aangetaste lumbale ruggenmerg weefsel van sporadische ALS patiënten, alsook van *SOD1*$^{G93A}$ muizen, die een ziektebeeld ontwikkelen dat representatief is voor het ziektebeeld bij de mens, hebben we vastgesteld dat de Notch signaalcascade abnormaal geactiveerd is. Dit was voornamelijk het geval in de reactieve door de ziekte aangetaste GFAP-positieve astrocyten, maar niet in gezonde controle astrocyten. Ook merkten we op dat één van de Notch liganden, namelijk Jagged-1, zowel bij de sporadische ALS patiënten als bij het muismodel, in deze door de ziekte aangetaste GFAP-positieve astrocyten tot expressie komt, terwijl dit niet het geval is in gezonde controle astrocyten.

Voorts hebben Cre-lox gemedieerde modulatie experimenten ons geleerd dat de expressie van het ligand Jagged-1 een protectieve functie heeft, aangezien astrocyt-specifieke deletie van Jagged-1 de Notch activatie versterkt en ook het ziekteproces versnelt na het optreden van de eerste symptomen van motor neuron degeneratie. In tegenstelling tot het voorgaande, werkt deletie van Jagged-1 in alle

celtypes waar het tot expressie komt protectief in vrouwelijke SOD1$^{G93A}$ muizen, want we stelden vast dat het begin van de ziekte later optreedt en bijgevolg dat de muizen langer leven. Uit receptor modulatie experimenten leerden we dat veralgemeende deletie van RBPjk, de cofactor die noodzakelijk is voor de activatie van de canonieke Notch signaalcascade, levensbedreigende gastro-intestinale toxiciteit induceert. De studie van de veralgemeende deletie van de Notch-1 receptor toonde geen effect op het ziektebeeld van de SOD1$^{G93A}$ muizen. Dit laatste suggereert het belang van andere Notch receptoren in het ziektemechanisme van ALS.

Ter conclusie, de resultaten voorgesteld in deze doctoraatsthesis suggereren dat abnormaal verhoogde activatie van de Notch signaalcascade bijdraagt tot het ziektemechanisme van ALS, en potentieel zowel schadelijke als protectieve functies omvat. Bij gevolg is het noodzakelijk dat het interfereren met deze Notch signaalcascade met de grootste voorzichtigheid gedaan wordt. Dit om nadelige neveneffecten te vermijden en om te verhinderen dat de complexe balans tussen de schadelijke trans-activatie en de protectieve cis-inhibitie verstoord wordt.

# HONEST SCIENTIFIC CONDUCT STATEMENT

## Scientific acknowledgements

This work was supported by the Fund for Scientific Research Flanders (FWO; G.0703.12N), the Interuniversity Attraction Poles Programme (P7/16) initiated by the Belgian Science Policy Office, ALS Therapy Alliance, the Association Belge contre les Maladies neuro-Musculaires (ABMM) and Research Fund KU Leuven (GOA/11/014). Prof. Dr. Wim Robberecht is supported through the E von Behring Chair for Neuromuscular and Neurodegenerative Disorders, the European Research Council under the European's Seventh Framework Programme (FP7/2007-2013)/ ERC grant agreement (n° 340429), the Laevers Fund for ALS Research, the fund 'Een Hart voor ALS'. Prof. Dr. Wim Robberecht and Prof. Dr. Ludo Van Den Bosch are supported by the ALS Liga België and the fund 'Opening the Future'. Annelies Nonneman was granted a PhD fellowship provided by the Agency for Innovation by Science and Technology in Flanders (IWT).

## Personal contribution

The candidate designed, organized and performed most of the experiments. For the immunohistochemical staining of NICD-1 the candidate received help and advice from Nathan Criem and Prof. Dr. An Zwijsen (KU Leuven, Center for Molecular and Vascular Biology). The human RNA expression results were analyzed by Dr. Sebastian Lewandowski (Karolinska Institutet, Sweden). Under the supervision of the present candidate Rik Nuyts, Begga Schevenels and Séraphina Penninckx assisted with genotyping of the mice used for this study and with some of the motor performance tests. Prof. Dr. Wim Robberecht supervised the project and inspired the candidate with ideas. The candidate wrote the manuscript, and Prof. Dr. Wim Robberecht and Prof. Dr. Ludo Van Den Bosch provided feedback.

## Conflict of interest

No competing interests to declare.

# LIST OF REFERENCES


1. Gladman M, Zinman L. The economic impact of amyotrophic lateral sclerosis: a systematic review. Expert Rev Pharmacoecon Outcomes Res. 2015;15(3):439-50.

2. Cavaleri F. Review of Amyotrophic Lateral Sclerosis, Parkinson's and Alzheimer's diseases helps further define pathology of the novel paradigm for Alzheimer's with heavy metals as primary disease cause. Med Hypotheses. 2015;85(6):779-90.

3. Swinnen B, Robberecht W. The phenotypic variability of amyotrophic lateral sclerosis. Nat Rev Neurol. 2014;10(11):661-70.

4. Kiernan MC, Vucic S, Cheah BC, Turner MR, Eisen A, Hardiman O, et al. Amyotrophic lateral sclerosis. Lancet. 2011;377(9769):942-55.

5. Hardiman O, van den Berg LH, Kiernan MC. Clinical diagnosis and management of amyotrophic lateral sclerosis. Nat Rev Neurol. 2011;7(11):639-49.

6. Taylor JP, Brown RH, Jr., Cleveland DW. Decoding ALS: from genes to mechanism. Nature. 2016;539(7628):197-206.

7. Al-Chalabi A, Hardiman O. The epidemiology of ALS: a conspiracy of genes, environment and time. Nature Reviews Neurology. 2013;9(11):617-28.

8. Lattante S, Ciura S, Rouleau GA, Kabashi E. Defining the genetic connection linking amyotrophic lateral sclerosis (ALS) with frontotemporal dementia (FTD). Trends Genet. 2015;31(5):263-73.

9. Li HF, Wu ZY. Genotype-phenotype correlations of amyotrophic lateral sclerosis. Transl Neurodegener. 2016;5.

10. Sreedharan J, Blair IP, Tripathi VB, Hu X, Vance C, Rogelj B, et al. TDP-43 mutations in familial and sporadic amyotrophic lateral sclerosis. Science. 2008;319(5870):1668-72.

11. Kwiatkowski TJ, Jr., Bosco DA, Leclerc AL, Tamrazian E, Vanderburg CR, Russ C, et al. Mutations in the FUS/TLS gene on chromosome 16 cause familial amyotrophic lateral sclerosis. Science. 2009;323(5918):1205-8.

12. Johnson JO, Mandrioli J, Benatar M, Abramzon Y, Van Deerlin VM, Trojanowski JQ, et al. Exome sequencing reveals VCP mutations as a cause of familial ALS. Neuron. 2010;68(5):857-64.

13. Renton AE, Chio A, Traynor BJ. State of play in amyotrophic lateral sclerosis genetics. Nat Neurosci. 2014;17(1):17-23.

14. Guerreiro R, Bras J, Hardy J. SnapShot: Genetics of ALS and FTD. Cell. 2015;160(4):798 e1.

15. Therrien M, Dion PA, Rouleau GA. ALS: Recent Developments from Genetics Studies. Curr Neurol Neurosci Rep. 2016;16(6):59.

16. Al-Chalabi A, Hardiman O. The epidemiology of ALS: a conspiracy of genes, environment and time. Nat Rev Neurol. 2013;9(11):617-28.

17. Eykens C, Robberecht W. The genetic basis of amyotrophic lateral sclerosis: recent breakthroughs. Advances in genomics and genetics. 2015;5:327-45.

18. Laferriere F, Polymenidou M. Advances and challenges in understanding the multifaceted pathogenesis of amyotrophic lateral sclerosis. Swiss Med Wkly. 2015;145:w14054.

19. Chen S, Sayana P, Zhang X, Le W. Genetics of amyotrophic lateral sclerosis: an update. Mol Neurodegener. 2013;8:28.

20. Gordon PH. Amyotrophic lateral sclerosis: pathophysiology, diagnosis and management. CNS Drugs. 2011;25(1):1-15.

21. Salameh JS, Brown RH, Jr., Berry JD. Amyotrophic Lateral Sclerosis: Review. Semin Neurol. 2015;35(4):469-76.

22. Bucchia M, Ramirez A, Parente V, Simone C, Nizzardo M, Magri F, et al. Therapeutic development in amyotrophic lateral sclerosis. Clin Ther. 2015;37(3):668-80.

23. Takei K, Watanabe K, Yuki S, Akimoto M, Sakata T, Palumbo J. Edaravone and its clinical development for amyotrophic lateral sclerosis. Amyotroph Lateral Scler Frontotemporal Degener. 2017;18(sup1):5-10.

24. Van Damme P, Robberecht W, Van Den Bosch L. Modelling amyotrophic lateral sclerosis: progress and possibilities. Dis Model Mech. 2017;10(5):537-49.

25. Philips T, Rothstein JD. Rodent Models of Amyotrophic Lateral Sclerosis. Curr Protoc Pharmacol. 2015;69:5 67 1-21.

26. Gurney ME. Transgenic-mouse model of amyotrophic lateral sclerosis. N Engl J Med. 1994;331(25):1721-2.

27. Wong PC, Pardo CA, Borchelt DR, Lee MK, Copeland NG, Jenkins NA, et al. An adverse property of a familial ALS-linked SOD1 mutation causes motor neuron disease characterized by vacuolar degeneration of mitochondria. Neuron. 1995;14(6):1105-16.

28. Bruijn LI, Becher MW, Lee MK, Anderson KL, Jenkins NA, Copeland NG, et al. ALS-linked SOD1 mutant G85R mediates damage to astrocytes and promotes rapidly progressive disease with SOD1-containing inclusions. Neuron. 1997;18(2):327-38.

29. Saccon RA, Bunton-Stasyshyn RK, Fisher EM, Fratta P. Is SOD1 loss of function involved in amyotrophic lateral sclerosis? Brain. 2013;136(Pt 8):2342-58.

30. Nolan M, Talbot K, Ansorge O. Pathogenesis of FUS-associated ALS and FTD: insights from rodent models. Acta Neuropathol Commun. 2016;4(1):99.

31. Sharma A, Lyashchenko AK, Lu L, Nasrabady SE, Elmaleh M, Mendelsohn M, et al. ALS-associated mutant FUS induces selective motor neuron degeneration through toxic gain of function. Nat Commun. 2016;7:10465.

32. Devoy A, Kalmar B, Stewart M, Park H, Burke B, Noy SJ, et al. Humanized mutant FUS drives progressive motor neuron degeneration without aggregation in 'FUSDelta14' knockin mice. Brain. 2017;140(11):2797-805.

33. Batra R, Lee CW. Mouse Models of C9orf72 Hexanucleotide Repeat Expansion in Amyotrophic Lateral Sclerosis/ Frontotemporal Dementia. Front Cell Neurosci. 2017;11:196.

34. Weishaupt JH, Hyman T, Dikic I. Common Molecular Pathways in Amyotrophic Lateral Sclerosis and Frontotemporal Dementia. Trends Mol Med. 2016;22(9):769-83.

35. Robberecht W, Philips T. The changing scene of amyotrophic lateral sclerosis. Nat Rev Neurosci. 2013;14(4):248-64.

36. Morgan S, Orrell RW. Pathogenesis of amyotrophic lateral sclerosis. Br Med Bull. 2016;119(1):87-98.

37. Hardiman O, Al-Chalabi A, Chio A, Corr EM, Logroscino G, Robberecht W, et al. Amyotrophic lateral sclerosis. Nat Rev Dis Primers. 2017;3:17071.

38. Kabashi E, Valdmanis PN, Dion P, Spiegelman D, McConkey BJ, Vande Velde C, et al. TARDBP mutations in individuals with sporadic and familial amyotrophic lateral sclerosis. Nat Genet. 2008;40(5):572-4.

39. Vance C, Rogelj B, Hortobagyi T, De Vos KJ, Nishimura AL, Sreedharan J, et al. Mutations in FUS, an RNA processing protein, cause familial amyotrophic lateral sclerosis type 6. Science. 2009;323(5918):1208-11.

40. Blokhuis AM, Groen EJ, Koppers M, van den Berg LH, Pasterkamp RJ. Protein aggregation in amyotrophic lateral sclerosis. Acta Neuropathol. 2013;125(6):777-94.

41. Ilieva H, Polymenidou M, Cleveland DW. Non-cell autonomous toxicity in neurodegenerative disorders: ALS and beyond. J Cell Biol. 2009;187(6):761-72.

42. De Vos KJ, Hafezparast M. Neurobiology of axonal transport defects in motor neuron diseases: Opportunities for translational research? Neurobiol Dis. 2017;105:283-99.

43. Naumann M, Pal A, Goswami A, Lojewski X, Japtok J, Vehlow A, et al. Impaired DNA damage response signaling by FUS-NLS mutations leads to neurodegeneration and FUS aggregate formation. Nat Commun. 2018;9(1):335.

44. Farg MA, Konopka A, Soo KY, Ito D, Atkin JD. The DNA damage response (DDR) is induced by the C9orf72 repeat expansion in amyotrophic lateral sclerosis. Hum Mol Genet. 2017;26(15):2882-96.

45. Rothstein JD, Van Kammen M, Levey AI, Martin LJ, Kuncl RW. Selective loss of glial glutamate transporter GLT-1 in amyotrophic lateral sclerosis. Ann Neurol. 1995;38(1):73-84.

46. Kretschmer BD, Kratzer U, Schmidt WJ. Riluzole, a glutamate release inhibitor, and motor behavior. Naunyn Schmiedebergs Arch Pharmacol. 1998;358(2):181-90.

47. Barber SC, Mead RJ, Shaw PJ. Oxidative stress in ALS: a mechanism of neurodegeneration and a therapeutic target. Biochim Biophys Acta. 2006;1762(11-12):1051-67.

48. Manfredi G, Xu Z. Mitochondrial dysfunction and its role in motor neuron degeneration in ALS. Mitochondrion. 2005;5(2):77-87.

49. Jaronen M, Goldsteins G, Koistinaho J. ER stress and unfolded protein response in amyotrophic lateral sclerosis-a controversial role of protein disulphide isomerase. Front Cell Neurosci. 2014;8:402.

50. Pramatarova A, Laganiere J, Roussel J, Brisebois K, Rouleau GA. Neuron-specific expression of mutant superoxide dismutase 1 in transgenic mice does not lead to motor impairment. J Neurosci. 2001;21(10):3369-74.

51. Lino MM, Schneider C, Caroni P. Accumulation of SOD1 mutants in postnatal motoneurons does not cause motoneuron pathology or motoneuron disease. J Neurosci. 2002;22(12):4825-32.

52. Jaarsma D, Teuling E, Haasdijk ED, De Zeeuw CI, Hoogenraad CC. Neuron-specific expression of mutant superoxide dismutase is sufficient to induce amyotrophic lateral sclerosis in transgenic mice. J Neurosci. 2008;28(9):2075-88.

53. Ralph GS, Radcliffe PA, Day DM, Carthy JM, Leroux MA, Lee DC, et al. Silencing mutant SOD1 using RNAi protects against neurodegeneration and extends survival in an ALS model. Nat Med. 2005;11(4):429-33.

54. Boillee S, Yamanaka K, Lobsiger CS, Copeland NG, Jenkins NA, Kassiotis G, et al. Onset and progression in inherited ALS determined by motor neurons and microglia. Science. 2006;312(5778):1389-92.

55. Kang SH, Li Y, Fukaya M, Lorenzini I, Cleveland DW, Ostrow LW, et al. Degeneration and impaired regeneration of gray matter oligodendrocytes in amyotrophic lateral sclerosis. Nat Neurosci. 2013;16(5):571-9.

56. Gong YH, Parsadanian AS, Andreeva A, Snider WD, Elliott JL. Restricted expression of G86R Cu/Zn superoxide dismutase in astrocytes results in astrocytosis but does not cause motoneuron degeneration. J Neurosci. 2000;20(2):660-5.

57. Yamanaka K, Chun SJ, Boillee S, Fujimori-Tonou N, Yamashita H, Gutmann DH, et al. Astrocytes as determinants of disease progression in inherited amyotrophic lateral sclerosis. Nat Neurosci. 2008;11(3):251-3.

58. Nave KA. Myelination and the trophic support of long axons. Nat Rev Neurosci. 2010;11(4):275-83.

59. Nave KA. Myelination and support of axonal integrity by glia. Nature. 2010;468(7321):244-52.

60. Simons M, Lyons DA. Axonal selection and myelin sheath generation in the central nervous system. Curr Opin Cell Biol. 2013;25(4):512-9.

61. Lee Y, Morrison BM, Li Y, Lengacher S, Farah MH, Hoffman PN, et al. Oligodendroglia metabolically support axons and contribute to neurodegeneration. Nature. 2012;487(7408):443-8.

62. Morrison BM, Lee Y, Rothstein JD. Oligodendroglia: metabolic supporters of axons. Trends Cell Biol. 2013;23(12):644-51.

63. Philips T, Bento-Abreu A, Nonneman A, Haeck W, Staats K, Geelen V, et al. Oligodendrocyte dysfunction in the pathogenesis of amyotrophic lateral sclerosis. Brain. 2013;136(Pt 2):471-82.

64. Stieber A, Gonatas JO, Gonatas NK. Aggregates of mutant protein appear progressively in dendrites, in periaxonal processes of oligodendrocytes, and in neuronal and astrocytic perikarya of mice expressing the SOD1(G93A) mutation of familial amyotrophic lateral sclerosis. J Neurol Sci. 2000;177(2):114-23.

65. Kang SH, Fukaya M, Yang JK, Rothstein JD, Bergles DE. NG2+ CNS glial progenitors remain committed to the oligodendrocyte lineage in postnatal life and following neurodegeneration. Neuron. 2010;68(4):668-81.

66. Niebroj-Dobosz I, Rafalowska J, Fidzianska A, Gadamski R, Grieb P. Myelin composition of spinal cord in a model of amyotrophic lateral sclerosis (ALS) in SOD1G93A transgenic rats. Folia Neuropathol. 2007;45(4):236-41.

67. Boggs JM. Myelin basic protein: a multifunctional protein. Cell Mol Life Sci. 2006;63(17):1945-61.

68. Braak H, Del Tredici K. Poor and protracted myelination as a contributory factor to neurodegenerative disorders. Neurobiol Aging. 2004;25(1):19-23.

69. Philips T, Rothstein JD. Oligodendroglia: metabolic supporters of neurons. Journal of Clinical Investigation. 2017;127(9):3277-86.

70. Geloso MC, Corvino V, Marchese E, Serrano A, Michetti F, D'Ambrosi N. The Dual Role of Microglia in ALS: Mechanisms and Therapeutic Approaches. Front Aging Neurosci. 2017;9:242.

71. Philips T, Rothstein JD. Glial cells in amyotrophic lateral sclerosis. Exp Neurol. 2014;262 Pt B:111-20.

72. Souza PV, Pinto WB, Rezende FMF, Oliveira AS. Far beyond the motor neuron: the role of glial cells in amyotrophic lateral sclerosis. Arq Neuropsiquiatr. 2016;74(10):849-54.

73. Ransohoff RM. A polarizing question: do M1 and M2 microglia exist? Nat Neurosci. 2016;19(8):987-91.

74. Henkel JS, Beers DR, Zhao W, Appel SH. Microglia in ALS: the good, the bad, and the resting. J Neuroimmune Pharmacol. 2009;4(4):389-98.

75. Luo XG, Chen SD. The changing phenotype of microglia from homeostasis to disease. Transl Neurodegener. 2012;1(1):9.

76. Ohgomori T, Yamada J, Takeuchi H, Kadomatsu K, Jinno S. Comparative morphometric analysis of microglia in the spinal cord of SOD1(G93A) transgenic mouse model of amyotrophic lateral sclerosis. Eur J Neurosci. 2016;43(10):1340-51.

77. Turner MR, Cagnin A, Turkheimer FE, Miller CC, Shaw CE, Brooks DJ, et al. Evidence of widespread cerebral microglial activation in amyotrophic lateral sclerosis: an [11C](R)-PK11195 positron emission tomography study. Neurobiol Dis. 2004;15(3):601-9.

78. Brites D, Vaz AR. Microglia centered pathogenesis in ALS: insights in cell interconnectivity. Front Cell Neurosci. 2014;8:117.

79. Liddelow SA, Guttenplan KA, Clarke LE, Bennett FC, Bohlen CJ, Schirmer L, et al. Neurotoxic reactive astrocytes are induced by activated microglia. Nature. 2017;541(7638):481-7.

80. Yamanaka K, Komine O. The multi-dimensional roles of astrocytes in ALS. Neurosci Res. 2017.

81. Zhou Y, Danbolt NC. Glutamate as a neurotransmitter in the healthy brain. J Neural Transm. 2014;121(8):799-817.

82. Van den Bosch L, Van Damme P, Bogaert E, Robberecht W. The role of excitotoxicity in the pathogenesis of amyotrophic lateral sclerosis. Bba-Mol Basis Dis. 2006;1762(11-12):1068-82.

83. Maragakis NJ, Rothstein JD. Mechanisms of Disease: astrocytes in neurodegenerative disease. Nat Clin Pract Neurol. 2006;2(12):679-89.

84. Stobart JL, Anderson CM. Multifunctional role of astrocytes as gatekeepers of neuronal energy supply. Front Cell Neurosci. 2013;7:38.

85. Kushner PD, Stephenson DT, Wright S. Reactive astrogliosis is widespread in the subcortical white matter of amyotrophic lateral sclerosis brain. J Neuropathol Exp Neurol. 1991;50(3):263-77.

86. Nagy D, Kato T, Kushner PD. Reactive astrocytes are widespread in the cortical gray matter of amyotrophic lateral sclerosis. J Neurosci Res. 1994;38(3):336-47.

87. Schiffer D, Cordera S, Cavalla P, Migheli A. Reactive astrogliosis of the spinal cord in amyotrophic lateral sclerosis. J Neurol Sci. 1996;139 Suppl:27-33.

88. Levine JB, Kong J, Nadler M, Xu Z. Astrocytes interact intimately with degenerating motor neurons in mouse amyotrophic lateral sclerosis (ALS). Glia. 1999;28(3):215-24.

89. Barbeito LH, Pehar M, Cassina P, Vargas MR, Peluffo H, Viera L, et al. A role for astrocytes in motor neuron loss in amyotrophic lateral sclerosis. Brain Res Brain Res Rev. 2004;47(1-3):263-74.

90. Wilhelmsson U, Bushongt EA, Price DL, Smarr BL, Phung V, Terada M, et al. Redefining the concept of reactive astrocytes as cells that remain within their unique domains upon reaction to injury. P Natl Acad Sci USA. 2006;103(46):17513-8.

91. Van Damme P, Bogaert E, Dewil M, Hersmus N, Kiraly D, Scheveneels W, et al. Astrocytes regulate GluR2 expression in motor neurons and their vulnerability to excitotoxicity. Proc Natl Acad Sci U S A. 2007;104(37):14825-30.

92. Haidet-Phillips AM, Hester ME, Miranda CJ, Meyer K, Braun L, Frakes A, et al. Astrocytes from familial and sporadic ALS patients are toxic to motor neurons. Nat Biotechnol. 2011;29(9):824-8.

93. Lasiene J, Yamanaka K. Glial cells in amyotrophic lateral sclerosis. Neurol Res Int. 2011;2011:718987.

94. Nijssen J, Comley LH, Hedlund E. Motor neuron vulnerability and resistance in amyotrophic lateral sclerosis. Acta Neuropathol. 2017;133(6):863-85.

95. Boillee S, Vande Velde C, Cleveland DW. ALS: a disease of motor neurons and their nonneuronal neighbors. Neuron. 2006;52(1):39-59.

96. Shaw PJ, Eggett CJ. Molecular factors underlying selective vulnerability of motor neurons to neurodegeneration in amyotrophic lateral sclerosis. J Neurol. 2000;247 Suppl 1:I17-27.

97. Kaplan A, Spiller KJ, Towne C, Kanning KC, Choe GT, Geber A, et al. Neuronal matrix metalloproteinase-9 is a determinant of selective neurodegeneration. Neuron. 2014;81(2):333-48.

98. Artavanis-Tsakonas S, Rand MD, Lake RJ. Notch signaling: cell fate control and signal integration in development. Science. 1999;284(5415):770-6.

99. Lai EC. Notch signaling: control of cell communication and cell fate. Development. 2004;131(5):965-73.

100. Kopan R, Ilagan MX. The canonical Notch signaling pathway: unfolding the activation mechanism. Cell. 2009;137(2):216-33.

101. Ilagan MX, Kopan R. SnapShot: notch signaling pathway. Cell. 2007;128(6):1246.

102. Bray SJ. Notch signalling: a simple pathway becomes complex. Nat Rev Mol Cell Biol. 2006;7(9):678-89.

103. Kageyama R, Ohtsuka T, Shimojo H, Imayoshi I. Dynamic Notch signaling in neural progenitor cells and a revised view of lateral inhibition. Nat Neurosci. 2008;11(11):1247-51.

104. del Alamo D, Rouault H, Schweisguth F. Mechanism and significance of cis-inhibition in Notch signalling. Curr Biol. 2011;21(1):R40-7.

105. Andersen P, Uosaki H, Shenje LT, Kwon C. Non-canonical Notch signaling: emerging role and mechanism. Trends Cell Biol. 2012;22(5):257-65.

106. D'Souza B, Meloty-Kapella L, Weinmaster G. Canonical and non-canonical Notch ligands. Curr Top Dev Biol. 2010;92:73-129.

107. Schweisguth F. Regulation of notch signaling activity. Curr Biol. 2004;14(3):R129-38.

108. Ables JL, Breunig JJ, Eisch AJ, Rakic P. Not(ch) just development: Notch signalling in the adult brain. Nat Rev Neurosci. 2011;12(5):269-83.

109. Mathieu P, Adami PV, Morelli L. Notch signaling in the pathologic adult brain. Biomol Concepts. 2013;4(5):465-76.

110. Lathia JD, Mattson MP, Cheng A. Notch: from neural development to neurological disorders. J Neurochem. 2008;107(6):1471-81.

111. Imayoshi I, Sakamoto M, Yamaguchi M, Mori K, Kageyama R. Essential roles of Notch signaling in maintenance of neural stem cells in developing and adult brains. J Neurosci. 2010;30(9):3489-98.

112. Louvi A, Artavanis-Tsakonas S. Notch signalling in vertebrate neural development. Nat Rev Neurosci. 2006;7(2):93-102.

113. Hamada Y, Kadokawa Y, Okabe M, Ikawa M, Coleman JR, Tsujimoto Y. Mutation in ankyrin repeats of the mouse Notch2 gene induces early embryonic lethality. Development. 1999;126(15):3415-24.

114. Huppert SS, Le A, Schroeter EH, Mumm JS, Saxena MT, Milner LA, et al. Embryonic lethality in mice homozygous for a processing-deficient allele of Notch1. Nature. 2000;405(6789):966-70.

115. Oka C, Nakano T, Wakeham A, de la Pompa JL, Mori C, Sakai T, et al. Disruption of the mouse RBP-J kappa gene results in early embryonic death. Development. 1995;121(10):3291-301.

116. Yoon K, Gaiano N. Notch signaling in the mammalian central nervous system: insights from mouse mutants. Nat Neurosci. 2005;8(6):709-15.

117. Sato C, Zhao G, Ilagan MX. An overview of notch signaling in adult tissue renewal and maintenance. Curr Alzheimer Res. 2012;9(2):227-40.

118. Zhao C, Suh H, Gage FH. Notch keeps ependymal cells in line. Nat Neurosci. 2009;12(3):243-5.

119. Giachino C, Taylor V. Notching up neural stem cell homogeneity in homeostasis and disease. Front Neurosci. 2014;8:32.

120. Lugert S, Basak O, Knuckles P, Haussler U, Fabel K, Gotz M, et al. Quiescent and active hippocampal neural stem cells with distinct morphologies respond selectively to physiological and pathological stimuli and aging. Cell Stem Cell. 2010;6(5):445-56.

121. Zhang R, Engler A, Taylor V. Notch: an interactive player in neurogenesis and disease. Cell Tissue Res. 2018;371(1):73-89.

122. McDaniell R, Warthen DM, Sanchez-Lara PA, Pai A, Krantz ID, Piccoli DA, et al. NOTCH2 mutations cause Alagille syndrome, a heterogeneous disorder of the notch signaling pathway. Am J Hum Genet. 2006;79(1):169-73.

123. Joutel A, Corpechot C, Ducros A, Vahedi K, Chabriat H, Mouton P, et al. Notch3 mutations in CADASIL, a hereditary adult-onset condition causing stroke and dementia. Nature. 1996;383(6602):707-10.

124. Zhang B, Fan QR, Li WH, Lu N, Fu DK, Kang YJ, et al. Association of the NOTCH4 Gene Polymorphism rs204993 with Schizophrenia in the Chinese Han Population. Biomed Res Int. 2015;2015:408096.

125. Woo HN, Park JS, Gwon AR, Arumugam TV, Jo DG. Alzheimer's disease and Notch signaling. Biochem Biophys Res Commun. 2009;390(4):1093-7.

126. Berezovska O, Xia MQ, Hyman BT. Notch is expressed in adult brain, is coexpressed with presenilin-1, and is altered in Alzheimer disease. J Neuropathol Exp Neurol. 1998;57(8):738-45.

127. John GR, Shankar SL, Shafit-Zagardo B, Massimi A, Lee SC, Raine CS, et al. Multiple sclerosis: re-expression of a developmental pathway that restricts oligodendrocyte maturation. Nat Med. 2002;8(10):1115-21.

128. Jurynczyk M, Selmaj K. Notch: a new player in MS mechanisms. J Neuroimmunol. 2010;218(1-2):3-11.

129. Aparicio E, Mathieu P, Pereira Luppi M, Almeira Gubiani MF, Adamo AM. The Notch signaling pathway: its role in focal CNS demyelination and apotransferrin-induced remyelination. J Neurochem. 2013;127(6):819-36.

130. Caraballo-Miralles V, Cardona-Rossinyol A, Garcera A, Torres-Benito L, Soler RM, Tabares L, et al. Notch signaling pathway is activated in motoneurons of spinal muscular atrophy. Int J Mol Sci. 2013;14(6):11424-37.

131. Ishikura N, Clever JL, Bouzamondo-Bernstein E, Samayoa E, Prusiner SB, Huang EJ, et al. Notch-1 activation and dendritic atrophy in prion disease. Proc Natl Acad Sci U S A. 2005;102(3):886-91.

132. Arumugam TV, Chan SL, Jo DG, Yilmaz G, Tang SC, Cheng A, et al. Gamma secretase-mediated Notch signaling worsens brain damage and functional outcome in ischemic stroke. Nat Med. 2006;12(6):621-3.

133. Wang S, Sdrulla AD, diSibio G, Bush G, Nofziger D, Hicks C, et al. Notch receptor activation inhibits oligodendrocyte differentiation. Neuron. 1998;21(1):63-75.

134. Hu QD, Ang BT, Karsak M, Hu WP, Cui XY, Duka T, et al. F3/contactin acts as a functional ligand for Notch during oligodendrocyte maturation. Cell. 2003;115(2):163-75.

135. Nakahara J, Kanekura K, Nawa M, Aiso S, Suzuki N. Abnormal expression of TIP30 and arrested nucleocytoplasmic transport within oligodendrocyte precursor cells in multiple sclerosis. J Clin Invest. 2009;119(1):169-81.

136. Jurynczyk M, Jurewicz A, Bielecki B, Raine CS, Selmaj K. Inhibition of Notch signaling enhances tissue repair in an animal model of multiple sclerosis. J Neuroimmunol. 2005;170(1-2):3-10.

137. Arumugam TV, Cheng YL, Choi Y, Choi YH, Yang S, Yun YK, et al. Evidence that gamma-secretase-mediated Notch signaling induces neuronal cell death via the nuclear factor-kappaB-Bcl-2-interacting mediator of cell death pathway in ischemic stroke. Mol Pharmacol. 2011;80(1):23-31.

138. Balaganapathy P, Baik SH, Mallilankaraman K, Sobey CG, Jo DG, Arumugam TV. Interplay between Notch and p53 promotes neuronal cell death in ischemic stroke. J Cereb Blood Flow Metab. 2017:271678X17715956.

139. Wei Z, Chigurupati S, Arumugam TV, Jo DG, Li H, Chan SL. Notch activation enhances the microglia-mediated inflammatory response associated with focal cerebral ischemia. Stroke. 2011;42(9):2589-94.

140. Shimada IS, Borders A, Aronshtam A, Spees JL. Proliferating reactive astrocytes are regulated by Notch-1 in the peri-infarct area after stroke. Stroke. 2011;42(11):3231-7.

141. Zhan L, Hanson KA, Kim SH, Tare A, Tibbetts RS. Identification of genetic modifiers of TDP-43 neurotoxicity in Drosophila. PLoS One. 2013;8(2):e57214.

142. Yang D, Abdallah A, Li Z, Lu Y, Almeida S, Gao FB. FTD/ALS-associated poly(GR) protein impairs the Notch pathway and is recruited by poly(GA) into cytoplasmic inclusions. Acta Neuropathol. 2015;130(4):525-35.

143. von Grabowiecki Y, Licona C, Palamiuc L, Abreu P, Vidimar V, Coowar D, et al. Regulation of a Notch3-Hes1 pathway and protective effect by a tocopherol-omega alkanol chain derivative in muscle atrophy. J Pharmacol Exp Ther. 2015;352(1):23-32.

144. Bonini SA, Ferrari-Toninelli G, Montinaro M, Memo M. Notch signalling in adult neurons: a potential target for microtubule stabilization. Ther Adv Neurol Disord. 2013;6(6):375-85.

145. Berezovska O, McLean P, Knowles R, Frosh M, Lu FM, Lux SE, et al. Notch1 inhibits neurite outgrowth in postmitotic primary neurons. Neuroscience. 1999;93(2):433-9.

146. Redmond L, Oh SR, Hicks C, Weinmaster G, Ghosh A. Nuclear Notch1 signaling and the regulation of dendritic development. Nat Neurosci. 2000;3(1):30-40.

147. Sestan N, Artavanis-Tsakonas S, Rakic P. Contact-dependent inhibition of cortical neurite growth mediated by notch signaling. Science. 1999;286(5440):741-6.

148. El Bejjani R, Hammarlund M. Notch signaling inhibits axon regeneration. Neuron. 2012;73(2):268-78.

149. Shi M, Liu Z, Lv Y, Zheng M, Du F, Zhao G, et al. Forced notch signaling inhibits commissural axon outgrowth in the developing chick central nerve system. PLoS One. 2011;6(1):e14570.

150. de Bivort BL, Guo HF, Zhong Y. Notch signaling is required for activity-dependent synaptic plasticity at the Drosophila neuromuscular junction. J Neurogenet. 2009;23(4):395-404.

151. Grandbarbe L, Michelucci A, Heurtaux T, Hemmer K, Morga E, Heuschling P. Notch signaling modulates the activation of microglial cells. Glia. 2007;55(15):1519-30.

152. Cao Q, Lu J, Kaur C, Sivakumar V, Li F, Cheah PS, et al. Expression of Notch-1 receptor and its ligands Jagged-1 and Delta-1 in amoeboid microglia in postnatal rat brain and murine BV-2 cells. Glia. 2008;56(11):1224-37.

153. Cao Q, Kaur C, Wu CY, Lu J, Ling EA. Nuclear factor-kappa beta regulates Notch signaling in production of proinflammatory cytokines and nitric oxide in murine BV-2 microglial cells. Neuroscience. 2011;192:140-54.

154. Yin J, Li H, Feng C, Zuo Z. Inhibition of brain ischemia-caused notch activation in microglia may contribute to isoflurane postconditioning-induced neuroprotection in male rats. CNS Neurol Disord Drug Targets. 2014;13(4):718-32.

155. Yao L, Kan EM, Kaur C, Dheen ST, Hao A, Lu J, et al. Notch-1 signaling regulates microglia activation via NF-kappaB pathway after hypoxic exposure in vivo and in vitro. PLoS One. 2013;8(11):e78439.

156. Yao L, Cao Q, Wu C, Kaur C, Hao A, Ling EA. Notch signaling in the central nervous system with special reference to its expression in microglia. CNS Neurol Disord Drug Targets. 2013;12(6):807-14.

157. Marumo T, Takagi Y, Muraki K, Hashimoto N, Miyamoto S, Tanigaki K. Notch signaling regulates nucleocytoplasmic Olig2 translocation in reactive astrocytes differentiation after ischemic stroke. Neurosci Res. 2013;75(3):204-9.

158. Xing F, Kobayashi A, Okuda H, Watabe M, Pai SK, Pandey PR, et al. Reactive astrocytes promote the metastatic growth of breast cancer stem-like cells by activating Notch signalling in brain. EMBO Mol Med. 2013;5(3):384-96.

159. Zhang Y, He K, Wang F, Li X, Liu D. Notch-1 signaling regulates astrocytic proliferation and activation after hypoxia exposure. Neurosci Lett. 2015;603:12-8.

160. Kamei N, Kwon SM, Ishikawa M, Ii M, Nakanishi K, Yamada K, et al. Endothelial progenitor cells promote astrogliosis following spinal cord injury through Jagged1-dependent Notch signaling. J Neurotrauma. 2012;29(9):1758-69.

161. Kim H, Shin J, Kim S, Poling J, Park HC, Appel B. Notch-regulated oligodendrocyte specification from radial glia in the spinal cord of zebrafish embryos. Dev Dyn. 2008;237(8):2081-9.

162. Genoud S, Lappe-Siefke C, Goebbels S, Radtke F, Aguet M, Scherer SS, et al. Notch1 control of oligodendrocyte differentiation in the spinal cord. J Cell Biol. 2002;158(4):709-18.

163. Liu A, Li J, Marin-Husstege M, Kageyama R, Fan Y, Gelinas C, et al. A molecular insight of Hes5-dependent inhibition of myelin gene expression: old partners and new players. EMBO J. 2006;25(20):4833-42.

164. He L, Lu QR. Coordinated control of oligodendrocyte development by extrinsic and intrinsic signaling cues. Neurosci Bull. 2013;29(2):129-43.

165. Snyder JL, Kearns CA, Appel B. Fbxw7 regulates Notch to control specification of neural precursors for oligodendrocyte fate. Neural Dev. 2012;7:15.

166. Rabadan MA, Cayuso J, Le Dreau G, Cruz C, Barzi M, Pons S, et al. Jagged2 controls the generation of motor neuron and oligodendrocyte progenitors in the ventral spinal cord. Cell Death Differ. 2012;19(2):209-19.

167. Popko B. Notch signaling: a rheostat regulating oligodendrocyte differentiation? Developmental Cell. 2003;5(5):668-9.

168. Park HC, Appel B. Delta-Notch signaling regulates oligodendrocyte specification. Development. 2003;130(16):3747-55.

169. Givogri MI, Costa RM, Schonmann V, Silva AJ, Campagnoni AT, Bongarzone ER. Central nervous system myelination in mice with deficient expression of Notch1 receptor. J Neurosci Res. 2002;67(3):309-20.

170. Mason HA, Rakowiecki SM, Gridley T, Fishell G. Loss of notch activity in the developing central nervous system leads to increased cell death. Dev Neurosci. 2006;28(1-2):49-57.

171. Yang X, Klein R, Tian X, Cheng HT, Kopan R, Shen J. Notch activation induces apoptosis in neural progenitor cells through a p53-dependent pathway. Dev Biol. 2004;269(1):81-94.

172. Slezak M, Goritz C, Niemiec A, Frisen J, Chambon P, Metzger D, et al. Transgenic mice for conditional gene manipulation in astroglial cells. Glia. 2007;55(15):1565-76.

173. Barnabe-Heider F, Goritz C, Sabelstrom H, Takebayashi H, Pfrieger FW, Meletis K, et al. Origin of new glial cells in intact and injured adult spinal cord. Cell Stem Cell. 2010;7(4):470-82.

174. Rabin SJ, Kim JM, Baughn M, Libby RT, Kim YJ, Fan Y, et al. Sporadic ALS has compartment-specific aberrant exon splicing and altered cell-matrix adhesion biology. Hum Mol Genet. 2010;19(2):313-28.

175. Beel S, Moisse M, Damme M, De Muynck L, Robberecht W, Van Den Bosch L, et al. Progranulin functions as a cathepsin D chaperone to stimulate axonal outgrowth in vivo. Hum Mol Genet. 2017;26(15):2850-63.

176. Staats KA, Humblet-Baron S, Bento-Abreu A, Scheveneels W, Nikolaou A, Deckers K, et al. Genetic ablation of IP3 receptor 2 increases cytokines and decreases survival of SOD1G93A mice. Hum Mol Genet. 2016;25(16):3491-9.

177. d'Ydewalle C, Krishnan J, Chiheb DM, Van Damme P, Irobi J, Kozikowski AP, et al. HDAC6 inhibitors reverse axonal loss in a mouse model of mutant HSPB1-induced Charcot-Marie-Tooth disease. Nat Med. 2011;17(8):968-74.

178. Dearmond SJ, Bajsarowicz K. PrPSc accumulation in neuronal plasma membranes links Notch-1 activation to dendritic degeneration in prion diseases. Mol Neurodegener. 2010;5:6.

179. D'Souza B, Miyamoto A, Weinmaster G. The many facets of Notch ligands. Oncogene. 2008;27(38):5148-67.

180. Hansson EM, Lanner F, Das D, Mutvei A, Marklund U, Ericson J, et al. Control of Notch-ligand endocytosis by ligand-receptor interaction. J Cell Sci. 2010;123(Pt 17):2931-42.

181. He W, Hu J, Xia Y, Yan R. beta-site amyloid precursor protein cleaving enzyme 1(BACE1) regulates Notch signaling by controlling the cleavage of Jagged 1 (Jag1) and Jagged 2 (Jag2) proteins. J Biol Chem. 2014;289(30):20630-7.

182. LaVoie MJ, Selkoe DJ. The Notch ligands, Jagged and Delta, are sequentially processed by alpha-secretase and presenilin/gamma-secretase and release signaling fragments. J Biol Chem. 2003;278(36):34427-37.

183. Le Bras S, Loyer N, Le Borgne R. The multiple facets of ubiquitination in the regulation of Notch signaling pathway. Traffic. 2011;12(2):149-61.

184. Larabee JL, Shakir SM, Barua S, Ballard JD. Increased cAMP in monocytes augments Notch signaling mechanisms by elevating RBP-J and transducin-like enhancer of Split (TLE). J Biol Chem. 2013;288(30):21526-36.

185. Kochert K, Ullrich K, Kreher S, Aster JC, Kitagawa M, Johrens K, et al. High-level expression of Mastermind-like 2 contributes to aberrant activation of the NOTCH signaling pathway in human lymphomas. Oncogene. 2011;30(15):1831-40.

186. Petrovic J, Galvez H, Neves J, Abello G, Giraldez F. Differential regulation of Hes/Hey genes during inner ear development. Dev Neurobiol. 2015;75(7):703-20.

187. Hatakeyama J, Bessho Y, Katoh K, Ookawara S, Fujioka M, Guillemot F, et al. Hes genes regulate size, shape and histogenesis of the nervous system by control of the timing of neural stem cell differentiation. Development. 2004;131(22):5539-50.

188. Mukhopadhyay A, Jarrett J, Chlon T, Kessler JA. HeyL regulates the number of TrkC neurons in dorsal root ganglia. Dev Biol. 2009;334(1):142-51.

189. Fior R, Henrique D. A novel hes5/hes6 circuitry of negative regulation controls Notch activity during neurogenesis. Dev Biol. 2005;281(2):318-33.

190. Zhang Y, Chen KN, Sloan SA, Bennett ML, Scholze AR, O'Keeffe S, et al. An RNA-Sequencing Transcriptome and Splicing Database of Glia, Neurons, and Vascular Cells of the Cerebral Cortex. Journal of Neuroscience. 2014;34(36):11929-47.

191. Almad A, Maragakis NJ. A stocked toolbox for understanding the role of astrocytes in disease. Nat Rev Neurol. 2018.

192. Swiatek PJ, Lindsell CE, del Amo FF, Weinmaster G, Gridley T. Notch1 is essential for postimplantation development in mice. Genes Dev. 1994;8(6):707-19.

193. Kiernan AE, Xu J, Gridley T. The Notch ligand JAG1 is required for sensory progenitor development in the mammalian inner ear. PLoS Genet. 2006;2(1):e4.

194. Zanotti S, Canalis E. Notch signaling in skeletal health and disease. Eur J Endocrinol. 2013;168(6):R95-103.

195. Buas MF, Kadesch T. Regulation of skeletal myogenesis by Notch. Exp Cell Res. 2010;316(18):3028-33.

196. Buas MF, Kabak S, Kadesch T. Inhibition of myogenesis by Notch: evidence for multiple pathways. J Cell Physiol. 2009;218(1):84-93.

197. Conboy IM, Rando TA. The regulation of Notch signaling controls satellite cell activation and cell fate determination in postnatal myogenesis. Dev Cell. 2002;3(3):397-409.

198. McCombe PA, Henderson RD. Effects of gender in amyotrophic lateral sclerosis. Gend Med. 2010;7(6):557-70.

199. Choi CI, Lee YD, Gwag BJ, Cho SI, Kim SS, Suh-Kim H. Effects of estrogen on lifespan and motor functions in female hSOD1 G93A transgenic mice. J Neurol Sci. 2008;268(1-2):40-7.

200. Zhou M, Goto N, Goto J, Moriyama H, He HJ. Gender dimorphism of axons in the human lateral corticospinal tract. Okajimas Folia Anat Jpn. 2000;77(1):21-7.

201. Bae JS, Sawai S, Misawa S, Kanai K, Isose S, Shibuya K, et al. Effects of age on excitability properties in human motor axons. Clin Neurophysiol. 2008;119(10):2282-6.

202. English AW, Widmer CG. Sex differences in rabbit masseter muscle function. Cells Tissues Organs. 2003;174(1-2):87-96.

203. Vagnerova K, Koerner IP, Hurn PD. Gender and the injured brain. Anesth Analg. 2008;107(1):201-14.

204. Chillakuri CR, Sheppard D, Lea SM, Handford PA. Notch receptor-ligand binding and activation: insights from molecular studies. Semin Cell Dev Biol. 2012;23(4):421-8.

205. Andersson ER, Lendahl U. Therapeutic modulation of Notch signalling--are we there yet? Nat Rev Drug Discov. 2014;13(5):357-78.

# CURRICULUM VITAE


## Annelies Nonneman

*nonneman.annelies@hotmail.com*


## Education

### 2011-present | PhD in Biomedical Sciences (Neuroscience) | KU Leuven

- Project: The functional meaning of the Notch signaling pathway for neurodegeneration: a translational approach
- PhD fellowship from the Agency for Innovation by Science and Technology (IWT) (2012-2015)
- Laboratory: VIB, Center for Brain & Disease research, Laboratory of Neurobiology
- Promotor: Prof Dr Wim Robberecht

### 2009-2011 | Master in Biomedical Sciences (Magna cum laude) | KU LEUVEN

- Thesis: Notch-1 signaling in amyotrophic lateral sclerosis, Laboratory of Neurobiology

### 2006-2009 | Bachelor in Biomedical Sciences (Cum laude) | KU LEUVEN

- Including 6 months Erasmus experience at Università degli Studi di Perugia, Italy
- Student researcher internship at
    - Laboratory of Neurobiology (KU Leuven)
    - Department of Experimental Medicine and Biochemical Science, Section Biochemistry and Molecular Biology (Università degli Studi di Perugia, Italy)

# Publications

## Peer-Reviewed Publications:

- **Nonneman A**, Criem N, Lewandowski SA, Nuyts R, Thal DR, Pfrieger F, Ravits J, Van Damme P, Zwijsen A, Van Den Bosch L, Robberecht W. Astrocyte-derived Jagged-1 mitigates deleterious Notch signaling in amyotrophic lateral sclerosis. Neurobiol Disease. 2018;119:26-40.

- Eykens C*, **Nonneman A***, Jenssen C, Iavarone A, Van Damme P, Van Den Bosch L, Robberecht W. Conditional deletion of Id2 or Notch1 in oligodendrocyte progenitor cells does not ameliorate disease outcome in $SOD1^{G93A}$ mice. Neurobiol Aging. 2018;68:1-4. ** shared first author*

- Bento-Abreu A, Jager G, Swinnen B, Rué L, Hendrickx S, Jones A, Staats KA, Taes I, Eykens C, **Nonneman A**, Nuyts R, Timmers M, Silva L, Chariot A, Nguyen L, Ravits J, Lemmens R, Cabooter D, Van Den Bosch L, Van Damme P, Al-Chalabi A, Bystrom A, Robberecht W. Elongator subunit 3 (ELP3) modifies ALS through tRNA modification. Hum Mol Genet. 2018:1;27(7):1276-1289.

- **Nonneman A**, Robberecht W, Van Den Bosch L (2014). The role of oligodendroglial dysfunction in amyotrophic lateral sclerosis. Neurodegenerative Disease Management, 2018:4 (3), 223-239.

- Philips T, Abreu Bento A, **Nonneman A**, Haeck W, Staats K, Geelen V, Hersmus N, Küsters B, Van Den Bosch L, Van Damme P, Richardson W, Robberecht W. Oligodendrocyte dysfunction in the pathogenesis of amyotrophic lateral sclerosis. Brain. 2013:136 (Pt 2), 471-82.

## Published Conference Proceedings:

- **Nonneman A**, Philips T, Dupont P, Lemmens R, Van Damme P, Van Den Bosch L, Robberecht W (2014). The involvement of the notch signaling pathway in amyotrophic lateral sclerosis. Society for Neuroscience Abstract Viewer and Itinerary Planner, 44.

- **Nonneman A**, Philips T, Eykens C, Vandenberghe R, Robberecht W (2013). The involvement of Notch in the non-cell autonomous pathogenesis of amyotrophic lateral sclerosis. Society for Neuroscience Abstract Viewer and Itinerary Planner, 43.

# Presentations at International Conferences

- **Nonneman A**, Van Den Bosch L, Robberecht W. Notch signaling: a target to modify the pathogenesis of amyotrophic lateral sclerosis? The Notch Meeting IX, Athens, Greece. October 4-8, 2015. ***POSTER***

- **Nonneman A**, Philips T, Dupont P, Lemmens R, Van Damme P, Van Den Bosch L, Robberecht W. The involvement of the Notch signaling pathway in amyotrophic lateral sclerosis. The 44th Annual Meeting of the Society for Neuroscience, Washington, DC. November 15-19, 2014. ***POSTER***

- **Nonneman A**, Van Damme P, Van Den Bosch L, Robberecht W. Characterization of the Notch signaling pathway in amyotrophic lateral sclerosis. The 12th Annual Meeting of the European Network for the Cure of ALS (ENCALS), Leuven, Belgium. May 22-24, 2014. ***POSTER***

- **Nonneman A**, Philips T, Eykens C, Vandenberghe R, Robberecht W. The involvement of Notch in the non-cell autonomous pathogenesis of amyotrophic lateral sclerosis. The 43rd Annual Meeting of the Society for Neuroscience, San Diego, CA. November 9-13, 2013. ***POSTER***